Proceedings of the 21st International Ship and Offshore Structures Congress (ISSC 2022) – Xiaozhi Wang and Neil Pegg (Eds.)

Volume 2

COMMITTEE V.1

ACCIDENTAL LIMIT STATES

COMMITTEE MANDATE

Concern for accidental limit states (ALS) of ships and offshore structures and their structural components under accidental conditions. Types of accidents considered shall include collision, grounding, dropped objects, explosion, and fire. Attention shall be given to hazard identification, accidental loads and nonlinear structural consequences including residual strength together with related risks. Uncertainties in ALS models for design shall be highlighted. Consideration shall be given to the practical application of methods and to the development of ISSC guidance for quantitative assessment and management of accidental risks.

AUTHORS/COMMITTEE MEMBERS

Chairman: Bruce Quinton
Gaetano De Luca
Topan Firmandha
Mihkel Körgesaar
Hervé Le Sourne
Ken Nahshon
Gabriele Notaro
Kourosh Parsa
Smiljko Rudan
Katsuyuki Suzuki
Osiris Valdez Banda
Carey Walters
Deyu Wang
Zhaolong Yu

KEYWORDS

Accidental Limit States, Accident Risk Assessment, Collision, Grounding, Fire, Explosion, Benchmark, Nonlinear Structural Behaviour, Consequence Analysis, Resilience

CONTENTS

1. INTRODUCTION

Ships and offshore structures may be subject to accidental actions during their operation. Design for preventing or minimizing the effects of accidents is termed accidental limit states (ALS) design and is characterized by preventing/minimizing loss of life, environmental damage, and loss of the structure. Collision, grounding, dropped objects, explosion, and fire are traditional accident categories. ALS design seeks to improve the outcomes of accidents by designing in flexibility/redundancy/durability that will permit the operator & crew to deal with the accident more effectively. Mitigations such as redundant systems, fault tolerant systems, and structural-system-level ductility will tend to improve accident outcomes. ALS design is inherently a scenario-driven exercise. Different structures may be subject to different accident scenarios depending on the type of structure and its intended purpose. Determination of appropriate accident scenarios for a particular structure for a particular operation is typically performed via hazard and risk assessment.

In general, this committee report discusses newer publications (from approximately 2017 to mid-2021) and references older publications as required for clarity. Chapter 1 introduces the basic terminology, definitions and background information required to discuss ALS. Chapter 2 presents an overview of rule and code design for ALS. Chapter 3 discusses accident hazard and risk analysis. Chapter 4 discusses recent publications relating to analytical, experimental, and numerical modeling of ALS. Chapter 5 discusses ALS related publications for new and emerging research areas. Chapter 6 presents a summary and the recommendations of this committee report. Finally, the appendix contains a benchmark study examining the capability of commercially available finite element analysis software to predict fracture for structures subject to an evolving state of stress. The benchmark study models novel large-pendulum impact experiments on full-scale ship structures.

1.1 Terminology, Definitions and Background

A limit state represents the state of a structure for some potential failure. If a limit state is realized, then the structure can no longer fulfil its intended function and is said to have failed. Limit states design attempts to ensure that a structure's capacity to withstand a particular limit state (e.g., elastic buckling, plastic collapse, fatigue failure, etc.) is greater than the demand placed on the structure. Limit states design typically includes the use of safety factors to account for uncertainty in structural strength and/or in the applied loads.

Structural limit states are generally divided into four basic categories: Serviceability Limit States (SLS), Fatigue Limit States (FLS), Ultimate Limit States (ULS), and Accidental Limit States (ALS). SLS are defined such that if exceeded, the normal operation of a structure is impaired. FLS are associated with fatigue related damage to structures. ULS are typically associated with structural collapse failures resulting from overload. ULS are not directly a concern of this report, however accidental actions that may lead to ULS are. ALS are the focus of this report. ALS result from accidental actions (e.g., abnormal events such as fire, collision, grounding, and explosions) that either directly or indirectly cause excessive structural damage that endangers the safety of personnel, the structure, and/or the environment. One example of many is fire. Fire may not directly affect the load applied to a structure, but it may compromise the strength of the structure resisting the applied load. Another example is a dropped object, which obviously directly affects the loads applied to the struck structure.

With respect to ALS, failure occurs when the main safety functions of the structure are impaired by the accident. The primary ALS design requirement is avoidance/minimization or loss of life, pollution, and significant economic losses. To accomplish this, appropriate accidental limit states (ALS) for the structure must be defined and not practically exceeded. Foreseeable accidental actions and their effects must be addressed in the design of ships and offshore structures.

2. PRINCIPLES, STANDARDS AND RULES FOR ALS

This chapter gives an overview of the principles, rules, and standards applicable to design for accidental events for ships and offshore structures and identifies known shortcomings and problems with the current approaches. Where applicable, guidance and recommendations are also provided. Design standards provide good explanations of the principles underlying the design for accidental events and are referenced in this chapter. Accidental events are addressed differently in the design of offshore facilities, ships, and other assets like fish farm as well as floating bridges.

2.1 Design for Accidental Limit States

As described in ISO 19900 (2019) "The aim of the design of a structure against accidental loads is to ensure that the accidental action does not lead to the complete loss of integrity or performance of the structure and related maritime systems". It shall prevent that an incident develops into an accident disproportional to the original cause and shall ensure a safety level where the main safety functions are not impaired by the accident or within a certain time following the accident. In other words, the intention is to prevent that the consequences of an accident are disproportional to the original cause and avoid loss of life, pollution, and significant economic losses.

An accidental limit state is defined in relation to the danger of failure when the structure is subjected to an accidental action, and also in relation to the performance of the damaged structure when exposed to normal actions. As part of the design for accidents, engineers shall define an acceptance criterion to evaluate the performance of the damaged structure. Some examples are: the ability of a damaged structure to withstand environmental actions; critical deformation of structures or components following impact loads (collision or dropped objects) to avoid damage to other equipment such as risers, pipes etc.; critical deformation to avoid leakage of compartments with consequence of oil spill or loss of water tightness of a few compartments such that the stability of the unit is jeopardized; degradation of the resistance of a structure exposed to fire loads over a given time shall be smaller than the demand from functional loads and any environmental load to allow for safe evacuation; and the ALS checks include the identification and quantification of the design accidental action with a given annual probability of exceedance, the consequences on the structure, and assessment of the performance following the damage.

NORSOK N-001 (2010) describes a two-step procedure to investigate performance against accidental events: 1. Resistance to accidental actions: the effects caused by accidental actions on the intact structure shall be determined; and 2. Resistance in damaged condition: following local damage which may have been demonstrated in the first step, or following more specifically defined local damage, the facility shall continue to resist defined environmental conditions without suffering extensive failure, overall collapse, free drifting, capsizing, sinking or extensive damage to the external environment (i.e. pollution).

2.2 Design Standards, Classification Rules and Guidelines

Offshore structures are designed and assessed against international standards such as NORSOK N-series, ISO 1990X (series of standards for offshore structures) and API (American Petroleum Institute). Accidental actions are explicitly addressed in these standards, which provide an overview of the design scenario and approaches that can be used to identify and assess the effects of accidental actions.

The most relevant standards providing provisions and instructions related to Accidental Limit States are: API RP 14J – Recommended Practice for Design and Hazards Analysis for Offshore Production Facilities (2001); API RP 2FB – Recommended practice for the design of offshore facilities against fire and blast loading (2006); NORSOK N-001 Integrity of Offshore Structures (2010); NORSOK N-003 Actions and Action Effects (2017); N-004 Design of steel

structures (2004); Z-013 Risk and emergency preparedness assessment (2010); ISO 19900 General requirements for offshore structures (2019), ISO 19901-3 Specific requirements for offshore structures – Part 3: Topsides structure (2014); ISO 19902 Fixed steel offshore structures (2020); ISO 19903 Concrete offshore structures (2019); ISO 19904-1 Floating offshore structures – Part 1: Ship-shaped, semi-submersible, spar and shallow-draught cylindrical structures (2019); ISO 19905-1 Site-specific assessment of mobile offshore units – Part 1: Jack-ups (2016); ISO 19905-3 Site-specific assessment of mobile offshore units – Part 3: Floating units (2021); and ISO 19906 Arctic offshore structures (2019).

Classification Societies have developed their own requirements typically reflecting the above standards. Examples of such standards are DNV GL Offshore Standards (DNVGL-OS Series), ABS Rules for Building and Classing Offshore Installations, and Lloyd's Rules for the Classification of Offshore Units. In some cases, differences between standards and corresponding rules can be found; examples are the demand for energy dissipation during a collision event specified in the DNV GL Offshore Standard and NORSOK. Another difference is the loading condition for the post accidental capacity check. For example, NORSOK N-001 specifies a 100-year load (without material and load factor) for correlated events while DNVGL-OS-C101 (2019) indicates 1-year actions. These differences are further addressed in DNVGL-SI-0166 (2018), which addresses the compliance with Norwegian Shelf regulations.

Guidelines and methodologies addressing accidental events can be found in various Recommended Practice and Guidance Notes issued by the Classification Societies. Some examples (not an exhaustive list) are: DNVGL-RP-C204 (2019) and DNVGL-RP-C208 (2019), ABS's Guidance Notes on Accidental Load Analysis and Design for Offshore Structures (2013a) and Lloyd's Register's Guidance Notes for Calculation of Probabilistic Explosion Loads (2015).

The practice followed in the shipping industry is generally based on prescriptive requirements derived from experience. International standards (e.g. SOLAS (1974) and MARPOL (1973)) and Classification Society Rules (such those by DNV GL, Lloyd's Register, ABS, and RINA) provide the framework for consideration of accidental limit states. In this context, design methodologies explicitly incorporating ALS considerations have not been widely adopted in the shipping industry, but design against accidental events is implicitly addressed by the prescriptive requirements such as the depth of the double side and double bottom, location of cargo containment system etc. Different requirements may be expected depending on the type of ship. There is however a growing interest in the use of direct analysis to explore specific items related to accidental scenarios which are not fully reflected or covered by today's regulations. In relation to an accidental event, equivalent strength studies can be performed to document sufficient protection of the cargo containment system or gas fuel tanks for designs deviating from prescriptive requirements, or to document sufficient protection for battery systems for hybrid propelled ships as well as protection of LNG fuel tanks against dropped objects. Lloyd's Register (2016) describes a procedure for assessing equivalent protection of fuel tanks.

Besides the traditional oil and gas and maritime facilities, other types of installation are being designed to operate at sea. Offshore wind turbines, fish farms and floating bridges are example of structures that are also exposed to accidental events, and therefore such threats must be addressed in the design phase.

2.3 Design against Accidental Events for Offshore Facilities

The following sections describe the accidental events to be addressed when designing an offshore facility. Attention is given to the design principles, methodologies, and recommended practice.

2.3.1 Design accidental actions and probability of occurrence

NORSOK N-001 (2010) indicates that offshore facilities shall be designed addressing accidental events with associated effects. Relevant accidental actions should be determined by risk

assessment and relevant accumulated experience. Typical accidental actions to be addressed in the design phase are collision, grounding, dropped object, fire, explosion, unintended flooding, loss of heading (dead ship scenario), and other relevant events. Depending on the type, offshore facilities and load bearing structures are exposed to different types of actions characterized by different probability levels. Only accidental actions are meant to be included in the ALS assessment. Other actions may be covered by the design process and ultimate limit state (ULS) assessments.

ISO 19902 (2007) gives a categorization of events in terms of probability of occurrence and with this criterion three groups are defined: 1. Hazards with a probability of occurring or being exceeded of the order of 10^{-2} per annum (return periods of the order of 100 years); 2. Hazards with a 10 to 100 times lower probability of occurring or being exceeded, i.e. probabilities of the order of 10^{-3} to 10^{-4} per annum (return periods of the order of 1 000 to 10 000 years); and 3. Hazards with a probability of occurring or being exceeded markedly lower than 10^{-4} per annum (return periods well more than 10 000 years). These probabilities (return periods) are an indication of the order of magnitude rather than as precise numbers, since accurate databases for such low probabilities of occurrence rarely exist.

As indicated in NORSOK N-003 (2017), Section 9.1, the ALS design check should be carried out with a characteristic value for each accidental action, which corresponds to an annual exceedance probability of 10^{-4} for the installation; hence covering the hazards belonging to group 2 in the above list. Accidental actions with a characteristic value falling into Group 2 are covered by the design against accidental events, while group 3 is typically neglected in the design phase and group 1 is covered by the design process.

2.3.2 Collision

Design principles and dissipation of strain energy

Iceberg and ship collision actions are described in DNVGL-RP-C204 (2019) as complex events characterized by an initial kinetic energy, governed by the mass (including hydrodynamic added mass) and the velocity of the striking body at the instant of impact which needs to be dissipated during the impact. Depending on the impact conditions (direction, eccentricity, masses of the two bodies, etc.) part of the kinetic energy may remain as kinetic energy after the collision. The remaining energy must be dissipated as strain energy (deformations) of the two objects. Eccentric collision with respect to colliding ship's centre of gravity will yield smaller demands for strain energy dissipation compared to centric collision. For simplicity, these processes are often decoupled into external dynamics and internal mechanics. The former considers rigid body motions of the impacting structures and determines the amount of energy to be dissipated as strain energy and may depend on the type of installation, impact direction, mass of the objects and their hydrodynamic masses, and the impact speed. The latter deals with the dissipation of strain energy by structural deformation prior to onset of a failure mechanism or exceedance of a given acceptance criterion related to stability, pollution, or load bearing capacity following the accident.

Simplified equations accounting for the external dynamics in a decoupled approach are given in DNVGL-RP-C204 (2019) and NORSOK N-004 (2004). Assuming a central impact, the strain energy that shall be dissipated during the impact can be computed from the masses, speed, and hydrodynamic masses for different types of installations such as complaint, single point anchored reservoirs (SPAR) platforms, and fixed and articulated structures. Additional discussion about the external dynamics is given in Section 4.1.1.

The distribution of deformation energy between the two colliding objects is governed by their relative strength. Typically, the softer structure deforms more, contributing to the energy dissipation by structural deformation. When it comes to the energy dissipation, an illustrative description of design strategies is given in NORSOK N-004 (2013), and represented here in

Figure 1. These principles apply to various collision scenarios, including ship-to-ship, offshore structure-to-visiting ship, ship/offshore structure-to-iceberg, ship to bridge etc., and can also be extended to dropped objects and grounding.

The structure can be designed according to ductile, shared energy, and strength design schemes. These three schemes will set different demands on the structural design to achieve the desired energy dissipation depending on the relative strength between the involved objects.

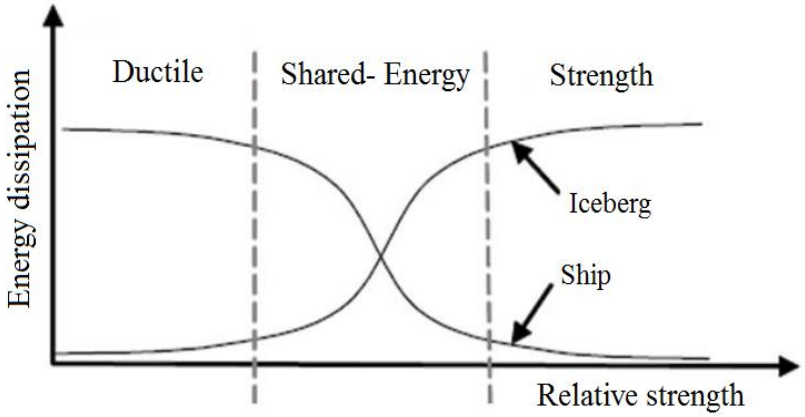

Figure 1: Illustration of ductile, shared-energy, and strength design (NORSOK N-004:2004, 2004).

In ductile design, the structure is designed to dissipate all the available impact energy by undergoing significant deformations; in this case the striking object (visiting ship or iceberg) can be simplified as rigid. Consequently, the demand on deformability may be increased (i.e., wider double side) to avoid, for example, premature oil spill. Conversely, in strength design, the structure is designed to withstand the collision load with small, or no permanent deformations. Hence, it must be designed to resist a given action similar to a ULS scenario. In this case the striking object is "crushed" and dissipates the majority of the impact energy. A shared-energy design implies that both objects are deforming, and thereby both are contributing to the energy absorption. This can be investigated in several ways by considering simplified methods (see Figure 2) or more advanced methods such as nonlinear finite element analysis where both objects are explicitly modelled and, in case of iceberg collision, a constitutive model for the ice is implemented.

The structural response of the visiting ship and installation can be illustrated by the load-deformation relationship shown in Figure 2 and the strain energy dissipated by the ship and installation equals the total area under the load-deformation curves. The load-deformation relationship for the ship and the installation is often established independently of each other assuming the other object to be infinitely rigid (continuous lines in Figure 2); this has, however, some limitation as, in reality, both structures will dissipate energy and the relative strength may also change with the progressive deformation and changes in the contact surface (dashed lines).

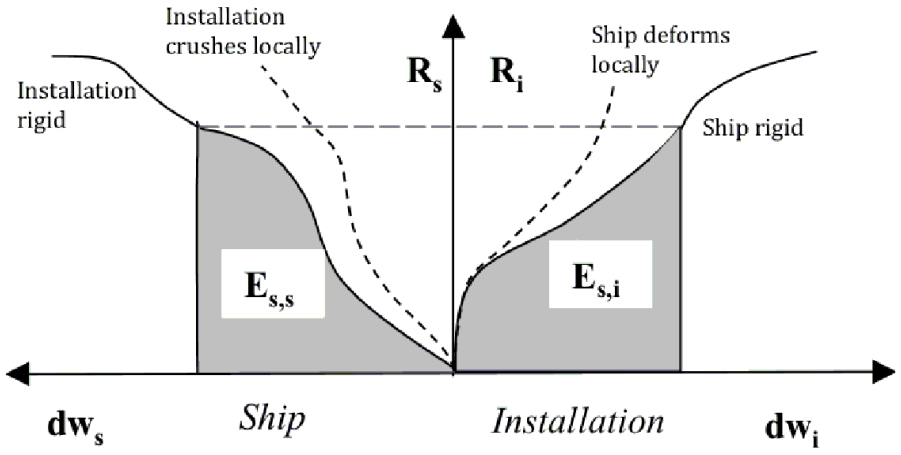

Figure 2: Dissipation of strain energy, Es, in ship and platform (DNVGL-RP-C204, 2019).

Collision actions and design energy

Reflecting the hazard characterization described in section 2.3.1, ISO 19902 (2020) and Veritec (1988) describe the collision events that shall be considered in the design process in terms of energy and occurrence:

A low-energy collision (≤ 1 MJ), representing the most frequent condition, are typically caused by small vessels with impact speeds related to normal operations. The associated probability of occurrence is larger than 10^{-2} per annum (return periods of the order of 100 years) and are covered by the normal design.

Accidental collision is often associated with a high energy level, representing a rare condition based on the type of vessel operating in the proximity of the installation and drifting out of control in the worst sea state or with head-on speed. The probability is in the range of 10^{-4} and these collisions are covered by the ALS checks.

Catastrophic collision which results in the total loss of the platform and with a frequency significantly lower than 10^{-4} are typically not covered in the design.

Additional events to consider are passing ships, shuttle tanker collisions, Floatel and facility-facility collisions. Traditionally, the generic collision load event was based on a 5000 tonne offshore supply vessel (OSV) with a drifting speed of 2 m/s (ISO 19902 (2020), NORSOK N-003 (2017), DNVGL-OS-A101 (2019)), however ISO specifies that "the representative velocity and size of the vessels used for impact analyses should correspond to those used in the operation and servicing of the platform." while DNVGL-OSA-101 indicates that "In applications where supply vessels are of much larger size this will need to be accounted for in defining the collision load." The concerns related to the size of the OSV, and hence available collision energy, and type of bow design are explicitly addressed in other references.

A comprehensive Guidance Note for risk-based collision analysis was published by Lloyd's Register (2014a). The guidance provides a summary of recognized and practiced guidelines on risk assessment and numerical analysis. The guidance highlights that in previous years, the size of the supply vessels operating on the Norwegian and UK continental shelves has increased and vessels in the range of approximately 8000 tonnes are now normal. The Guidance Note points out that additional research was recommended to assess in greater detail the influence of bow design (e.g., axe vs bulbous vs raked, ice reinforced vs non-ice reinforced, forecastle location, size, and stiffness, etc.) on energy dispersion and associated load-indentation.

NORSOK N-003 (2017), indicates design energy levels for vessel collision to be used unless further evaluations are performed. For a visiting supply vessel and intervention vessel, the

indicated value is 50 MJ (for head-on impact). This corresponds to a 10000 tonne OSV with a speed of 3 m/s. For side and stern impact, the speed remains 2 m/s.

It is worth nothing that with regard to stability and subdivision for floating offshore units, NORSOK N-003 (2017) addresses the case where the risk analysis shows that the greatest relevant accidental collision event is a drifting vessel with a displacement exceeding 5000 tonnes. In this case the prescriptive requirements given in Norwegian Maritime Directorate regulations (1991) cannot be applied and damage has to be calculated based on the collision energy from the risk analysis.

NORSOK N-003 (2017) addresses the difference between ship bow designs and implications with respect to their collision resistance (via load-indentation curves). Traditionally, a raked bow vessel was used as a basis to define the design collision event. Bulbous bow and ice reinforced vessels shall now be considered when defining the collision load. These designs are characterised by a different (likely stiffer) collision response compared to the raked bow. This aspect is addressed in the recommendations on ship collision given in DNVGL-RP-C204 (2019) which includes updated typical force-deformation relationships for standard supply vessels with a displacement of 6500 to 10000 tonnes for broad-side, bow, stern end, and stern corner impact. Force-deformation curves for bulbous bow with and without ice class are also included and are shown here in Figure 3. The bow deformation curve for a raked bow without bulb may be used to represent the resistance of the forecastle of the supply vessel.

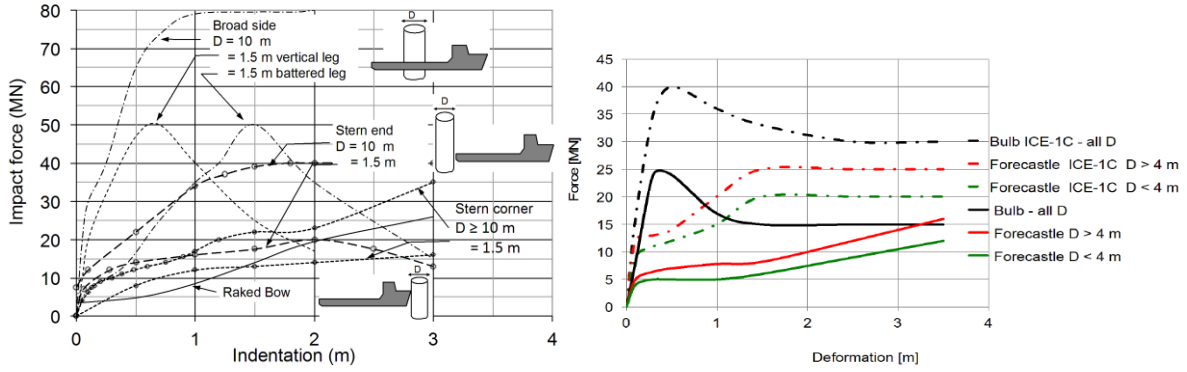

Figure 3: Recommended resistance curve for OSV DNVGL-RP-C204 (2019).

The presented curves are determined from bow, side, and stern FE models of a representative North Sea OSV. The FE models are included in the DNV GL library of FE models suitable for collision analysis and are part of the DNVGL-RP-C208 (2019). The models are available in ABAQUS and LS-DYNA formats. The curves indicate a significant increase in the OSV resistance compared to the traditional raked bow vessel. This, together with the increasing demands for collision energy, may imply that the facility should be designed following a "strength design approach".

Platform legs or braces often experience impacts, and the dissipation of impact energy can be classified as local denting or bending of the members. To establish the energy dissipated by a standard OSV bow (i.e. not ice reinforced) as a function of the brace bending resistance R0, DNVGL-RP-C204 (2019) includes an updated table describing the energy dissipated in the eventuality of an impact with the bulb of an OSV (previously only raked bow type of vessels, i.e. resistance above the main deck, was covered). A corrective factor is proposed to account for an ice reinforced OSV. Local denting can also contribute to energy dissipation. This contribution is often small for brace members in typical jackets and should be neglected. Force-deformation relationships for denting of tubular members are also given and local denting may be disregarded if the denting compactness given in the code is fulfilled. This approach is considered to be generally correct for braces or sections with small diameter, but additional

consideration should be made when considering large diameter tubes as, for example, jacket legs, where some denting is likely to occur before onset of bending deformations. Neglecting this aspect would overestimate the local resistance predicting deformation of the striking vessel structure. DNVGL-RP-C204 (2019) and NORSOK N-004 (2013) also provide failure criteria for the deformation member; such as joint failure and denting cannot exceed ½ of the diameter.

Tensile failure is currently not discussed in the last revision of the DNVGL-RP-C204 (2019). When structures are analyzed with nonlinear finite element analysis, suitable tensile failure criteria and material characterization are given in DNVGL-RP-C208 (2019). Storheim et al. (2018) have performed a critical analysis of the material characterization offered in DNVGL-RP-C208 (2019) and compared them with other models used in the engineering community and academia. They conclude that material model properties and fracture criterion specified in the new RP-C208 are unnecessarily conservative.

2.3.3 Dropped object

The dropped object load is defined by the kinetic energy of the falling object, determined by the mass and the speed at the instant of impact. Most of the kinetic energy must be dissipated as strain energy in the impacted member and, in some cases, by the dropped object itself. The principles on the relative strength explained in Figure 2 also apply to the present case. The object may be modelled as rigid or deformable, depending on the circumstances. For example, a container may be modelled as deformable while a hammer used on a wind turbine installation vessel may be assumed to be rigid. DNVGL-RP-C204 (2019) recommends assuming mean material properties for the object while modelling the characteristic strength of the impacted structure. Large deformation and fracture may often be accepted; the dropped object shall not fall through the impacted structure and the impacted structure should not hit important inventories or structures underneath (with some margin). As an additional safety factor, DNVGL-RP-C204 (2019) recommends that the "limiting impact energy for violation of the acceptance criteria is reduced by 20%". Dropped objects are rarely critical to the global integrity of the structure but may lead to puncturing of the buoyancy tanks, jeopardizing the stability of a floating installation. It should be noted that puncturing of a single tank is normally covered by the general stability requirements.

2.3.4 Fire loads and explosion

Fire and explosion events are associated with hydrocarbon leakage from flanges, valves, equipment seals, nozzles, etc. The accidental actions resulting by the combination of the two shall also be considered. The structural layout should be selected to limit the effect of fire and explosion.

The design fire action can be described in terms of the thermal flux as function of time and space, or as a standard temperature-time relation. The fire load leads to temperature rise in exposed members which causes the structural resistance to degrade. The temporal and spatial variation of the temperature depends on factors such as the fire intensity and insulation. The degradation of the structural resistance over a certain time should be limited to allow for safe evacuation or shall be smaller than the demand for functional and environmental loads. Procedures to evaluate structural resistance against fire loads is given in Eurocode EN 1991-1-2 (2002) and EN 1993-1-2 (2005). Material degradation data as function of the temperature, formulae to calculate the temperature increase in members, and design formulas to calculate the time that such members can withstand the given fire loads are given. Such calculations can also be performed by using nonlinear FE analysis. DNVGL-RP-C204 (2019) includes an updated section on design against accidental fire with guidelines on the (a) combustion process analysis, (b) heat transfer analysis, and (c) structural integrity using nonlinear FE analysis. To account for the effect of residual stresses and fabrication imperfections, the buckling resistance shall be modelled with an equivalent imperfection. The material modelling refers to the stress strain relationships given in EN 1993-1-2. A comprehensive Guidance Note for risk-based analyses

of fire loads and protection was published by Lloyd's Register (2014b). These guidelines address the type of fires, design conditions, fire protection system and principles, design loads, mitigation measures, and calculation of response to fire load. The guidance is aligned with Eurocode.

Although full CFD fire simulation can be used to capture a more realistic exposure of the structure to the thermal environment during a fire, the computational cost generally makes this impractical for most industrial applications. The gap between a full-blown CFD and practical engineering tools is large at this time and requires further research. Recently, Hodges et al. (2019) developed a reduced-order neural network driven approach to capture temperatures and velocities within a compartment that closely mirrors the results of CFD analyses.

Aluminum structures are particularly susceptible to fire due to a loss in modulus at temperatures as low as 200°C. Rippe and Lattimer (2021) developed a material model capable of capturing the post-fire degradation of 6061-T6 due to different levels of thermal exposure.

The design accidental explosion may be given as an average pressure with a certain duration over a structural member. The damage should be determined considering the system dynamics and when found necessary, nonlinear FE analysis should be applied. Lloyd's Register (2015) issued a Guidance Note for risk-based analysis of explosion loads with recommendations regarding the definition of the loads and applications.

2.3.5 Wave-in-deck loading – Current industry practices

Special consideration is required to assess possible abnormal environmental conditions or unforeseen action effects at an annual exceedance probability of 10^{-4}, e.g., by model testing for new and novel concepts. The offshore industry is currently exploring in deeper waters as well as harsher environments than they traditionally have. The target return period of waves for the design of structures has also increased over the years. For existing offshore fixed platforms, it is very common that the air gap is not adequate and design event extreme/abnormal waves will inundate the deck resulting in large wave-in-deck.

One of the major challenges that the industry faces for life extension projects is to demonstrate the suitability of the aged platforms for an increased design return period, air gap and possible wave-in-deck loading. Wave-in-deck loading arises when there is insufficient air gap for the crest in an extreme event to clear the platform topsides deck, leading to very large impulsive loads. Most of the existing jacket structures have been designed based on the requirements of API RP 2A (the latest version of which is API RP 2A (2014)) that historically required a minimum air gap of 1.5 metres for a design wave of a 100-year return period. However, these requirements are valid mostly for the Gulf of Mexico region where extreme events are hurricane dominated. The platforms in these regions are de-manned prior to occurrence of an extreme event as the path of hurricanes may be accurately predicted well in advance. This criterion would not be valid for regions like the North Sea where there is higher uncertainty for the prediction of extreme wave events. The New Year Wave that hit the Draupner platform on 1st January 1995 attracted a lot of research interest in the area of extreme wave events. The current codes such as NORSOK N-003 (2017) and ISO 19902 (2020) require a positive air gap with an annual probability of exceedance of 10^{-4} as part of the ALS strength requirements. However, the determination of the crest wave heights, wave properties, wave particle kinematics, and the derivation of associated wave in deck loads for an abnormal wave have always been a challenge.

ISO 19901-1 (2015) gives guidance on derivation of the maximum height of an individual wave for long return periods. The standard recommends that the method employed for derivation of the crest height should account for the long-term uncertainty of occurrence of a storm event and the short-term uncertainty in the severity of the occurrence of a maximum wave within a

given sea state or storm. Both NORSOK N-003 (2017) and ISO 19901-1 (2015) recommend a Forristal distribution for statistical modelling of waves in a short-term sea-state.

The latest API RP 2A WSD 22nd Edition (2014) recommends for new platforms in the Gulf of Mexico that the elevation for the underside of the deck shall not be lower than 1000-year return period maximum crest elevation. It also recommends that site-specific data should be developed in accordance with the requirements of API RP 2MET (2019).

Several joint industrial projects have been undertaken by leading international experts and major oil companies. The most recent being the CREST JIP, SHORTCREST JIP, BREAKIN JIP and LOADS JIP. The results and conclusions of the JIPs are yet to be harmonised with latest codes and practises.

Haver (2019) studied various met-ocean induced uncertainties affecting the prediction of air-gap and the major uncertainty is related to the adequacy of second-order wave theory. The paper recommends an increase of 5-10% on the predicted wave crest elevation for a robust design to account for these uncertainties. L. A. Pangestu et al. (2020) studied the significant difference in the calculation of wave force between the API RP2A-WSD based silhouette method and detailed component method. The simulation was carried on two fixed platforms situated in South China Sea. The silhouette method assumes the deck is simplified as a silhouette with suitable projected areas facing the wave crest as compared to detailed component method which calculates wave forces on individual topside elements. The results indicated that the detailed component method is less conservative than the silhouette method, showing lesser reduction to the reserve strength ratio (RSR). The detailed component method is dependent on the individual topside arrangements and hence indicates a more realistic estimate of the RSR under wave in deck loading. Ma and Swan (2020) illustrate an extensive laboratory study undertaken for improving the physical understanding of the wave-in-deck loading for a wide range of sea-state severity. The research attempts to address the nonlinear amplification of crest elevations beyond second order and the occurrence of wave breaking in both intermediate and deeper waters. The study shows that the wave in deck loads are dependent on the wave shapes and the water particle kinematics at the highest elevations within the wave crest. At the extreme sea-states, both the wave shapes (steepness) and higher crest velocities lead to wave breaking. A breaking wave-in-deck is an entirely different loading scenario compared to that of the traditional regular-wave based load estimation which is less conservative. The paper suggests detailed model testing to establish relevant wave-in-deck loads for design or reassessment. Otherwise, extensive and problem-specific calibration of the forces from regular wave assessment is required for a realistic estimate of wave-in-deck loads.

2.4 Design against Accidental Events for Ship Structures

2.4.1 Liquified gas carrier

The IMO International Code for the Construction and Equipment of Ships Carrying Liquefied Gases in Bulk (IGC Code) (2014) provides an international standard for the safe carriage, by sea in bulk, of liquefied gasses (and certain other substances). Already in the Preamble of the IGC Code it is noted that severe collisions or stranding could lead to cargo tank damage and result in uncontrolled release of the product. The IGC Code also recognizes the risks of fire and explosion as well as collision risk during berthing manoeuvres for ships at fixed locations (re-gasification or gas discharge operations). The purpose of the IGC Code is to minimize these risks. The IGC Code prescribes hazardous areas where an explosive gas atmosphere may be expected. Ship types are classified according to the transported gas and are denoted as type 1G, 2G, 2PG and 3G. A Type 1G ship is a gas carrier intended for the transportation of products considered to present the greatest overall hazard. Types 2G/2PG and type 3G ships carry products of progressively lesser hazards. The type of ship defines requirements with respect to the location of the cargo containment system, damage stability, and flooding.

The cargo containment system shall meet the criteria for collision, fire and flooding as defined by the IGC Code. Considering collision loads the IGC Code prescribes the collision load to be determined on the cargo containment system under the fully loaded condition with an inertial force corresponding to 0.5g in the forward, and 0.25g in the aft direction (where g is gravitational acceleration). Considering fire on board, the Code requires resistance to fire and flame spread, including a need for electrical apparatus considerations in the hazardous area. For a novel design cargo containment system configuration, a Load and Resistance Factor Design format is applied. At the same time, both 3D finite element and hydrodynamic analyses are required for identification of all the failure modes.

2.4.2 Gas fuelled ship

The IMO International Code of Safety for Ships using Gases or other Low-flashpoint Fuels (IGF Code) (2015) is the only document issued by IMO which addresses gas as a fuel and describes the functional requirements to be met for natural gas fueled ship. The current version includes regulations to meet the functional requirements for natural gas fuel. Regulations for other low-flashpoint fuels will be added to this Code as, and when, they are developed by the Organization. In the meantime, for other low-flashpoint fuels, compliance with the functional requirements of this Code must be demonstrated through alternative design. As stated in clause 3.2.1 “The safety, reliability and dependability of the systems shall be equivalent to that achieved with new and comparable conventional oil-fueled main and auxiliary machinery.” Chapter 5 regulates the ship design and arrangement with specific measures to protect the fuel tank(s) and piping from mechanical damage caused by collision and grounding and gives measures to guarantee sufficient ventilation to prevent accumulation of escaped gas. Further it stipulates that machinery spaces shall be designed to minimize the probability of gas explosion. In addition, Section 5.3.1 states “Fuel storage tanks shall be protected against mechanical damage.” Prescriptive requirements to protect tanks from external damage caused by collision or grounding are included in Section 5.3.3 where minimum distance from the outer shell are specified (B/5 or 11.5 m, whichever is less, from the side of the ship). This has become industry practice.

No requirements are given in the IGF code with respect to protection against dropped objects, however a risk assessment shall be carried out to investigate potential hazards. It is believed that the threats to the natural gas tank from a dropped object depend on the actual operating profile for the ship, as well as lifting operations; hence making difficult to establish general criteria which can ensure a sufficient level of safety for all operating profiles. The operating profiles shall be considered when establishing an appropriate prescriptive requirement aimed at preventing damage to the tank and further escalations. Possible hazards related to dropped object and protection should be addressed by the designer.

DNVGL-RU-SHIP Pt.6 Ch.2. (2020) provides criteria for safe and environmentally friendly systems using natural gas as fuels. This includes LNG (Section 5), Low-flash point liquid (Section 6) in supplement to the IGF Code, Gas ready (Section 8), and Gas fueled ship installations – Gas fueled (Section 13). In general, these rules cover several aspects of the systems including accidental design conditions for the containment system such as collision load (i.e., design acceleration) and fire and flooding. For LNG, collision and grounding protection for fuel tanks are generally covered by statutory requirements (i.e., thee IGF Code). These rules explicitly cover the prescriptive requirements for liquified petroleum gas (LPG) fueled vessels which are not formally covered by the IGF code. The arrangement shall ensure that the probability for the tank(s) to be damaged following a collision or grounding is reduced to a minimum, taking into account the safe operation of the ship and other hazards that may be relevant to the ship. The given prescriptive requirements are in line with the provisions given by the IGF code for natural gas and, as an alternative, a probabilistic method is given to calculate an acceptable location for the fuel tanks.

Lloyd's Register's Guidance Notes for Collision Assessment for the Location of Low-flash-point Fuel Tanks (2016) address aspects of ALS design for gas fueled ships. In cases where the prescriptive requirement cannot be satisfied, these rules, in accordance with the IGF Code, allow consideration of a 'reduced distance' by use of a probabilistic calculation. Where space is limited, both the prescriptive and probabilistic requirements on fuel tank location can be difficult to meet. However, if the hull structure in way of the tank is strengthened, higher collision resistance is provided. This can reduce damage penetration from a striking ship and may allow a 'reduced distance' to be considered. Lloyd's Register (2016) describes a procedure for assessing equivalent protection and determining the strengthening needed to reach an equivalent level of safety according to SOLAS (IMO, 1974) Chapter II-1 Part B-1.

2.4.3 Fuel cell

The use of fuel cells is currently not covered by international conventions and hence such installations will require additional acceptance by the flag authorities. DNVGL-RU-SHIP Pt.6 Ch.2 Sec. 3 (2020) provides additional requirements to those given in SOLAS Ch.II-2 (IMO, 1974) with respect to fire safety.

2.4.4 Seaborn transport of hydrogen and alternative fuels

The use of alternative fuels such has ammonia and hydrogen will present challenges that need to be addressed in the near future. Although hydrogen is gradually becoming a popular topic as an alternative to traditional fossil fuels and towards the global reduction of CO2 emission, rules do not yet explicitly address the seaborn transportation of hydrogen. The International Convention for the Safety of Life at Sea ("the Convention") (i.e. SOLAS) (IMO, 1974) and the International Code for the Construction and Equipment of Ships Carrying Liquefied Gases in Bulk ("the IGC Code") (IMO, 2014) currently do not specifically provide requirements for carriage of liquefied hydrogen in bulk by sea: the code covers hydrogen in the scope, but currently lacks specific requirements for hydrogen. An IMO interim resolution (IMO, 2016) provides the only available guidelines for maritime transport of hydrogen (not as fuel). As explained in Section 2.1 of the interim resolution "The Interim Recommendations for the carriage of liquefied hydrogen in bulk have been developed based on the results of a comparison study of similar cargoes listed in chapter 19 of the Code". This is intended to facilitate agreement for pilot ship and demonstration projects of long-haul carriage of hydrogen. Currently, hydrogen carriers are classified as a 2G ship, like LNG carrier.

According to a recent report (Maritime Knowledge Centre et al., 2017), the storage tank sizes needed to accommodate these alternative fuels (ammonia, hydrogen) should be significantly larger compared with the marine diesel oil (MDO) tanks used in current ships so as to facilitate a reasonable operation range. For example, liquified hydrogen, having a density of 70.8kg/m^3, would require 4.2 times the storage volume of MDO to achieve the same energy output. To accommodate larger storage volumes alternative arrangements that go beyond current empirically prescriptive B/5 or 11.5m rules must be employed (Vredeveldt et al., 2021). Moreover, this can affect computational methods that are used for assessment of equivalent safety, which are currently based on a simplistic rigid striking ship assumption (Lloyd's Register, 2016). Further discussion of hydrogen as a ship fuel is given in section 5.10.

2.4.5 Battery systems for electric propulsion ships

In recent years there are an increased number of vessels in operation propelled by a hybrid or a fully electric system. The battery system, also called Electrical Energy Storage (EES) poses some concern related to potential accidental scenarios associated with the integrity of the EES. DNV GL Ship Rules, DNVGL-RU-SHIP Pt.6 Ch.2. Sec. 1 (2020) addresses several issues related to the arrangement of EES spacing. The arrangement of the EES spaces shall be such that the safety of passengers, crew and the vessel is ensured and, as well, addresses potential hazards such as gas development, fire, explosion, ventilation, and external hazards such as

water ingress and collision. Electrical Energy Storage (EES) spaces shall be positioned aft of the collision bulkhead. Boundaries of EES spaces shall be part of the vessel structure or enclosures with equivalent structural integrity.

2.5 Accidental Events for other Facilities/Structures

Aside from the traditional oil and gas maritime facilities, ALS must be considered during the design of other types of offshore installations. Offshore wind turbines, fish farms and floating bridges are examples of structures that are also exposed to accidental events, and therefore such threats shall be addressed in the design phase. Due to the relative novelty of such construction, the regulatory framework is not as established as it is for more traditional marine structures.

DNVGL-ST-0119 (2018) describes accidental loads for floating wind turbine structures. For a floating wind turbine unit, accidental limit states are survival conditions in a damaged condition or in the presence of abnormal environmental conditions caused by, for example: impacts from unintended collisions by drifting service vessels, unintended change in ballast distribution, loss of mooring line or tendon, dropped object, fire and explosion, as well as flooding. Primary and secondary structures near the waterline for wind turbine columns shall be designed for service vessel impacts as a normal event. Primary structure shall be dimensioned considering abnormal events, such as impact loads resulting from accidental events. In DNVGL-ST-0437 (2016), normal and abnormal events follow different philosophies in the definition of the characteristic impact energy, with the former being related to operating conditions and the latter to unintended collision. Further discussion of offshore wind turbines is given in section 5.3.

Accidental events/loads to be considered for the design and installation of floating fish farms are addressed in DNVGL-RU-OU-0503 (2018). The design shall comply with the generic safety principles described in DNVGL-OS-A101 (2019), as well as the requirements given in NS-9415 (Standards Norway, 2009). A risk assessment shall be carried out to identify hazardous events that need to be covered in the design. This may include ship collision or other accidental loads that can lead to progressive breaks, loss of the mooring lines, drifting, loss of stability and capsize, or sinking as well as escape of fish (i.e., by damaging the net pen). Further discussion of floating fish farms is given in section 5.6.

2.6 Guidance and Recommendations for ALS Rule Design

Present day standards and rules incorporate experience and knowledge and have matured over time and tend to follow and adapt to the industry needs. An example of this is the increased collision energy from 11MJ to 50MJ in the latest release of NORSOK N-003 (2017). Over time, engineering methods to solve practical problems evolve. For example, in the last two decades the use of complex nonlinear finite element analysis (NLFEA) has become more prominent. Classification Societies have correspondingly developed Recommended Practices and Guidance Notes on the safe and reliable use of NLFEA. Examples are DNVGL-RP-C208 (2019) and ABS (2021). A different example is the development of an exhaustive section on fire loads in DNVGL-RP-C204 (2019). However, and especially in sectors where the framework is defined by prescriptive requirements, industry needs may evolve at a faster pace than the supporting rules and regulations. The use of prescriptive requirements is challenged when novel cases are introduced, or in cases when the adopted operational profile does not correspond to the one intended by the rules; examples are the use of fuel cells and seaborn transportation of hydrogen, which are presently not covered by international conventions. In other circumstances, such as the hazards related to dropped objects for LNG tanks installed on deck, a case-by-case assessment is required. Some cases, for example the use of battery powered propulsion abord ships, are partly covered by rules, but need further development.

The use of direct analysis to explore specific items related to accidental scenarios not fully reflected or covered by today's rules and regulations is increasing, however many such assessments require more research to ensure that they are incorporating appropriate design and failure

criteria; an example is assessment of the effects of fire – either via simulation or other direct methods.

3. HAZARD IDENTIFICATION AND RISK ANALYSIS

This chapter reviews hazard and risk analyses for ships and offshore structures and identifies known shortcomings and problems with the current approaches. Where applicable, guidance and recommendations are also provided.

3.1 Foundations

Hazard and risk analyses are essential tasks for establishing new structural designs against accidental events for marine structures (Mousavi et al., 2017; Ozbas, 2013; Valdez Banda et al., 2019). Hazard identification is the process of recognizing hazards that may arise from a system or its environment, documenting the related unwanted consequences, and analyzing their potential causes (Siddharth et al., 2020; Valdez Banda et al., 2014). The hazards can be aligned to issues linked to the design and operation of the system. The analysis of hazards commences with a preliminary analysis in the early stages of a project and continues throughout the system's life cycle.

An important consideration in risk analyses concerns the conceptual understanding of risk and the corresponding risk perspective. Risk is understood as uncertainty about, and severity of, consequences with respect to something that humans value (Aven, 2010). The execution of the risk analysis provides the initial establishment of the risk picture; supports the comparison of different alternatives and solutions; identifies factors, conditions, systems, and design aspects that are critical with respect to risk; and demonstrates the effects on various measures on risk (Aven, 2015). Risk analyses provide a basis for choosing the optimal of various alternative design solutions in the planning phase of a system; the drawing of conclusions on whether the design solutions meet stated requirements; and the documentation of the acceptable risk level of the selected design solution.

Hazard and risk analyses for structural designs against accidental events for marine structures need to consider the demands on the operation of the entire maritime ecosystem. Therefore, the implementation of systemic approaches to analyse and manage the risks is essential to the current demands of maritime traffic operations. Hazard and risk analyses can be carried out at various phases in the lifetime of the ship or offshore structure and the entire maritime ecosystem. The analyses start from the early concept design phase, through the more detailed planning phases and the constructions phase, and up to the operation and decommissioning phases. The fulfilment of regulatory requirements is an essential task of systemic hazard and risk analyses. This task is commonly aligned to the need for finding the right balance between ensuring safety and the costs for it.

The approaches for analyzing hazards and risks are evolving to include understanding the demands of the design and operation of marine structures considering the entire ecosystem. Today, hazard and risk analyses for accidental events for ships and offshore structures must consider the introduction of higher levels of automation and more digitalized systems. Autonomous and remote-control ships have become a topic of high interest in the maritime transport industry. Recent progress in the development of technologies enabling autonomous systems and the development of smart ship concepts have culminated in the first fully autonomous ship, the MV Yara Birkeland (container vessel), recently completing its maiden voyage (Schuler, 2021). However, one essential aspect for ensuring the correct functioning of autonomous ships is the management of risks and the assurance of safety. A criterion for an autonomous ship is that it be at least as safe as the most advanced crewed ships (Abilio Ramos et al., 2020; Chaal et al., 2020; Jalonen et al., 2017; Rødseth & Burmeister, 2015). This is an initial high-level demand that requires innovative approaches to analyse the risks and to develop the safety management strategies for autonomous/smart ships at the earliest design phase.

In the context of risk analysis, the International Maritime Organization (IMO) provides guidelines in the Formal Safety Assessment (FSA) (IMO, 2018). “The Formal Safety Assessment (FSA) is a structured and systematic methodology, aimed at enhancing maritime safety, including protection of life, health, the marine environment and property, by using risk analysis and cost-benefit assessment.” (From Section 1.1.1 IMO, 2018). The FSA is utilized to perform a balanced analysis between various technical and operational issues, and between safety and costs (Purba et al., 2020). The FSA consists of five steps: 1. Identification of hazards; 2. Risk analysis; 3. Risk control options; 4. Cost-benefit assessment; and 5. Recommendations for decision making (Section 3.1.1.1 IMO, 2018). In the context of hazard identification and risk analysis in accidental limit states, the structure of the FSA provides a supportive process for identifying and analysing the risks of collisions, groundings, explosions, and fires in ships and marine structures.

3.2 The Importance of the System Description in Risk Analysis

A clear understanding of the components and context of the system and their relation to accidents is essential for defining the scope of the risk analysis and for identifying the main factors influencing the performance of the operations of ships and marine structures (Basnet et al., 2020; Valdez Banda et al., 2019). The system description supports the delimitation of the scope of the maritime ecosystem that is covered in the context of the analysis. The system description should also be aligned with the analysis of selected accidents which can affect the resistance, integrity, and performance of ships and marine structures. Particularly, this focuses on the analysis of hazards and risks that may trigger accidental loads produced from collisions, groundings, explosions, and fires.

3.2.1 Collision

Collision risk in the maritime industry has been studied extensively (P. Chen, 2020; Du, Goerlandt, et al., 2020; Goerlandt et al., 2015; Goerlandt & Kujala, 2014; Paik, 2020c; Qu et al., 2011; Szłapczyński & Szlapczynska, 2016; Y.-F. Wang et al., 2020). Analysis of historical accident data suggests that ship-to-ship collisions are the most common accidents occurring in the development of maritime traffic operations (Bakdi et al., 2019; Du, Valdez Banda, et al., 2020; Goerlandt & Kujala, 2011). In order to better understand the cause of these accidental events, a clear description of the components of the system needs to be incorporated in the hazard and risk analysis. Ship-to-ship collisions and ship-to-marine structures collision is normally correlated with the ship traffic density of the area, ship manoeuvring operations (e.g., ship on meeting, ship passing, ship crossing, etc.), weather and navigational conditions (e.g., current, waves, visibility, ice, etc.), implementation of official navigational requirements (e.g., COLREGS and Traffic Separation Schemes), the coordination of support and assistance operations (e.g. piloting, VTS, icebreakers, etc.), and the influence of the human performance (e.g., the role of the master, officers and mariners influencing the manoeuvring of the ship). These are essential components that need to be considered for elaborating the system description included in the hazard and risk analysis.

3.2.2 Grounding

Ship grounding is one of the most common maritime traffic accidents (Bužančić Primorac et al., 2020; Mazaheri, 2009; Pedersen, 2010). Ship groundings account for about one-third of commercial ship accidents (D. Jiang et al., 2021; Samuelides et al., 2009). Ship grounding is a type of marine accident that involves the impact of a ship with the seabed or waterway side. It results in damage of the submerged part of the hull and, in particular, the bottom structure, potentially leading to water ingress and compromise of the ship's structural integrity and stability. Grounding applies extreme loads onto ship structures and is a marine accident of great importance due to the potential impacts on the safety of crew, the ship, and the local environment. In less grave accidents, grounding might result in some local hull damage, however, in most serious accidents it might lead to oil spills, human casualties and total loss of the vessel.

Ship grounding events are categorized into two major groups: powered grounding and drift grounding. Powered grounding has the largest portion of total groundings (Bin Liu et al., 2021; Otto et al., 2002). It happens when the ship is moving forward (or backward) under its own power, and generally occurs because of navigational error. Errors in nautical charts or late update of these charts is the other main reason for powered grounding. Drift grounding happens when the ship is not under its own power (for example due to mechanical problems) and drifts onto the coast or a shoal by current, wave and/or wind actions. In addition to mechanical failure, unfavourable weather conditions, failed anchoring and failed tug assistance might also contribute to the occurrence of drift grounding. Therefore, in the description of the system components connected to the main causes of accidental ship grounding, the overall scope covered is similar to that of ship collision, but it includes the essential elements of the hydrographical characteristics of the area regarding navigation (e.g., navigation in shallow waters).

3.2.3 Explosions

Oil and gas are essential sources of energy that may be produced in demanding oceanic environments where their extraction is linked to tasks with fire and explosion hazards (Czujko & Paik, 2015). Offshore platforms are the most likely structures to be exposed to hazards such as hydrocarbon explosion (Czujko & Paik, 2012). A number of major accidents involving offshore installations have been reported, such as the Piper Alpha accident of 6 July 1988 in the North Sea and the Deepwater Horizon accident of 20 April 2010 in the Gulf of Mexico. Explosions generate extreme loads that pose a huge challenge for structural maritime engineers. In the systemic description for analysing the risk of explosion in the offshore industry, the main elements to be included in the analysis are those covered in the design, reassessment, and maintenance of offshore installations.

3.2.4 Fire

The development of safety strategies to prevent fire hazards on board ships has been traditionally achieved through compliance with prescriptive rules issued by regulatory bodies (Azzi & Vassalos, 2011). The approach has now changed with the introduction of performance-based design for fire safety in the marine sector, which has instigated practical investment in prevention (as opposed to mitigation) and triggered the wide demand and use of first-principles modelling tools (Vassalos et al., 2010). The main elements to be included in the analysis of fire onboard ships include: potential sources of ignition; storing and protection of flammable materials; machinery spaces; fire detection devices; fire suppression; analysis of human factors; fire doors; response reaction plans; weather conditions; and location of the vessel (Ventikos et al., 2006).

3.2.5 Smart/autonomous ships

Studies have been conducted to analyse the risks associated with autonomous ships. Some of these include the analysis of safety risks for the general concept of autonomous ships; identifying challenging aspects for the execution of operations and prevention of accidents (de Vos et al., 2021; Wróbel et al., 2016, 2017). Others include the analysis of safety risks for a particular type of vessel and its autonomous system; reviewing a semi-defined operative context and a determined escalation process representing diverse degrees of autonomy (Burmeister, Bruhn, & Rødseth, 2014; Burmeister, Bruhn, Rødseth, et al., 2014; Rødseth & Burmeister, 2015). Other studies focused on the challenges for transferring the roles of personnel involved in the management of safety to the foreseen operational context of autonomous vessels (Abilio Ramos et al., 2019; Ahvenjärvi, 2016; Man et al., 2015; Utne et al., 2020; Wahlström et al., 2015). Some of these studies have presented analyses based on data lacking specific details about the autonomous ship and autonomous maritime ecosystem description (e.g. design characteristics of the ship, its operative context, and the practices for managing the safety of its operation), nevertheless, these studies have achieved the identification of safety gaps and challenges, and demands for the design for the autonomous maritime ecosystem. Further, some studies have

provided initial design solutions for managing the safety of autonomous shipping (Valdez Banda et al., 2019, 2021). These studies have also evidenced the need to design and implement methods and tools for systemic hazard and risk analysis that can support the design of such ecosystems.

3.3 Hazard Identification

Hazard identification is part of the definition of the accidental scenario and is a key task within quantitative risk assessment and management. Hazard identification recognizes the sources, causes, and potential consequences of hazards associated with accidents such as collisions, grounding, fire, and explosions. For example, collisions are an event where a striking structure is colliding with a struck structure and includes ship-ship collision (and allision), ship-offshore platform collision, ship-iceberg collision, offshore platform-iceberg collision, etc. The process for hazard identification commonly focuses on the collection and review of information about hazards in an operational context, information from safety reviews, reports of incidents and accidents, accident investigations, and preliminary analysis to discuss the implementation of changes in the operational context or during the development of new design concepts (OSHA, 2016). It would be highly advantageous if an omnibus historical database of such material was available. Such a database would allow identification of the frequency (probability) of the certain accidents, and how accidental events can be formulated in terms of random parameters affecting the event. For example, for the case of ship-ship collisions, appropriate random parameters might be the size of striking and struck ships, speed of striking ship, types of ships involved, collision angle, collision location, etc. The existence of such a database would allow each of the individual parameters to be characterized in a probabilistic manner. However, the risk analysis is not dependent on the existence of available data. For cases where actual accident data are not available, it may be produced from simulations, drills and/or discussion with experts.

In risk analysis, the initial step in the process is to define the type of accidents covered in the analysis. An accident represents an undesired and unplanned event that results in a loss; including loss of human life or injury, property damage, equipment damage, environmental pollution, delays in system operations, and repair costs (Valdez Banda & Goerlandt, 2018). The accident identification specifies the accident types which may cause loss during the design and operation of the system. Commonly, the identification of accidents focuses on determining and describing the most critical accidents to be prevented and/or to provide a post-accidental response for. Hazard identification focuses on detecting those hazards which can lead to the defined accidents. The aim is to detect a certain system state or set of conditions, which in a particular set of worst case conditions in the operational context, leads to the defined accidents (Leveson, 2011). This enables the development of the initial systematic and systemic connection between the accidents and their linked hazards.

3.3.1 Collision

Collision risk is commonly associated with the identification of hazards such as weather conditions (e.g., waves, currents, winds, light conditions, fog, ice, etc.); ship maneuvering operations (e.g., passing, meeting, crossing) which can be combined with a challenging operational context (e.g., navigation in a narrow fairway, traffic density, navigation in ice channel, etc.); and human erroneous performance (e.g., inadequate situational awareness, violations of COLREGs, inexperience, etc.).

3.3.2 Grounding

Grounding is commonly associated with hazards such as weather conditions (e.g., waves, currents, winds, light conditions, fog, sea ice drifting, tide, swell, availability of weather forecast, etc.); ship manoeuvring operations (e.g., passing, meeting, crossing); vessel specifications (e.g., length, breadth, draught and size); the route characteristics (e.g., traffic volume density, navigation in a narrow fairway, navigation in shallow waters, availability and quality of

nautical charts, etc.); human erroneous performance (e.g., inadequate situational awareness, violation of the traffic separation schemes, lack of navigational experience in the area, etc.); and availability and quality of assistance and support services (e.g., pilots, tugs, VTS, etc.).

3.3.3 Explosions

Explosions outside of the military domain can result from various causes, such as terrorism, ignition of fuel-air or dust-air mixtures, battery cookoff, etc. Explosions generate elevated levels of pressure on surrounding structures and systems that are not limited to the immediate region of the explosion. Internal explosions typically result in high-pressure reaction products that transmit past the compartment or space in which the explosion occurs and propagate through doors, hatches, stairways, and other such boundaries. Often, such explosions are accompanied by fire. External explosions typically result in pressure waves that can cause damage to topsides equipment such as radar systems and antennas far away from the source of the explosion.

3.3.4 Fire

The identification of fire hazards onboard ships is mainly related to the detection of potential ignition sources (Ventikos, 2013; L. Wang et al., 2021). Electricity is one of the main factors triggering the ignition process. Cigarettes, matches or similar smoking paraphernalia represent the second most common ignition source. The source is normally associated with the contribution of human factors to the occurrence of a fire incident. Another ignition source is related to the hot surfaces commonly associated to areas like kitchens/galleys and machinery rooms where heat coupled with cooling/ventilation system failures may stop providing the necessary support for safe performance.

3.3.5 Autonomous/smart ships

Initial analyses have identified a significant number of potential hazards in the design of new autonomous ship concepts and the design of their operational context (Abilio Ramos et al., 2020; Fan et al., 2020; Thieme et al., 2018; Utne et al., 2020; Valdez Banda et al., 2019; Wróbel et al., 2018). Wróbel et al. (2017) used the Human Factors Analysis and Classification System for Marine Accidents (HFACS-MA) method and what-if analysis for over 100 reported maritime accidents. They limited their analysis to safety hazards and concluded that obtained results indicate that the introduction of unmanned vessels will be very challenging from the safety point of view. They also state that actions aiming at reducing accidents must be implemented at early stages of systems design.

New intelligent ships have to consider the traditional hazards of manned vessels as well as the new hazards deriving from the new implementation of automated technologies and digitalized services. In preliminary hazard analysis for new autonomous ship concepts, studies have identified new hazards such as object detection sensor error; ship structural sensor status errors; erroneous software specifications; position reference equipment failure; unclear specifications of safety roles and responsibilities; insufficient specification for system robustness and redundancy; and cyber safety and security issues. It is important to note that autonomous ships will also be dependent on the safety and reliability of systems that are not onboard the ships but are allocated elsewhere in the context of the autonomous maritime ecosystem. Thus, hazards linked to the functionality of satellite services, internet connectivity, intelligent equipment allocated in fairways, buoys, etc. need to be considered in the analysis of the risks of the autonomous ship operations (Thieme et al., 2018). In addition, as humans are transferred to a different system area, the hazards from human erroneous actions need to be considered from an entirely new perspective (Porathe et al., 2018).

3.4 Risk Analysis

According to ISO 31000 (2018), risk is the "effect of uncertainty on objectives" and an effect is a positive or negative deviation from what is expected. Goerlandt and Montewka (2015)

provide nine definitions of risks: 1) risk is the expected value of the probability of an event occurrence and the utility of the consequences, 2) risk is defined risk as the probability of an undesirable event, or the chance of a loss, 3) risk is defined as objective uncertainty, i.e. a probability distribution over an outcome range (known through calculations or from statistical data analysis), 4) risk represents definitions where risk is equal to uncertainty, understood as a statistical variation compared with an average value, 5) risk is defined as the possibility of an unfortunate occurrence, 6) risk is the combination of the probability of occurrence of an event and consequences, without combining these in one unit, 7) risk is objective states of the world, which are considered existing independent of an assessor, 8) risk is the combination of events, consequences and the uncertainties of these, where uncertainty is understood as an assessor's uncertainty about the occurrence of the events/consequences, and 9) risk is an effect on stated objectives (i.e. a consequence), due to the presence of uncertainty.

In a risk analysis, risk is measured/described with the purpose of informing a decision. The overall aim of the risk analysis in the maritime industry is to identify and analyze the potential issues that could compromise the overall functionality of the maritime systems. Its aim is to support decisionmakers to avoid or mitigate the risks covered in the analysis (Goerlandt et al., 2019; Goerlandt & Montewka, 2015).

Quantitative risk analysis has been utilized to analyse the reliability and safety of the maritime ecosystem and its component. A quantitative risk analysis commonly follows a hazard identification, and it continues with a consequence assessment, probability calculation, and finally risk quantification (Meng et al., 2010, 2011; Nguyen et al., 2021; Qu et al., 2014). In some specific contexts (e.g. offshore structures), engineers may follow the indications given in design standards (ISO 1990X or NORSOK N-003 (2017)). An exercise of quantitative risk assessment may also be carried out if there are other hazards not specified in the standards, or if something is not relevant for the given facility.

3.4.1 Collision

The overall methodology for ship–ship collision risk analysis as commonly applied in the maritime industry includes the analysis of accident/incident frequency data, traffic data, accident frequency data, environmental data and analysis of the severity of the consequences (Goerlandt & Kujala, 2014). In a simplified description, the approach consists of finding a number of vessel conflicts in nautical traffic data and assigning a probability of collision to each of these conflicts to find a collision frequency. For the execution of this approach different methods are commonly utilized:

Fuzzy quaternion ship domain in ship traffic data. It commonly focuses on the utilization of risk indices such as ship speed dispersion, ship acceleration/deceleration, and a vessel conflict index.

Blind navigation collision candidates in ship traffic simulation. It focuses on the estimation of the ship–ship collision frequency by analysing the number of collision candidates, i.e., the number of pairwise vessel contacts in a given time period determined under the assumption that no evasive action is taken, and the so-called causation probability, defined as the probability of failing to avoid a collision when on a collision course. Its value depends on the encounter type.

Projected domain violation in ship traffic data. It focuses on the ship-ship collision frequency by analysing the number of vessel conflicts, the critical situation where a vessel is expected to enter another vessel's ship domain in the next time interval, and the probability of failing to avoid a collision for a given vessel conflict.

3.4.2 Grounding

The analysis of the risk of ship grounding focuses mainly on the frequency and consequences of the accidental event. Normally, a frequency analysis can be conducted by utilizing historical

databases of grounding accidents and a consequence analysis can be performed using the non-linear finite element method (NLFEM) modeling, or physical model testing. Specific parameters must be considered in the analysis of ship grounding, these include the mass, forward speed, and trim angle of the grounded ship, as well as the eccentricity of the impacted rock tip and the length, width an height of the rock (Paik, 2020d).

3.4.3 Fire and explosions

Three types of research on offshore fire/explosion risk analysis are commonly carried out (Y.-F. Wang et al., 2015): the first is using statistical methods to estimate fire/explosion risk based on historical data (Paik et al., 2011); the second is the implementation of risk analysis using commercial software (Yan-jie, 2011); and the third is integrating new theory with traditional risk assessment methods (Røed et al., 2009). For fire and explosions, there is no given a design scenario, but a risk assessment shall be done to identify if some situation deserves further attention with a consequence assessment (e.g., structural analysis with fire loads).

3.4.4 Autonomous/smart ships

The analysis of the risks of autonomous/smart ships with quantitative risk assessment is a complex task due to the lack of available data on the design and operation of such ships. Thieme et. al. (2018) investigated ship risk models available in the literature, 644 of them, applicable for risk assessment of Marine Autonomous Surface Ships (MASS) and concluded that none of them are suitable to be directly used for risk assessment of MASS. Abilio Ramos et al. (2019) considered operator's tasks and human failure events in the context of collision avoidance on MASS and concluded that interactions between operators and a system for collision avoidance must be considered, probably by human surveillance from an onshore control centre.

The interpretation of risk simply as a product of probability and consequence can lead to the misconception that risk is just a number and becomes divorced from the scenarios of concern and available background knowledge (Montewka et al., 2018). Applying this perspective, much of the relevant information needed for risk management is not properly reflected or even missing (Aven, 2011). In several maritime risk analyses, a lot of effort is put into producing as “accurate” risk numbers as possible, however, it is futile to calculate high precision values in risk analysis if other parameters essentially are “guesstimates” made by the analyst. In the extreme cases, the numbers obtained from databases and analyses are considered “the ultimate truth” about the probability of an accident in the analysed area, without proper reflection of the context and background knowledge.

For Accidental Limit States, the estimation of how the structure of an autonomous/smart ship resists accidental loads and maintains its integrity and performance may be calculated in a manner similar to conventional ships. The understanding of the nature of accidents and identifying hazards and risks for autonomous/smart ships, however, demands a different approach; particularly for a qualitative risk assessment (QRA), where the following implications need to be considered:

There are no existing databases for autonomous ships. For important accident types like collision and grounding, existing data are hardly relevant at all.

The inclusion of software increases the complexity of the systems and makes them harder to analyse. There is an increased possibility that we are unable to understand fully how the system works and that mistakes are made in the design of the software and hardware.

New technology also implies that new types of accidents and, in particular, new causes of accidents are introduced. We may not be able to identify these with our current methods for hazard identification (which often are based on checklists of different types).

In general, the background knowledge pertaining to autonomous/smart ships is much less than for traditional shipping concepts.

3.5 Recommendations

3.5.1 Collisions

Ship collision is one of the most frequent accident types during maritime traffic operations (Du, Valdez Banda, Huang, et al., 2021). The European Maritime Safety Agency reported that ship collisions accounted for 13% of all casualties with ships in the years 2014 to 2020 (EMSA, 2021). In the context of hazard and risk analysis, many methods have been proposed for the analysis of waterways and to support the decision making for the prevention of and response to collision risk (Lim et al., 2018). Automatic identification system (AIS) data has become a valuable source for providing information about ship traffic, and therefore many works have been conducted to detect non-accident critical events based on AIS data (Szłapczyński & Niksa-Rynkiewicz, 2018). The International Regulations for Preventing Collisions at Sea (IMO, 2007) provides guidance for ship collision avoidance. All ships are required to follow the COLREGs. In congested waters, multi-vessel encounter happens frequently, however the majority of the studies still only consider the risk of collision between two ships at a time.

New methods have been developed for the analysis of near misses and the patterns and behavior of ships during encounter situations (Du, Valdez Banda, Goerlandt, et al., 2021). New alternatives for the analyses of risk of collision should consider the dynamic nature of ship manoeuvring with the support of RADAR, AIS and other sensor data. In addition, new methods for risk analyses need to consider the application of COLREGS and the evaluation of the context in ship–multi-vessel encounters. With these critical aspects considered, the development of diverse risk management strategies for different ship types could support a better execution of evasive manoeuvring and better monitoring and advising of ship traffic operations. These new alternatives and advanced methods could support the prevention of dangerous ship encounters and provide recommendations for the direction of traffic flow, the designation of safe speeds and safe distances, and the enhancement of communication among traffic management authorities. Methods for collision risk analyses must be validated by testing them in the context of traffic operation in different waterways and sea areas. Further discussion on this topic is presented in section 5.2.

3.5.2 Grounding

Statistics show that ship grounding is the most common type of accident after ship collision (Eliopoulou et al., 2016). A ship going aground may have catastrophic consequences for humans, the natural environment and property (Youssef & Paik, 2018). Collision and grounding accidents in the context of an oil or chemical tanker could lead to irreversible effects on the natural environment. Methodologies such as the Formal Safety Assessment (FSA) with the support of risk analysis tools such as Fault Tree Analysis (FTA), HazOp, and Probabilistic Risk Analysis (PRA) tools such as Bayesian Networks have been used as the basis for the analysis of the risk of ship groundings (Z. Yang et al., 2018). These methods and tools have been focused on estimating the probability of grounding as well as the consequences of a grounding accident. Existing methods provided the identification of the main causal factors of groundings such as navigational season, water levels, currents, waterway navigational complexity, time of the day, extraordinary weather conditions (e.g. storms, rain, snow, winds, fog, etc.). Some of these methods also incorporate the analysis of human factors and the safety culture onboard the ships. In a study presented by Jiang et al (2021), ship grounding hazards are grouped by organization, human, ship technical and environmental factors. The interconnection and dependency of the elements included in these categories are essential to clearly understand the risk of ship grounding in a specific case scenario (ship operation and its context). The historical data reported in accidents and near misses has been essential to develop the assessment of the risk of ship grounding. The use of historical data and PRA tools seem to be optimal for the analysis of ship technical and environmental factors. However, statistical data and PRA tools are not sufficient to process the analysis and the proper understanding of organizational and

human factors. Therefore, new alternatives should focus on the implementation and proper linking of methodology for the analysis of the socio-technical interaction in the context of ship navigation.

3.5.3 Autonomous/smart ships

In the context of autonomous/smart ships, a more systemic approach for analyzing risk should be adopted. This would: allow a systematic and hierarchical description of the risk associated with a given system and the entire autonomous maritime ecosystem; support reasoning about risk control options (RCO) in light of available background knowledge; and provide a reflection of the effect of background knowledge on the evaluated risk and proposed RCOs (Montewka et al., 2014). This task can follow a similar shift of the risk paradigm in the offshore oil and gas industry. The industry moved from probability and consequence definition towards an uncertainty based perspective, which stresses the relevance of uncertainty assessment in the process of risk analysis, thus informing the end users about the quality of the obtained risk estimates (Haugen & Vinnem, 2015).

The transformation of the maritime industry with the introduction of autonomous/smart ships demands the development of an improved framework for risk management in the maritime industry in general, and in particular for autonomous shipping. The framework should contain: characteristics such as a flexible perspective on risk, where the aspect of background knowledge/uncertainty is incorporated; a focus on goal based and risk informed approaches to develop novel solutions while at the same time retaining consistent and acceptable risk levels also for new technology; it should allow the implementation of advanced and adequate risk analysis methods to enhance the analysis of highly complex systems with increased use of sensors, software, communication between ships and between ship and shore; and it should consider the new and different demands on the humans involved in the design and operation of autonomous/smart ships.

4. CONSEQUENCE ANALYSIS DUE TO ACCIDENTAL ACTIONS

This Chapter reviews recent publications regarding analytical, experimental, and numerical consequence analyses due to accidental actions. It identifies known shortcomings and problems with the current approaches, and where applicable, guidance and recommendations are provided.

4.1 Analytical Methods

Analytical methods for consequence analyses for floating structures most often consider external dynamics (considering global motions of the floating structure) and internal mechanics (considering deformation of the floating structure) separately; as discussed in section 2.3.2.

4.1.1 External dynamics

Analysis of ship or ice collisions is often decoupled into external dynamics and internal mechanics. The external dynamics model deals with global motions (ideally considering hydrodynamics) of the two interacting bodies prior to and after the collision. The main outcome of an external dynamics assessment is the energy loss during the collision, which will be dissipated by structural deformations in the assessment of internal mechanics. A few external dynamics models exist in the literature based on common rigid body kinematics and the impulse–momentum principle. The differences between them generally lie in the assumptions and simplifications made to solve for the considered collision scenarios, e.g. Popov et al. (1969) considers the resulting impulse in the normal direction; Pedersen and Zhang (1998) considers planar collisions, and Liu and Amdahl (2010) considers 6DOF collisions. More recently, Zhang et al. (2017) validated the method by Pedersen and Zhang (1998) with results from 58 model tests and 2 full-scale collisions and showed promising accuracy of the model. Liu and Amdahl (Z. Liu & Amdahl, 2019) reformulated the 6DOF+6DOF impact dynamics of two rigid bodies and unified the existing models in a consistent matrix formulation. Results predicted by

different methods were compared with experimental results and discussed. An equivalent friction factor was proposed which included contributions from both the Coulomb friction force and deformation resistance of structures due to sliding.

4.1.2 Internal mechanics

Simplified analytical methods are widely used for quick assessment of structural deformation resistance to accidental loads. The methods often provide reasonable predictions compared with numerical simulations and experiments, and some formulations are adopted in classification society rules.

Grounding

Hu et al. (2016) proposed a simplified model for predicting the structural responses of double bottom ships grounding on blunt seabed objects, which caused continuous sliding of structures but no rupture of the outer shell. The formulation included resistance of longitudinal girders, transverse floors, the outer plate, and the corresponding attached stiffeners. Compared with explicit time-integration finite element simulations using LS-DYNA, the model predicted total energy dissipation within a range of approximately -10% to +25% depending on the grounding scenario.

Analytical models were recently derived for ship grounding on paraboloid-shaped rocks. According to Sormunen et al. (2016), the parabolic shape allows for a better fit with real seabed rocks than does a conical one; which is commonly used in hard grounding simulations. Closed form expressions were derived from plastic analyses for ship bottom sliding (Pineau & Le Sourne, 2021) and raking (Pineau et al., 2021) over an elliptic paraboloid rock. The failure modes include steady state plate tearing and crushing of bottom floors and girders. The main mechanisms of energy absorption are friction, membrane straining, plastic bending and crack propagation. A super-element solver was then developed and successfully compared with numerical simulations by Le Sourne et al. (2021) within a collaborative benchmark study.

Collision

Liu and Soares (2016a) reviewed existing simplified models for predicting the crushing resistance of unstiffened web girders subjected to in plane loads and proposed a model for the resistance of stiffened web girders subjected to local in plane loads. The model was validated by comparison with experiments. Daley et al. (2017) presented a model for overload response of simple flat bar stiffened frames subjected to ice loading, and the effect of bending and shear is discussed while the axial force is not included. Yu et al. (2018) proposed a simplified approach for the assessment of large deformation resistance of stiffened panels subjected to lateral loading, considering the effect of boundary flexibilities, concentrated and pressure loading. Although the model was formulated in the quasi-static manner, it may be used in combination with the Biggs method for transient problems in explosions or slamming actions. Sha and Amdahl (2019) studied the deformation of ship deckhouse collisions with steel bridge girders and proposed a formulation for the collision resistance by summing up resistance from structural components including tearing of plates, crushing of girders and deformation of stiffeners. Zhang et al. (2019) validated the revised Minorsky model by Pedersen and Zhang (1998) for the prediction of energy absorption in collisions and groundings with a series of experiments and showed good agreement. More recently, Conti et al. (2021) introduced a methodology to assess the influence of ship structural design for use in the frame of damage stability analyses. Using a super-element solver to quickly simulate a high number of collision scenarios, statistical SOLAS damage distributions were reshaped for a reference cruise ship and her reinforced version, and it was quantitatively shown that risk control in terms of damage reduction over the whole range of damages was possible by adding a double hull or by deck reinforcement. Zhu et al. (2018) presented a method for predicting the dent resulting from objects dropped onto the deck of ships by application of the hinge-line method. This was verified via finite

element simulations using ABAQUS/Explicit. Zhu et al. (2020) applied hinge-line analysis to predict the energy absorbed during a collision with ice floes. This work was verified by comparison with finite element analysis using Ansys/LS-DYNA and experiments.

For ship collision with offshore tubular structures, Buldgen et al. (2014) presented closed form solutions for the resistance of a jacket leg subjected to ship impacts considering the complete behavior of tube deformation including local denting, global bending and membrane stretching. The different orientations and positions of the struck tube, and the shape of the striking ship stem were accounted for. The proposed method was verified to be of reason able accuracy using explicit time-integration finite element simulations with LS-DYNA. Pire et al. (2018) derived analytical expressions for energy absorption in two additional scenarios other than that wherein the impacted leg was laterally deformed. The first considered a leg punched by one or several compressed braces and the second considered buckling of a rear compressed leg near the mudline during the overall deformation of the jacket. Based on the concept of the super element method, Le Sourne et al. (2016) and Pire et al. (2017) proposed an efficient method that included simplified solutions for local denting, global bending, axial stretching, brace punching and buckling. The proposed method was verified to be of reasonable accuracy using explicit time-integration simulations with LS-DYNA. Yu and Amdahl (2018) presented a comprehensive review of structural responses and design of offshore tubular structures subjected to ship impacts. Different analytical models for the response of tubular members subjected to lateral impacts were compared and discussed. It was found that analytical models for the indentation of tubes are well established by Wierzbicki and Suh (1988) with a closed form solution. However, the reduction of bending capacity of tubes with increasing indentation seems to vary significantly using different models. More efforts are needed to verify and improve a model describing the complete tube behavior including local denting, global bending and axial stretching under lateral impacts. The residual strength of damaged tubular members is also of interest to explore further.

Post damage

Post damage hull girder strength is an important topic for collision, grounding, and explosion scenarios where the resulting strength is often below operational load requirements. Sun et al. (2016) assessed the residual strength of a grounded ship based on the progressive collapse method and compared with numerical simulations. Cerik & Chuong (2020) examined the role of collision damage on the residual strength of a bulk carrier, accounting for unsymmetrical bending effects due to heel at mild and severe heel angles, using an enhanced Smith's method approach that accounts for motion and rotation of the section neutral axis. Damage is accounted for in this case by removing damaged structure and treating it as entirely ineffective, an approach that is common in the salvage community. Leelachai (2020) presented extended results on damaged panel strength accounting for damaged state residual stress utilizing FEA. The resulting load-shortening curves accounting for severe local and multi-bay damage are included in a progressive collapse tool, ProColl.

Once damage occurs, the hull girder may be in a highly degraded state in which hog/sag cycles exceed peak girder capacity. Li et al. (2019) presented an analysis method for examining hull girder capacity under severe cyclical load using a reference point based load shortening formulation that accounts for strength reduction at the panel level. The results were compared to FEA of the entire cross section as well as the bilinear IACS formulation.

Tabri et al. (2020) presented an ultimate and residual strength assessment model for the early stage design of hull girder, based on the coupled beam (CB) method. In CB method the structural elements are represented with load-end shortening curves as opposed to discrete finite elements making the analysis computationally efficient compared to NLFEM. The original CB method was extended to assess post grounding ultimate strength by excluding the coupled beams from the damaged region. Approach was validated with comparative NLFEM

simulations. Compared with other simplified methods which are restricted to single section analysis CB method can properly model the behavior of the entire hull girder.

4.2 Experimental Methods

The structures and physical scale of the phenomena of interest are large, and it is impractical to conduct more than a handful of full-scale field test events for most of the hazards presented. Furthermore, full-scale field test events are generally conducted with a limited level of control over experimental inputs. Therefore, generating meaningful experimental data relating to ALS inherently involves some form of scaling of either the loading phenomena or the test structure. Additional challenges arise from the complex nature of loading phenomena and the challenges in generating experimental data e.g., pressure data from explosions, ice impact pressures, etc.

4.2.1 Similitude Methods for Structural Impact

The design of structures capable of crashworthiness has motivated many researchers to study the structural impact phenomena. It is believed that the full-scale experiment is the most reliable method of evaluating the crashworthiness performance of structures (W. Zhang et al., 2010). However, the high costs and environmental concerns impose restrictions on full-scale experiments. Instead, scaled model tests are commonly used to predict the damaging effect on the prototype structure. To obtain responses of the prototype structure efficiently, it is feasible to work with models designed by proper similarity laws (Ding et al., 2015; D. Wang et al., 2011). Significantly, structural impact involves events such as plastic flow and potential fracture, on which strain and strain rate strengthening effects have great influence (P. Jiang et al., 2006; Jones, 2012). And the fact that the nonlinear effects are not prone to scaling is a major obstacle for the use of scaled structures under impact loads (Oshiro & Alves, 2004).

Imperfect similarity occurs since several phenomena do not scale according to the same geometric factor. The law of similarity for structures has been extensively investigated (Baker et al., 1991; Barenblatt, 2003; Coutinho et al., 2016; Decius, 1948; Skoglund, 1967) and widely applied in significant research fields concerning non-scaling phenomena, for example structural failure (Atkins, 1999; Noam et al., 2014; Sadeghi et al., 2019), explosions (Fu et al., 2018; Gao et al., 2018; Kong et al., 2017; S. Ma et al., 2021; Snyman, 2010) and structural impact (Atkins, 1988; U. Cho et al., 2005; B. Liu et al., 2020; Mazzariol & Alves, 2019a, 2019b; Q. Song et al., 2017; S. Wang et al., 2021). Indirect similarity (U. Cho et al., 2005) established coefficients to infer the prototype behaviour applying loading scaling factors that results in scaled displacements differing from geometric scaling factors. Afterwards, recent developments of similarity laws in structural impact have focused on methods of altering the impact velocity or mass to overcome non-scaling effects including strain-rate effects, differences in material mechanical properties and distorted geometry configuration (Mazzariol & Alves, 2019b).

To name a few, Luo et al. (2014, 2015) discussed the applicability of the distortion models numerically when predicting the dynamic characteristics of a full size rotating thin wall short cylindrical shell. In their work, sensitivity analysis and governing equations were employed to relate the incomplete scaled-down model to the prototype, the improvement of which was to determine a necessary scaling law, applicable structure size intervals, and boundary functions that could guide the incomplete scaled-down model design. An important suggestion for how to deal with non-scaling phenomena occurring in scaled problems of mechanical impact and fracture was provided by Atkins (1988). According to his energy analysis, when the problem presents a mixture of surface and volume effects, a perfect replica scaling is unfeasible. Such a mixture is present in the majority of problems.

As a means to do so, Oshiro and Alves (2012) developed a method to allow a replica with geometrical distortions to forecast and represent the prototype structure behavior by changing the impact velocity. To validate its applicability, three analytical problems of structures

subjected to dynamic loads are analyzed. Mazzariol et al. (2019a, 2019b) attempted to give a comprehensive framework to compensate for the differences in material properties and small thickness distortions. A correction equation has been derived to relate the behavior of models and full-size steel structure based on the relationship between strain rates and impact velocity. Then it was employed to correct the impact velocity of the striker in scaled circular plates and double plate Calladine structure analytically and numerically.

Another efficient technique to correct non-scaling effects is to consider the relevance of the mass in the impact event, thus adding additional mass to the scaled model to balance the strain-rate effects. Lu et al. (2020) carried out experimental and numerical studies on dynamic characteristics for tubular K-joints in offshore platforms. On the basis of previous work (Wei & Hu, 2019), an indirect similarity method is developed in their work, which mainly scales the model by controlling the impact mass to balance the strain rate induced size effects.

Similitude theory has proven to be an efficient tool to conduct scaled model design in structural analysis and tests. Specifically, it affords a theoretic basis to study mechanical characteristics such as free and forced vibrations, buckling and impact responses, in several engineering fields by small-scale models. In the application of similitude methods, partial similitude may be best as results can be achieved considering non-scaling effects and manufacturing constraints. As simplifications are applied in the corresponding methodology focus on specific problems, the whole similarity process will have to be repeated for each structure. Besides, the influence of non-scaling effects can hardly be generalized since the main concerns in mechanical systems are sensitive to different parameters such as the geometric variables, material properties and load input parameters. Distortions may be viewed as manufacturing variabilities, or perturbations of a system with respect to a reference state that lead to differences in response. Thus, in practice, model distortion is the main obstacle to be overcome in the further study of similarity laws. In this context, the principal lines of research should focus on a generalized methodology, with the attempt to more easily derive the similarity conditions and scaling laws from a generalized set of scaling relationships, without having to apply the similitude theory to the various situations.

4.2.2 Scaled experiments and miniaturization

Chen et al. (2020) conducted a series of experiments to investigate the crushing behavior of vertical stiffeners in web girders. The specimens were in 1:6 scale with respect to actual ship bottom structure elements. The study is the continuation of earlier similar experiments by Liu et al. (2016b). Compared with this earlier study, the number of stiffeners and plate thicknesses are the varied parameters. From an experimental perspective, the study provides valuable insight into the crushing behavior of stiffened plates by presenting the interplay between the number of stiffeners, welds, and location of the indentation. From a numerical perspective, it is less straightforward to assess the added value. Although the authors claim that the established numerical model can be used to predict the crushing behavior of ship structures in collision and grounding, it is left for the reader to interpret what they exactly mean by that. For instance, it is recommended in the paper that element length in crushing simulations should not exceed 10 mm. However, such a recommended value should have a clear dependence on plate thickness since the susceptibility of the plate (i.e., element) to buckle and fold depends on the thickness. The strong effect of thickness on the localization in deformation was well exemplified by Kõrgesaar (2019).

More extreme scaling factors for structural components have been used lately by Calle and coworkers. Their initial study was made at a scale of 1:100 to reproduce the structural response during collision and grounding (Calle et al., 2017). In these tests, they neglected some of the structural details because of the small thickness. The limitation was removed by Calle et al. (2020) who performed scaled raking test with specimens produced using additive manufacturing. Nevertheless, because of the extreme scaling, similarity techniques were used to scale the

original structural dimensions to model scale. These techniques involved classical dimensional scaling combined with separate thickness scaling. The latter was introduced to enable model production with additive manufacturing. The thickness scaling depends on the failure mode (tearing, membrane or folding), meaning that failure mode must be known a priori for all structural components. If the wrong failure mode is assumed, the manufactured structural part has an incorrect thickness, which can lead to a cascade of errors compared with actual full-scale structural behavior. Failure mode identification is further exacerbated by the fact that often there is a strong interaction between modes. This uncertainty needs to be carefully addressed in future studies.

Raking experiments on full-scale plates were performed by Bijleveld et al. (2018) and Haag et al. (2017). These experiments helped to show how material failure could be modeled in dynamic, sliding contact. Notably, Bijleveld et al. (2018) showed that the maximum shear criterion (otherwise known as the single-parameter MMC model) was reasonably good at predicting failure in shell elements, with input taken from small-scale material tests.

4.2.3 Full-scale structural experiments

Paik et al. (2021) performed cold-temperature (-80°C) collapse testing of a stiffened steel plate composed of AH32 steel subject to axial compressive loading. Even though -80°C is below the tensile-to-brittle fracture transition temperature for AH32, they did not observe any brittle failure. The stiffened plate structure behaved similarly to similar tests conducted at room temperature (Paik et al., 2020a) (i.e. they observed essentially linear force-displacement curves until just prior to stiffener tripping), except that the cold temperatures induced a structural response that was 11.6% larger than that at room temperature. Paik et al. (2021) also developed a calibrated numerical model of the experiments which overpredicted the experimental results in both force-displacement modulus as well as peak load capacity; for both the -80°C and room temperature experiments. Paik et al. (2020b) performed further similar experiments at cryogenic temperatures (which may practically occur, for example, from accidental LNG spill). Here they observed sudden brittle fracture of the stiffened panel once the ultimate limit state was achieved. They reported no visible plastic deformation and significant portions of the structure were violently detached from the main structure. The maximum structural load achieved was 9% higher than the similar room temperature test.

Paik et al. (2021a, 2021b) conducted full-scale fire testing to collapse of steel stiffened plate structures subject to lateral patch loading. They did so for stiffened structure with (Paik, Ryu, et al., 2021a) and without (Paik, Ryu, et al., 2021b) passive fire protection. Their measured gas cloud temperature was approximately 15% less than the ISO 834 fire curve for most of the experiments. The time to structural collapse was 1600 seconds for the case without passive fire protection, and nearly twice that, at 3100 seconds, for the case with passive fire protection.

H. Kim, Daley et al. (2018) conducted full-scale ice load experiments on an IACS PC6 polar class stiffened grillage structure. They used a 1m diameter ice cone to quasi-statically apply ice loads normal to the stiffened grillage. They observed significant structural deformation and stiffener tripping, with small surface cracks visible at the ends of the central stiffener. These experiments demonstrate significant structural overload capacity. They also developed and calibrated a nonlinear finite element model that compared very well with the results of the experiments.

Gagnon et al. (2020) used a large-double pendulum apparatus to conduct ice-cone impact experiments against a novel ice-pressure sensor and recorded pressure distributions for various impact energies with a sampling rate of 500Hz. The maximum recorded pressures were in the range of 30-55 MPa, tending toward the higher end of the range.

4.3 Numerical Methods

4.3.1 Model setup

This section provides reference on numerical FE analyses setup parameters to aid analysts in performing the ALS analyses and reaching reliable results. Much valuable guidance is available in DNVGL-RP-C208 (2019) and ABS's Guidance Notes on Nonlinear Finite Element Analysis of Marine and Offshore Structures (2021).

Finite element analysis solver type

Selecting a solver type for ALS finite element analyses presents challenges. Historically, many nonlinear ALS FE analyses have been conducted using an explicit time-integration formulation solver. Quinton et al. (2017) present criteria for selecting an 'explicit solver' for moving/sliding loads on hull structures. Explicit solvers are generally robust for highly nonlinear transient dynamic events because it can capture large deformations, structural instabilities, contact, and fracture very well. Explicit solvers, however, generally rely on first-order elements and may have difficulty capturing higher frequency responses due to various sources of numerical noise including solver noise (which may be mitigated by modifying default analysis settings) and contact handling related noise (which also has several non-default options for mitigating noise; in particular by implementing 'two-way contact' algorithms as well as accounting for 'soft' contact). For ALS problems that occur over a period of time on the order of several seconds or more, the explicit solvers become inefficient due to their requirement for very small-time steps (typically 10^{-6} seconds or even much smaller). These small-time steps are required to maintain solution stability. As an example, a 'explicit' FE model with 10mm .x 10mm shell elements composed of steel (with mass density equal 7850 kg/m^3, Young's modulus equal to 207 GPa, and Poisson's ratio equal to 0.3), by the Courant-Friedrichs-Lewy stability criterion, requires a time step no larger than 1.85768E-06 seconds; therefore, simulation of 1 second requires the solution of over 530,000 time steps. One method of improving the efficiency of explicit solvers is to employ mass scaling. There are various mass scaling techniques, however, typically mass scaling involves artificially and drastically increasing the density of the smaller elements in the mesh so that their time step is artificially increased. This will, of course, significantly increase the mass of these elements which will affect their dynamic behaviour and may (or may not; depending on many factors) greatly affect the FE model solution. Mass scaling should be employed with caution and is discussed further below.

For analyses where contact and fracture do not play a central role, implicit time-integration solvers are attractive and facilitate the use of higher-order elements that generally will result in improved solution quality at an equivalent nodal spacing. Furthermore, the time step selected for an implicit time-integration analysis is chosen by the user and is generally based on the frequencies of interest (a typical rule is that the chosen time step is 1/20 the period of the highest frequency of interest). For cases where the geometry dictates small elements, the overall solution time is much less dependent on the element size than for an explicit solver. An additional advantage of implicit solver is the ability to include Rayleigh damping; doing so for an explicit solver may result in a reduced time step, and therefore a longer solution time.

Mass scaling

Efficiency of ALS numerical analysis is crucial for evaluations during the conceptual and early design stages. Many ALS scenarios may be approximated as quasi-static; implying that analysts may choose between implicit or explicit FE solvers. For the class of ALS analyses that often exhibit strong nonlinearities and contact, explicit solvers are often computationally more efficient, however, since the time step for explicit solvers has an upper limit in order to maintain solution stability, their use becomes computationally impractical to model quasi-static events in their natural time period. Hence, quasi-static simulations using explicit solvers may need to be accelerated; either by increasing the rates of the applied loads or by using mass scaling.

Increasing loading rates increases the material strain rate as well as the structural inertial response.

Regarding material strain rate sensitivity, mass-scaling may only be used when material strain rate sensitivity may be considered negligible. For ships and offshore structures built from metallic materials, this may or may not be the case, depending on many factors. Therefore, the use of mass scaling (which involves an artificial increase of material density that may be implemented using several methodologies (e.g., applied globally to the mesh, applied only to elements with a time step < n, etc.)) can increase the maximum stable time step, thereby reducing the number of time steps needed for the solution and thus, reducing the total simulation time. In other words, mass scaling may allow efficient modelling of events in their natural time scale using an explicit solver.

Regarding structural inertia, mass scaling should be done so that kinetic energy remains a fraction (1-5% ABAQUS manual, <1% DNV-RP-C208 (2019)) of deformation energy, so that problem solution retains its quasi-static character. The analyst should confirm that this check is made when the aim is to model quasi-static event. This general guideline is well established and appears to be consistently followed also in the scientific literature reviewed.

In transient dynamic analyses, the natural time scale is always important and an accurate representation of the physical mass and inertia in the model is required to capture the appropriate structural response. Although these analyses are computationally demanding, the application of mass scaling is less straightforward since scaled element masses affect their resulting inertia. In such cases, selective mass scaling could be used, however the current review could not identify any studies focusing on this practical issue. In other words, best practices and criteria for choosing selective mass scaling parameters for dynamic ALS analysis are missing; but urgently needed.

Element related

Storheim et al (2016) investigated the aspects of the numerical setup for simulation of collisions using ABAQUS and LS-DYNA, with attention to the differences between the two codes. Two examples of crushing simulations are presented: a bulbous bow hitting a rigid wall and the simulation of a folding experiment. The calculations indicate that the described folding mechanisms are very sensitive to the mesh refinements and numerical effects. The artificial stiffness from hourglassing and shell drilling were identified as the main source of differences. The authors pointed out that the drilling constraint is activated by default in ABAQUS and but not in LS-DYNA; likely due to the different evolution of the two codes. Equivalent results were obtained by setting the drilling constraints consistently in the two solvers. The effect of the drilling stiffness was shown to be mesh dependent and the simulated response seems to converge between the solvers when the mesh size is decreased. The authors recommended not to include the drilling stiffness in coarsely meshed shell structures. Quinton et al. (2017) recommend the enabling of drilling stiffness for the simulation of moving/sliding loads on hull structures.

4.3.2 Grounding

Le Sourne et al. (2021) studied the influence of buoyancy forces, failure strain and friction coefficient on the damage of a grounded ship. It was found that the damage extent can be several times larger when hydrodynamic loads (especially buoyancy forces) and ship motions are considered. Moreover, the length of the breach resulting from bottom raking significantly depends on both the friction coefficient between the rock and the hull plating and the criterion used to model the failure. Indeed, a shear failure criterion commonly used in such numerical analyses appears to be insufficient to accurately model the different failure mechanisms occurring in a ship raking process. Kim et al. (2021) also emphasized the importance of buoyancy

forces on structural damage and energy absorption in ship grounding when they conducted fluid structure interaction analysis using LS-DYNA/MCOL.

4.3.3 Collision

Ship-ship/offshore oil and gas platforms

Moan et al. (2019) presented the background for the update of the NORSOK N003 (2017) standard to meet the challenges of increased collision energy and new ship bow and structures designs. The consequences of increased design energy on the design of offshore oil and gas platforms were discussed. It is indicated that for typical North Sea jackets it will be difficult to design braces such that a single brace will absorb the required energy for standard bow collisions. A viable alternative may be to design the braces strong enough to penetrate and crush the bow of the impacting vessel, so that the vessel dissipates most of the energy. Amdahl and Yu (2021) discussed the new updates of DNV-RP-C204 (2019) and its impact on crashworthiness design. The challenges addressed in the updated recommended practice are discussed in the paper and include updated design collision energy and force-displacement curves, ship installation interactions, compactness criterion of offshore tubulars and external dynamic models. Mujeeb-Ahmed et al. (2020) conducted supply vessel collision simulations with an offshore jacket platform using explicit time-integration simulations with LS-DYNA. The hydrodynamic effects of the striking vessel are included using MCOL. The results showed that the local damage resistance of jacket tubulars agreed well with theoretical models. The majority of collision scenarios showed deformations on both forecastle and bulb, and the vessel may hit multiple braces and column members when hydrodynamic effects are included. Travanca and Hao (2015) simulated quite a few ship collision cases with three different jacket platforms using explicit time-integration simulations with LS-DYNA. The platforms were modelled with shell elements. They found that global elastic deflection energy can be important for jackets especially for large platforms. The portion of global elastic energy out of total energy were large for ship collision on strong legs and tubular joints, which have large local stiffness at the impact point. Travanca and Hao (2014) simulated ship collisions with jacket and jack-up platforms using explicit time-integration simulations with LS-DYNA with shell elements, and then simplified the platform global response with equivalent single-degree-of-freedom (SDOF) systems. They found that the equivalent SDOF models were able to simulate global deflections of platforms generally well. However, in eccentric collisions, both the lateral and tortional responses are prominent for jack-up platforms. Equivalent models in such cases should account for both lateral and tortional responses. The rotational response was found less important for jackets in the studied cases. Amdahl and Holmas (2016) analyzed the response of a typical jack-up subjected to a high-energy collision of 67 MJ on a corner leg using USFOS. The platform was installed in 110m water depth and the first eigenperiod was 7.8 s. It was found that the ship spent considerable time in the elastic unloading phase (1.9 - 5.2 s), and up to 25 MJ was stored as elastic energy mainly in the platform during impact. The inertia force was important, and the temporal impact force depended on the jack-up response, which could not be calculated a priori. The compliance of the platform contributed significantly to the survival of the impact and needed to be considered.

Ship-offshore wind turbine

For ship collisions with bottom fixed offshore wind turbines (OWT), Biehl and Lehmann (2006) studied the behavior of three foundation structures i.e., monopile, tripod, and jacket of offshore wind collided by single (200,000t) and double (45,000t) hull tankers, bulk carriers (25,000t), and container ships (52,000t). The ship caused large deformations of the turbine foundations, which were completely torn off in extreme cases. The nacelle and the rotor may fall onto the deck of the striking vessel. The collision loads caused local damage on the ship hull with possible oil leakage. Song et al. (2021) evaluated dynamic responses of a monopile-supported wind turbine under ship impacts using both numerical and analytical methods.

Precalculated wind loads and aerodynamic damping were included in the explicit time-integration LS-DYNA simulations through a user defined load subroutine. The differences of the maximum tower-top displacement by the analytical and numerical methods vary from 5% to 23%. It was found that the wind turbine response was significantly affected by the impact velocity and the wind direction. Bela et al. (2017) conducted numerical simulations of supply vessel collisions with a monopile based offshore wind turbine. Both rigid and deformable bows were considered. It is however recommended by the committee to use deformable ship bows as the turbine foundations are often strong enough to deform the bow of supply vessels. The studies emphasized the influence of wind directions and soil flexibilities. The assumption of fixed boundaries of the OWT at the mudline is found to lead to an overestimation of the plastic deformation of the collided structure. For ship collision with jacket foundation wind turbines, Ramberg (2011) conducted collision analysis with jacket OWTs from a tanker of 190,000 tons using USFOS. This gives a design energy of 500 MJ. With such huge amount of energy, it is not possible to design wind turbines to resist a tanker. The collapse may be induced either by buckling, yielding of the support structure, or foundation failure, e.g., piles being pulled out of the soil on the tension side. In many cases, the turbine collapsed into the sea in the drift direction of the tanker, thus preventing the nacelle from dropping down on the tanker, which is favourable. However, in some cases, the large inertia may cause local buckling and unfavourable failure of the tower towards the ship. Moulas et al. (2017) conducted explicit time-integration NLFEM simulations of monopile and jacket type bottom fixed turbines subjected to supply vessel impacts using ABAQUS. The failure mechanisms of turbine foundations are identified. The ship was modelled as a rigid body, which may exaggerate the damage on the turbine foundations.

For ship collision analysis with floating offshore wind turbines (FOWT), proper modelling of the hydrodynamic loads becomes essential. Echeverry Jaramillo et al. (2019) simulated a SPAR type floating offshore wind turbine subjected to collisions from a supply vessel of 5000 tons using explicit time-integration using LS-DYNA. Hydrodynamic effects were included using the LS-DYNA MCOL module. They emphasized the importance of introducing hydrodynamics for collision with a floating turbine. Yu et al. (2022) carried out dynamic response analysis of a 10 MW semi-submersible floating offshore wind turbine subjected to collisions from a supply vessel of 7500 tons and an oil tanker of 150,000 tons using USFOS. The hydrodynamic effects were modelled using the buoyancy module and the Morrison equation, while the wind loads were calculated using software based on blade element momentum theory. It was found that the semi-submersible turbine was in general safe from tower collapse under supply vessel impacts under a design energy of 50 MJ, while the platform may capsize in the event of tanker collisions with a design energy of 420 MJ. Zhang and Hu (2021) conducted supply vessel collision with a spar type floating wind turbine using explicit time-integration FEA using LS-DYNA. The wind loads and hydrodynamic loads including buoyancy, motion induced radiation loads and waves loads were included using a user load subroutine.

Ship-bridge collisions

Sha et al. (2019) posed two critical notions related to the topic of ship-bridge collisions: (i) rigid bridge assumption regarding foundations and piers might not be valid for bridge girders (ii) up to now the design and safety of bridge superstructures against collision have mainly been ignored. Therefore, Sha et al. performed parametric studies and showed that damage sustained by the bridge girder is dependent on the ship-bridge girder relative strength. They proposed a strengthening method for the bridge girder against ship forecastle collisions. Along the same lines, Sha and Amdahl (2019) proposed a simplified analytical method for predictions of ship deckhouse collision loads on steel bridge girders. They explicitly accounted for the specifics of interacting structures (girder geometries and deckhouse configurations) and characteristics of the developed line load.

Sha et al. (2019) presented a combined local and global analysis procedure to address ship collision with a floating bridge. The global analysis procedure was motivated by the significant compliance of the floating bridge and consequent strong interaction between the bridge and ship during the collision. They concluded that finite element simulations should be conducted to estimate the collision load for a specific collision scenario. Furthermore, the global analysis showed that in a particular analyzed case, 40% of collision energy was dissipated by the global bridge motion. Therefore, neglecting the global response of the bridge would yield a conservative estimation of the energy consumed through structural damage, and thus, a much more conservative design.

Song and Wang (2019) proposed an empirical impact load time-history model accounting for ship size and impact velocity, which could be used to substitute the FE models of ship-bridge collision events to predict the bridge response efficiently. The basis is decoupling the ship-bridge interaction and making a rigid bridge assumption. It is noteworthy that they validated the numerical simulation technique by drop hammer tests. Naturally, this model does not apply to floating bridges. Wan et al. (2019) investigated the collision safety of reinforced concrete bridge piers using numerical and experimental methods. In their quasi-static and dynamic scaled experiments (scale 1:10), they crushed ship bow models against the concrete piers. They showed that the pier concrete model assumptions (elastic, rigid, nonlinear inelastic) had a significant effect on the resulting bow crush depth and the impact force in high energy collision cases. To capture the interaction effects accurately, the authors advise using a nonlinear material relationship for concrete. Pu et al. (2019) investigated the dynamic responses of a long-span cable-stayed bridge under ship collision through FEA and presented a comparison of the collision forces with the recommendations in different design codes (AASHTO (2009), International Association for Bridge and Structural Engineering (IABSE code), CDRBC (2017), GSDHBC (2015)). Figure 8 in Pu et al. (2019) gives some insight into the level of conservativeness in the different rules considered. AASHTO consistently predicts the highest collision force versus ship tonnage, while CDRBC consistently predicts the lowest. The results in the paper may be useful for the further development of codified design rules and procedures.

Glacial ice impacts

Bergy bits and growlers (i.e., small glacial ice features) travelling with waves and currents can pose great threats to ships and offshore structures operating in ice infested waters. These relatively small glacial ice features are difficult to detect, monitor and to manage by concurrent ice management operations, therefore, it is important to quantify the probabilities and consequences of the potential glacial ice impacts with the structure of interest.

In efforts to ensure that involved petroleum industries maintain a high level of HSE and emergency preparedness, the Petroleum Safety Authority Norway (PSA) established a series of projects to study the structural safety in the central part of the Barents Sea. These projects have provided many insights into aspects of this technical challenge.

The ST5 project (Ekeberg et al., 2018) was carried out by DNV. The study described and identified concurrent knowledge and challenges in relation to structural safety in the High North and narrowed down the investigation to a specific scenario regarding the impact between glacial ice features (with a characteristic water line < 15 m) and a semi-submersible structure. The ST19 project (W. Lu, Yu, van den Berg, Lubbad, et al., 2019) carried out by NTNU and ArcISo substantially extended and enriched the work of ST5. The project analysed the probability distributions of impact velocities and locations on the structure and the collision energy under waves and currents and identified the critical scenarios that might potentially lead to structural damage. Further, nonlinear finite element simulations were carried out to calculate the structural damage under ice impacts. The shared-energy approach was adopted in analogy to the procedures for ship-installation impacts, where ice was presented as a pressure-area curve considering its energy absorption per unit volume and the structural resistance is by nonlinear finite

element simulations assuming rigid ice. It was concluded that the recommended impact energy for design is around 7.5 MJ for a 15 m long ellipsoidal glacial ice feature, with an annual probability of exceedance of 10^{-4}. With this design energy, the structure was safe from outer shell penetration and flooding risks, based on finite element simulation results. The ST20_2018 project (Ommani et al., 2018) was carried out by SINTEF Ocean, studying the hydrodynamic interactions between glacial ice and semisubmersible drilling units using CFD methods and potential flow theory. Possible position of impact, impact velocity and impact energy were assessed. It was found that the motion response of the glacial ice was highly influenced by the presence of a semisubmersible; both in the wave diffraction forces acting on the ice as well as the added mass coefficients for the ice mass. The nonlinear restoring and Froude-Krylov excitation forces were shown to be important due to large variation in the ice feature's waterplane area as it moves vertically, as well as the potential for the ice to be completely submerged as it moved in waves. The ST 20_2019 project (W. Lu, Yu, van den Berg, Monteban, et al., 2019) continued the work in ST 19 and conducted a more in-depth analysis of ice motions under waves and current using time domain simulations considering nonlinearities and structural damage under ice impacts. It was found the lower size limit of a detectable glacial ice feature by marine radars can easily be doubled to 30 m and thereby yield a higher impact energy. Three different approaches were used to calculate structural damage with various degrees of simplifications i.e., the integrated approach, the weakly-coupled approach and the fully coupled approach. The structural responses were found to be sensitive to local sharpness of ice geometry. With the most unfavorable local ice geometry, the structure was found to withstand a maximum impact energy level of around 15 MJ without shell puncture. The ST 20_2019 project ended with two journal publications, i.e. Lu et al. (2021) (Part I) and Yu et al. (2021) (Part II). A follow-up project, the ST20_2019_Extension project (W. Lu et al., 2020), summarized the findings from the above projects and formulated a report in the format of classification rules for the analysis and design against glacial ice impacts, which can be a useful reference for new rules to come. Further, Yu et al. (2021) developed a numerical solver for coupled simulation of glacial ice impacts accounting for the effects of hydrodynamic-ice-structure interaction. The solver adopted user subroutines provided in LS-DYNA and combines three different modules, i.e. the BWH (Bressan-Williams-Hill) criterion for the prediction of fracture of steels, a hydrostatic pressure dependent plasticity-based material model for constitutive modelling of ice, and linear potential flow theory for hydrodynamic loads. The model has been successfully implemented for ice collision simulations with a semi-submersible platform column considering hydrodynamic-ice-structure interaction with good efficiency and accuracy. Amdahl (2019) reviewed the principles for the analysis and design against glacial ice impacts in ALS conditions, including the pressure-area curve versus force-area curve of ice, the effects of local and global shape of the ice feature in energy absorption, material modelling of ice and ice structure interactions.

Cai et al. (2020) proposed to use a soil and concrete constitutive material model (keyword MAT_SOIL_CONCRETE in LS-DYNA) to represent ice material. The model is a hydrostatic pressure dependent plastic model similar to the ice models in Derradji-Aouat (2000) and Liu et al. (2011). Four groups of experiments were performed to study the dynamic behaviors of clamped plates impinged by a freshwater ice wedge. Good correlation was obtained between the numerical and single impact experimental results and later with repeated impacts in Cai et al. (2022). Herrnring and Ehlers (2021) adopted the Mohr-Coulomb material to model brittle ice behavior using the node splitting technique to simulate ice fracture. The simulated maximum ice forces and contact pressures were verified of good accuracy by comparison with ice extrusion and double pendulum tests Gagnon et al. (2020) . Ince et al. (2017) proposed a new constitutive equation for ice materials where the effects of strain rate, salinity and temperature were taken into account. Ductile and brittle behaviours were separated at a critical strain rate. Ice fracture was modelled with cohesive elements based on the crack-opening displacement. The model was used to simulate an ice drop test in Ince et al. (2017) and showed reasonable

agreement. Kim et al. (2018) conducted full-scale quasi-static experiments of large structural grillages subjected to ice loads. The structures were pushed into large plastic damage with considerable ice failure at the same time. Results of FE analysis showed a good agreement compared with the physical experimental results. Gagnon et al. (2020) conducted large double-pendulum ice impact tests and the contact pressure was measured using an advanced novel pressure-sensing technology. The pressure-sensing strip technology was shown to be robust and capable of providing accurate distribution maps of high-pressure zones (HPZ) and low-pressure zones (LPZ) over time. Patterns of HPZs that were surrounded by LPZs due to spallation of ice from the HPZs, were evident. The experiments were simulated in Andrade et al. (2020). Quasi-static and dynamic simulations showed a clear response difference in the structure.

4.4 Fluid Structure Interaction

4.4.1 Slamming

Water impact (slamming) is a strongly nonlinear phenomenon including significant fluid structure interactions. Potential consequences of water slamming may vary from structural vibrations to large permanent deformations and structural damage. In the extreme sea states, slamming loads may cause progressive collapse of structures and fatalities. An example is the recent accident of the COSL Innovator drilling rig in the North Sea, 2015, where a steep horizontal wave struck the unit on the front bulkhead of the forward box girder. Water intrusion caused extensive damage to cabins, killing one crew member with four injured (Viste-Ollestad et al., 2016).

Generally, ULS design is often adopted for the design against slamming, where the structure shall resist the design slamming pressure with minor damage. The structure, in this case, responds primarily with elastic vibrations, and the coupling between hydrodynamic pressure and the elastic response of the structure, known as hydroelasticity, matters and has been studied extensively. However, when violent water slamming occurs in extreme or abnormal events, large structural stresses may occur that exceed the material yield stress, causing large plastic flow and permanent damage. The elastoplastic or fully plastic response of the structure will be strongly coupled with the hydrodynamic pressure, termed as hydro-elastoplasticity or hydro-plasticity.

From the literature, the coupling effect between hydrodynamic pressure and structural response during water slamming is generally limited to the hydroelastic effect. Little information can be found on the effect of hydro-elastoplastic or hydro-plastic slamming. When structural damage is concerned in extreme slamming conditions, an uncoupled approach (e.g., Wang et al. (2002)) is often adopted by assuming a certain pressure profile, which is to be applied on the structure for the response. It is also unclear whether an artificial added mass should be added to the structure and, if so, the associated values to use.

As this topic is relatively new, a summary of the important previous works is presented. For the uncoupled methods, Jones (1973) proposed an analytical model for slamming damage of ship plates considering dynamics effects by assuming a triangular pressure impulse and rigid perfectly plastic material. The plates were assumed to deform in the same pattern as in quasi-static conditions. The results were given as non-dimensional curves of structural damage with respect to a pressure ratio and a normalized impulse. Design equations following similar principles are given by Paik and Shin (2006) and Ma et al. (2021). Many class rules (e.g. (ABS, 2013b)) are however, based on the equivalence concept of quasi-static pressure loads such that the well-established simplified models for quasi-static structural response apply. It is however well noted from structural mechanics under impulsive loading (e.g. Jones (2012)) that when the external pressure is larger than 3 times the pressure causing static collapse of structures, plastic hinges form in between the end and middle of the beam, and move towards the beam

middle span during deformation. The moving hinge response, as shown in Figure 4, is widely used for structures subject to explosions and blasts.

For coupled hydro-elastoplastic theory, a first attempt was made by Yu et al (2019a) to couple hydrodynamic loads and plastic structural response, where the moving hinge response of rectangular beams and stiffened panels were directly coupled with hydrodynamic loads represented by the potential flow theory. The results were presented using nondimensional diagrams, where a governing parameter of nondimensional velocity is identified. The formulations were validated against Arbitrary Lagrangian Eulerian (ALE) simulations in Yu et al. (2019b) and a recent experiment by Sintef Ocean in Yu et al. (2021). Abrahamsen et al. (2020) proposed a hydroplastic theory for the prediction of permanent deflections of thin plates subjected to extreme slamming. The model did not include travelling hinges. This is considered reasonable for thin plates, which are quickly dominated by membrane reactions. The proposed model was validated by comparison with drop tests. The coupled consideration of hydro-plastic or hydro-elastoplastic slamming remains limited in the literature and requires further effort to reach a mature understanding.

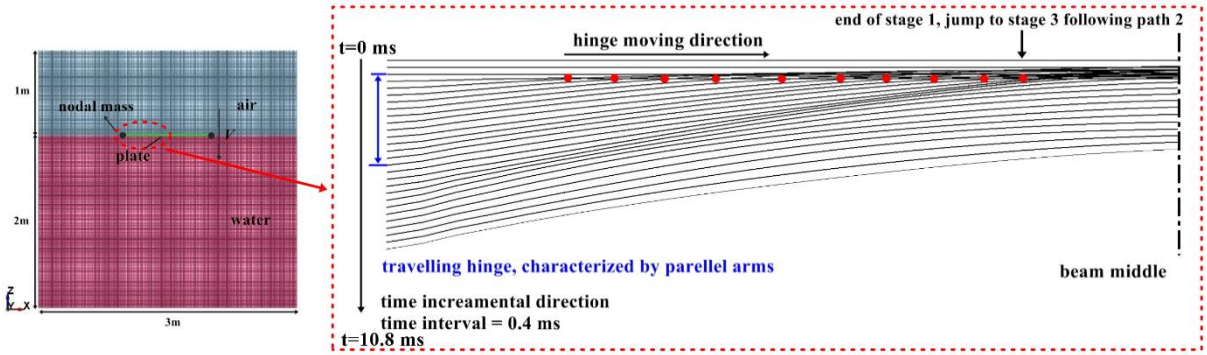

Figure 4: Snapshots of displacement profiles for half of a plate strip during water entry with ALE simulations; the plate thickness is 6 mm and the initial impact velocity is 10 m/s. The time interval is 0.4 ms. The red points denote positions of the travelling hinge at each time instant; from Yu et al. (2019).

Experiments and numerical methods are useful tools for the assessment of structural damage and associated coupling effect to extreme water slamming. Considerable information is summarized in the report of ISSC 2009, COMMITTEE V.7 IMPULSIVE PRESSURE LOAD-ING AND RESPONSE ASSESSMENT (2009). Regarding experimental methods, Abrahamsen et al. (2020) conducted drop tests of thin-walled aluminum plates at Marintek ocean basin. The complex hydrodynamics of the impact were captured using a high-speed camera from below, refer to Figure 5. The plate deformation was tracked using a three-dimensional digital image correlation (DIC) technique. The experimental results for flat plate impact showed large plastic deformation of the plate and significant fluid structure interactions. A large air pocket was trapped by the deformed plate during impact. Shin et al. (2018) conducted repeated drop tests of flat steel unstiffened plates with varied plate thickness and drop height. Seo et al. (2018) further performed similar experiments for unstiffened wedges with a deadrise angle of 10°. The cumulative deflection due to consecutive free drop was found to approach a constant value, which was about 1.6 - 4.0 times as that of the first drop at the center of wedge bottom plate depending on both drop height and plate thickness. Results indicated that the accumulated damage of ship plates under repeated water slamming cannot be neglected.

Regarding numerical methods, Cerik (2017) conducted parametric studies of aluminum plate damage subjected to slamming using ABAQUS/Explicit by assuming an idealized pressure

impulse. Truong et al. (2018) adopted similar procedures to study the effect of repeated slamming impacts. Empirical equations were recommended by fitting to the simulation results. Storheim and Lian (2018) applied a total of 775 measured slamming time series to three different structural models and studied the correlation between the load and response. Results showed a significant variability of extreme slamming loads from model tests, and that using the structural response as an indicator did not help resolve the variability. To account for fluid structure interactions during violent water slamming, the Arbitrary Lagrangian Eulerian (ALE) method, which is available in many commercial software packages, e.g. LS-DYNA and ABAQUS, are often adopted. Examples of the ALE method with respect to recent slamming applications are found in Truong al. (2020) , Cheon et al. (2016) , and Yu et al. (2019b). A better representation of the fluid and the air effect can be achieved by instead coupling with CFD solvers for the fluid domain, and NLFEM for the structures, e.g. Zu (2019) by coupling STAR-CCM+ and ABAQUS for slamming problems. Truong et al. (2021) presented a benchmark study on the slamming responses of flat stiffened plates. Different methodologies including include LS-DYNA ALE, LS-DYNA ICFD, ANSYS CFX, and Star- CCM+/ABAQUS, for the modelling of fluid-structure interactions are compared and discussed.

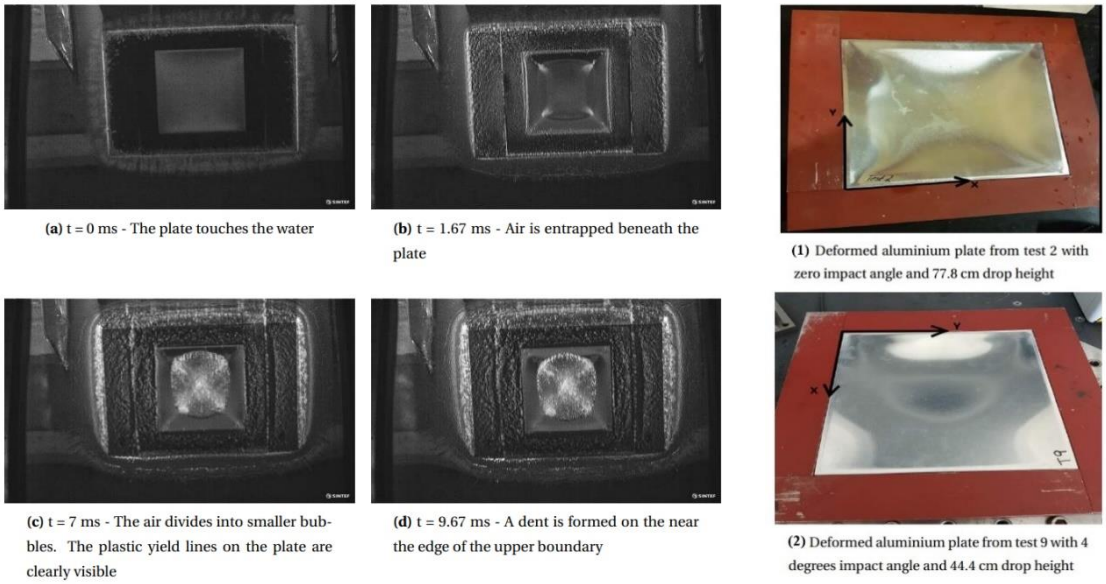

Figure 5: (left and centre) Pictures taken by the high speed camera for drop test of a 0.6 mm-thickness alluminium plate with zero deadrise angle and drop height 44.4 cm; (right) Plate deformation after experiments. From Abrahamsen et al. (2020).

4.4.2 Collision and grounding

The realistic analysis of ship dynamic response in accident scenarios requires the coupling of structural response (internal mechanics) with ship motions (external mechanics) that depend on the environment, operational conditions, and transient fluid motion. While hydrodynamic-structural response coupling implies significant computational effort, these analyses are becoming more accessible with the increased computational power that has become available over recent years. Currently, we can distinguish two types of coupling methods: fully and partially coupled. Fully coupled methods explicitly model the fluid (and therefore the fluid effects) by one of several computation fluid simulation techniques: the Arbitrary Lagrangian-Eulerian (ALE) technique; fully coupled CFD-FE; and smoothed particle hydrodynamics (SPH)-FE. Fluid effects in partial coupling methods are represented through algorithmic development of hydrodynamic forces (Yu, 2017).

Regarding fully coupled simulation techniques, only the ALE technique has been prevalent in collision and grounding studies. This is likely due to the associated extremely high computational requirements of coupled CFD-FEA and the novelty of using SPH modeled fluid in such scenarios. Regarding the SPH-FE, this is a computationally attractive option because it eliminates the need to track the fluid free surface, and fluid-structure interaction forces may be handled with standard Lagrangian contact algorithms. While collision and grounding research has yet to model fluid effects using SPH, Lee et al. (2020) suggest it may be used in studies of ships and offshore structures. Much work is required to ascertain whether SPH modeled fluid can accurately predict hydrostatic and hydrodynamic forces on ship hulls. The ALE technique typically models fluids with Eulerian elements and solids (i.e. the ship) using Lagrangian elements. Forces are transferred between fluids and solids via coupling algorithms, and between solids and solids via contact algorithms. For a recent review see Lee et al. (2017). Song et al. (2016) performed collision simulations between ships considering different parameters and compared the ALE method against a constant added mass representation of hydrodynamic effects. They concluded that the added value from the full coupling does not outweigh the excessive computational effort compared with partially coupled models. Nearly the same conclusion was reached by Rudan et al. (2019), who compared the ALE method to a partially coupled approach based on MCOL – LSDYNA coupling. MCOL is a code for the analysis of rigid body motions of a ship subjected to hydrodynamic forces (Le Sourne et al., 2001). During the coupling process, LS-Dyna and MCOL exchange data: contact force from LS-Dyna is transferred to MCOL and then the ship's centre of gravity (CoG) position, velocity, and acceleration are updated according to hydrodynamic reactions calculated by MCOL; which are returned to LS-Dyna for the next calculation step. Rudan et al. (2019) concluded that this approach is fast and stable, but requires hydrodynamic analysis of the considered ship in an independent software (e.g., HYDROSTAR). Furthermore, their study pointed to the complexity of choosing the correct ALE parameters and stability issues related to ALE method.

Two partially coupled approaches were also developed by Yu (2017) by using the "user-defined load and user common subroutines in LS-DYNA. Namely, the approaches differ in how hydrodynamic forces are calculated, either by manoeuvring model or by linear potential flow theory. User common subroutine allows storage of important history or external information, e.g., velocities of ship CoG and the impulse response function, and the load subroutine provides a way to apply load boundary conditions. Based on coupled simulation results, Yu et al. (2019) critically reviewed the assumptions behind the widely used analytical external dynamic models and concluded that: i) it is difficult to find a representative frequency to determine the constant added mass for the external dynamics models. ii) the external dynamics models assume that the collision duration is short, and the collision angle does not change before and after the collision. This is shown to be a good approximation for short duration collisions, but the accuracy becomes less for collisions with long durations. iii) The external dynamics models assume ideal collision of two rigid bodies with a common tangential plane at the contact point, however, in practice the striking and struck objects often do not have a common tangential plane before impact. It may not be straightforward to determine the normal vector of the contact plane as a function of the inputs of the external dynamics models. iv) In some cases, motions of the striking ship may be hindered by large deformation and rupture of the struck structures. This motion locking effect will significantly increase the total dissipated energy but is not considered in external dynamic models with the rigid body assumption. This may be remedied by giving the model an artificially large friction factor to forcefully enable a 'sticking' case when motion locking occurs. To summarize, the external dynamic models generally give quite good predictions of the collision energy, but the users should be aware of the assumptions made by the external dynamics models and circumstances where the accuracy may decrease due to invalidation of underlying assumptions.

The partially coupled approach based on LS-DYNA MCOL was extended by Kim et al. (2021) to account multi-physics effects during ship collision and grounding process. The impact

velocity in 6DOF considering evasive action was defined through manoeuvring analysis and the resistance force was evaluated using a CFD solver. Two scenarios corresponding to collision and grounding accidents with passenger vessels were considered. They concluded that the effect of resistance on the analysis results is negligible and that the hydrodynamic restoring forces may be the most influential on the structural dynamic response.

For a more general overview of damage assessment models used in the analysis of ship and offshore structures, but not limited to FE based approaches see Deeb et al. (2017).

4.4.3 Underwater explosions

Underwater explosions (UNDEX) have long been the focus of defence naval research. Today, non-military issues such as accidental underwater explosions near offshore installations (jackets, risers, etc.) as well as terrorist attacks against non-military vessels may be considered as accidental events. In this field, the main challenges/difficulties lie in understanding and modelling the physics of the interaction between the immersed structure and the surrounding water, both at early time (a few milliseconds) and long-time (a few tenth of a second) phases.

Theoretical studies performed by Kennard (1943), Bleich et al. (1970) and Newton (1978) give many insights in regard to fluid-structure interactions (FSI) occurring in such events like bulk cavitation that may develop in the vicinity of an immersed structure. Over the past decades, many researchers have brought several advances forth, and a considerable body of literature already exists. Cole (1948), Mair (1999), and Porfiri and Gupta (2009), and more recently Mouritz (2019),Tran et al. (2021) and Wanchoo et al. (2021) provided a wide overview of many of those underwater explosion studies.

Experimental methods

Early before World War I, experimental methods had been performed from full-scale and large-scale explosive testing to laboratory-controlled scale. Most full-scale and large-scale experiments have been mainly conducted at sea or in a detonic basin by defence organisations. Although the most precise to assess shock resistance of structures, these tests are very costly and require many precautions and safety measures; therefore, laboratory-scale installations like water-filled shock tubes, water-filled chambers, spherical pressure vessels and cubic tanks are nowadays commonly used at research centres and universities.

To obtain controlled loading and reproduce different water-structure contact conditions, an underwater shock loading simulator (USLS) was used by Avachat et al (2016) to provide a variety of load configurations with quantitative diagnostics. Important features of this facility include the ability to generate water-based impulsive loading of a wide range of intensity, the ability to simulate the loading of submerged structures, and integrated high-speed photographic and laser interferometric diagnostics. Figure 6 shows a schematic illustration of the cross-section of the USLS.

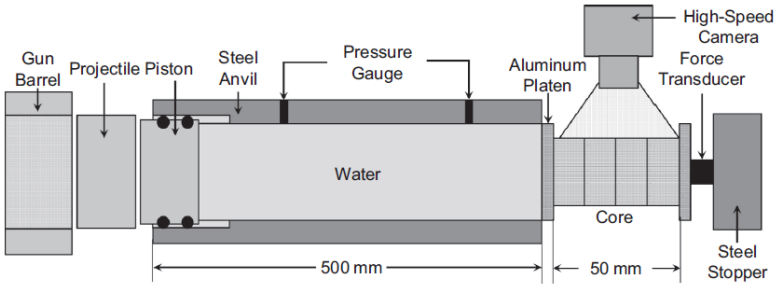

Figure 6: A schematic illustration of the dynamic compression test setup within the underwater shock loading simulator (USLS) (from Avachat et al (2016)).

Experimental investigations were carried out by Wu et al. (2018) in an artificial water pool on steel cylindrical shell-water-cylindrical shell structures subjected to near field or contact underwater explosion loading. Major deformation modes were analysed considering the effect of standoff distance, shell thickness and water interlayer thickness. In the same way, a ballistic pendulum system suspended on the top of an explosion vessel was employed by Ren et al. (2019) to investigate the response of water-back metallic sandwich panels. To generate an underwater shock wave, an explosive charge was fixed at the centre of a water filled PVC tube located at a given standoff distance from the panel. A large diameter test tank was used by Gauch et al. (2018) to study the behaviour of composite cylinders to near field (UNDEX) loading, including the effects of polyurea coatings. The transient response of the structure as well as its interaction with the expanding gas bubble were evaluated through high-speed photography coupled with 3D Digital Image Correlation. A similar measurement system was employed by Kishore et al. (2021) to investigate the interaction between the water and a cylindrical shell immersed at a near critical hydrostatic pressure and subjected to the implosion of another shell in proximity.

Laboratory-scale experiments require less preparation time and lower cost, whereas they are repeatable, safer, and more controllable than full-scale or large-scale experiments. Both structure response and shock wave pressure history can be captured by the aforementioned installations, whereas only a transparent shock tube system allows for direct observation of the entire process during the experiment, including inception and collapse of cavitation bubbles.

Analytical methods

Although it is well accepted that a quasi-static approach is suitable for ship grounding and collision analyses, structure inertial forces involved in UNDEX are much higher than resistant forces and, consequently, cannot be neglected when deriving analytical solutions. Among the earliest theoretical works, Taylor's one-dimensional FSI theory (Taylor, 1963) is a well-known and a widely adopted approach due to its simplicity and effectiveness. The major finding is that the momentum transferred to the plate could be substantially reduced by decreasing the plate areal mass or its acoustic impedance due to the FSI.

Among the most important works over the past decade, Schiffer and Tagarielli (2014) proposed an analytical model to predict the response of circular, fully clamped, orthotropic elastic plates loaded by a planar, exponentially decaying shock wave in water. The model considers the propagation of flexural waves in the plates as well as fluid-structure interaction prior and subsequent to water cavitation. Expressing the unavailability of closed-form analytical solutions for fully coupled FSI problems, the authors attempted a numerical approach that leads to geometry-specific results. They determined that the initial phase of response is dominated by the mode shape associated with the lowest vibration frequency. These analytical predictions were then successfully compared to those of detailed dynamic FE simulations and later to laboratory-scale experiments (Schiffer & Tagarielli, 2015).

Fluid-structure interaction solutions for the water blast response of marine composite sandwich panels with crushable foam cores were presented by Hoo Fatt and Sirivolu (2017). Reflected and radiated acoustic pressure waves were introduced using Taylor's FSI method into Lagrange's equations of motion for the sandwich plate and a resulting matrix differential equation system was solved numerically. The predicted elastic-plastic transient response of the panel from the proposed model was shown to be fairly consistent with results from ABAQUS/Explicit.

While Taylor's model predicts well for higher areal mass density plates, it fails to capture the FSI phenomenon accurately for low areal mass density plates. Kishore et al. (2020) derived an analytical model for immersed plates subjected to near field dynamic loads, addressing these shortcomings. The model compares well with the experimental results of a submerged

aluminum plate subjected to shock loading by predicting with great accuracy the pressure–time history of the plates' reflected pressure and transmitted pressure.

Sone-Oo et al. (2020) discussed the applicability of Taylor's theory to assess the underwater blast response of composite plates. The applicable limit of the approach was exposed in terms of the time ratio between the decay time of the loading and the plate in-air swing time as well as in terms of a FSI parameter that relates decay time and areal mass. Although the early-time interaction effect is properly accounted for, the late time response involving water inertial forces is not considered and Taylor's theory tends to underestimate the structural response. That is why Brochard et al. (2018) coupled a plastic-string-on-plastic-foundation model initially proposed by Hoo Fatt and Wierzbicki (1991) for air blasts with a two-step impulse-based approach for assessing the plastic damage of an immersed metallic cylinder subjected to an UNDEX primary shock wave. Here, the long-time interaction is considered through the introduction of a water added mass calculated in the cylinder damaged area. The method was later extended to deeply immersed cylinders, for which the action of hydrostatic pressure is of highest importance (Brochard et al., 2020). In the same way, Sone-Oo et al. (2021a) coupled closed form solutions for orthotropic rectangular panels subjected to UNDEX shock waves with a two-step approach to model both early and long-time fluid structure coupling. The internal mechanics solver, initially limited to small shell deflection, was later extended to large displacements and, at the same time, coupled with a Doubly Asymptotic Approximation solver to improve fluid structure interaction modelling (Sone Oo et al., 2021b).

Numerical methods

In the defence domain, national codes capable of capturing the full range of coupled explosion and target interactions exist. These numerical tools typically require a high level of computational resources and are available only for defence applications. Outside of defence applications, LS-DYNA and ABAQUS have been used to capture underwater explosion effects. This can be accomplished using either an acoustic-type or Eulerian fluid approach.

The acoustic approach is effective for far-field loading and is computationally efficient. With the development of Doubly Asymptotic Approximations (DAAs) during the 1970s by Geers (1978), the paradigm for treating UNDEX problems was shifted to a new era. DAAs have been implemented in Underwater Shock Analysis (USA) code and then incorporated into various commercial finite element tools such as LS-DYNA and DYTRAN (see DeRuntz, Jr. 1989). These time domain differential equations approach exactness at both high and low frequencies and allow for a smooth transition in between. They are expressed in terms of wet surface variables only, so it is not needed to explicitly model the surrounding fluid; however, such acoustic-type approaches encounter difficulties in capturing the effects of near-field explosions as well as cavitation. For example, Sone-Oo et al. (2021b) demonstrated that the DAA approach is accurate only for scenarios where bulk cavitation is negligible; that is, when the shock wave decay time is long compared to the plate response time.

The use of Euler type approaches has the advantage of directly capturing pressure and explosively generated gas bubble effects. These methods require Equation of State (EOS) parameters for the explosive material, water, and if relevant, air. They are however numerically challenging due to the extensive computational requirements of a large 3D water domain, as well as difficulties in achieving accurate and efficient fluid-structure coupling. In Wang et al. (2016), a simple method to determine the mesh size for numerical simulations of near field underwater explosion was developed. To this end, the mesh size effects on the shock wave propagation of underwater explosions were investigated for different charge weights, through which the correlation between mesh sizes and charge weights was identified. The proposed meshing rule allowed for adequate balance between solution accuracy and computational efficiency. Shams et al, (2017) proposed a modeling framework to investigate the two-dimensional, nonlinear hydroelastic response of thin composite structures. Panel dynamics were described using

nonlinear Euler-Bernoulli beam theory incorporating von Kármán nonlinearity. Potential flow theory was used to model the fluid flow, and a closed form solution was established for the hydrodynamic pressure as a function of the panel acceleration. A Galerkin discretization method was then implemented to cast the problem into a set of nonlinear ordinary differential equations, which were solved using a polynomial set of basic functions. In the same way, a coupled method utilizing advantages of the Runge-Kutta Discontinuous Galerkin scheme and finite elements was developed by Zhang et al. (2018) to investigate pressure characteristics and cavitation effects of near-field underwater explosions of cylindrical charges near single/double plates. Effects of both the plate thickness and the distance between the charge and the plate on pressure and cavitation characteristics were analyzed. Finally, Wu et al. (2020) utilized the Local Discontinuous Galerkin (LDG) method to capture the propagation of the shock wave in the fluid domain and employed the pressure cut-off model to calculate cavitation effects. The proposed model was used to investigate the interaction between an UNDEX shock wave and a submerged sphere. The LDG method was shown to better capture the shock discontinuous wave than the traditional acoustic approach.

4.4.4 Fires

Ryu et al. (2021) present transient thermal elastic-plastic large-deformation finite element models for the analyses of heat transfer and fire-induced progressive collapse behaviour of steel stiffened plate structures. They examine structures with and without passive fire protection. The numerical models were validated against full-scale test data. Paik (2020a) presents CFD models for predicting gas cloud temperature time histories in fires. Paik (2020b) presents computational models for structural crashworthiness analysis in fires. He discusses one-way and two-way models, citing that two-way models provide more realistic results.

4.5 Material Failure Criteria

Fracture criteria that account for stress state have become standard in the marine community to assess ductile fracture scenarios. The common assumption is that failure occurs in the plate field primarily under tensile states; thus, most advancements in developing fracture criteria have focused on corresponding stress states. In contrast, failure in out-of-plane shear-dominated loading states is a relatively unexplored territory in the context of shell elements. The probability of this failure mode increases with the decreasing ductility characteristic to high and extra-high strength steels.

Recent work by Woelke (2020) presented a constitutive model for shell elements that is tied to void fracture mechanics models. The work includes a careful consideration of calibration to test data as well as an energy-based method to account for element size effects. A remaining challenge is the development of analytical approaches for capturing through-thickness shear in the context of shell elements. Furthermore, simulations by Atli-Veltin et al. (2016) showed that fracture onset in maritime crash analysis is not limited to tensile loads and can equally well occur under lower triaxialities. Therefore, Kõrgesaar (2019) analyzed the quantitative effect of the low stress triaxialities on large-scale FE crash simulations with different fracture criteria. The simulation results with different criteria under membrane deformations (tensile loads) were quite consistent, while the results were far less consistent when the fracture occurred under lower triaxialities. The lower triaxialities were shown to prevail in stiffened structures. Therefore, it was suggested that future investigations and benchmark analyses be designed to evoke lower stress triaxialities, which would better reveal the limits of the fracture criteria. In the same study by Kõrgesaar (2019), the history of deformation and how this is interpreted by failure criterion was shown to have a strong influence on the analysis results. For instance, simulations with two stress state dependent fracture criteria that provided the same failure strain, but accounted damage history differently, led to very different force-displacement curves. Therefore, as a practical guideline, investigations should always report whether the used fracture criterion accounts for deformation history or not.

Recent developments in failure criteria have been geared towards a better identification of failure modes. For instance, Woelke et al. (2018) discuss the difference between fracture behavior of thin sheets under plane strain bending and tension as well as showcase how fracture initiation could be delayed under bending dominated loads. Pack and Mohr (2017) and Costas et al. (2019) developed approaches that can distinguish between membrane and bending deformation. The approach by Pack and Mohr (2017) was shown in Cerik et al. (2019) to give consistent element size independent results for a stiffened plate ruptured under membrane tension. The Pack and Mohr approach offers a middle ground between accuracy and calibration. First, a fracture locus is calibrated with different material tests on top of which a localization curve is added. The latter is relatively straightforward and can be automated once the fracture locus has been calibrated. The two approaches (i.e. Pack and Mohr (2017) and Costas et al. (2019)) that can distinguish between membrane and bending deformation mode were also employed by Kõrgesaar and Storheim (2020) in the numerical fracture simulations of different structural components relevant to marine structures. In these simulations the range of stress states was not limited to tension. In contrast to Cerik et al.'s results (2019), these simulations showed that the Pack and Mohr approach did not yield better accuracy compared to approaches that do not distinguish deformation modes. The probable reason for decreased accuracy is accumulation of deformation under stress states where a localization curve is not defined (stress triaxiality < 1/3). Instead, a Cockcroft–Latham failure criterion that was extended by bending mode indicator to account for bending damage Costas et al. (2019) gave the least scatter among different analyzed cases. This preliminary study should be extended with experimental verifications and consideration of additional fracture criteria used in the community (e.g. BWH).

Accounting for mesh size effects in capturing different deformation modes and fracture is an important aspect that continues to be investigated; e.g. by Wiegard and Ehlers (2020). As the mesh size increases, the strain at failure decreases due to the increased volume of lower strain material away from the crack. For cases where necking is well defined, e.g. plane strain tension, averaging approaches weighting material inside and outside the neck are effective. However, for cases where a necking occurs due to shear localization or is even suppressed (bending), this procedure is less well understood. Furthermore, the role of strain rate in mesh size dependency is unclear. Therefore, further efforts into the role of stress triaxiality and strain rate are required.

Kõrgesaar et al. (2021) presented a python routine called 'WELDINP' to identify the weld zone in ABAQUS models by automatically identifying structural intersections. This is especially useful for special treatments in fracture modelling near welds and material modelling in the heat affected zones.

Increasing marine operations in Arctic regions have stimulated the interest in fracture modelling with shell elements at low temperatures. Noh et al., (2018) validated the plasticity model of F-grade marine structural steel with drop-weight impact tests and showed that FH32 material remained ductile even at −60°C. In experiments, no fracture took place, so no fracture model was implemented. Their numerical simulation accuracy increased when strain rate effects were included in the plasticity model. As a further development they foresee a ductile fracture modelling approach tailored for low temperatures considering strain rate effects. The effect of low temperatures (down to −90°C) on fracture ductility under different stress states has been investigated by Tu et al. (2018) and Perez-Martin et al. (2019). Although they didn't work with marine grade structural steel, they report that the effect of low temperatures on the fracture locus is insignificant compared to room temperature fracture locus (see Figure 7). Cerik and Choung (2020) performed numerical simulations with steel grillages assuming three different material grades (DH32, DH36 and EH36) at three temperature levels (−50°C, −30°C, and room temperature). Necking criterion used in simulations is calibrated based on the tensile tests performed by Min et al. (2013), which showed improved work hardening characteristics and higher fracture strain at lower temperatures. This enhanced ductility reveals itself also in the grillage simulations, leading authors to the same conclusion reached by Ehlers and Ostby

(2012) that crashworthiness improves at low temperatures. Nevertheless, in both studies, crashworthiness was assessed only numerically without experimental verification. Whether extrapolation of quasi-static tensile test results lends itself for characterization of actual crashworthiness of steel structure with all its structural imperfections and material inhomogeneities (HAZ) remains to be answered. The HAZ caused inhomogeneities on crashworthiness of sandwich plates were numerically investigated by Berntsson et al. (2019) and Kõrgesaar et al. (2019) who varied the material parameters in the heat affected zone, which had a marked effect on the crashworthiness. Similar variations in response are possible at low temperatures caused by the differences between weld and base metal as well as ductile-to-brittle transition. This notion is supported also by experiments by Kim et al. (2016) who performed drop impact tests at -60°C. The unstiffened plates remained intact, but stiffened plates fractured in a brittle manner exhibiting ductile-to-brittle behavior. Ductile-to-brittle transition was also observed in full-scale collapse testing of stiffened plate structure by Paik et al. (2020b). The two most important conclusions from their analysis are that i) the failure modes of steel plated structures under axial compressive loads at cryogenic condition are totally different from typical collapse modes at room temperature, and ii) advanced computational models for structural crashworthiness at low temperature are needed. First efforts regarding the second point were taken by Mokhtari et al. (2021) who conducted thermal analysis with EH36 grade steel subjected to non-spreading cryogenic spills. Such basic investigations attempting to explain the underlying physics will eventually provide a pathway to better computational models applicable to large-scale.

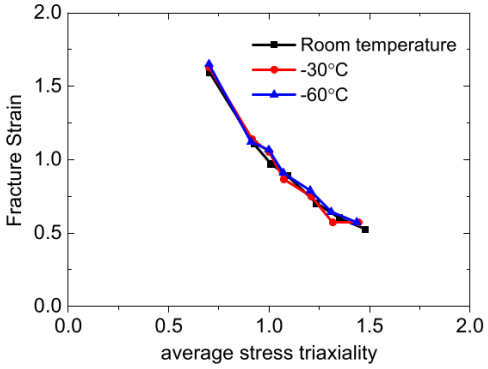

Figure 7: Fracture strain versus average stress triaxiality at different temperatures (Figure adopted from Tu et al., (2018)).

All of the aforementioned fracture models discussed above require calibration – i.e., determination of the material parameters that are used in the numerical model. This is an expensive process, and the specific material properties are often not available in design and analysis phases, so having some pre-existing calibrated values would be of tremendous use for industry. There have been recent attempts at publishing material parameters. For example, Paik et al. (2017) published plasticity and basic failure data for several materials that are of use in the maritime industry. Notably, Cerik et al. (2019) performed a calibration of a ductile failure locus for DH36 steel and compared it with two other calibrations from the literature. The fact that these three calibrations did not match indicates that test data from one steel cannot be readily applied for another steel – even if they are the same nominal grade and quality. These published values may nevertheless be useful references for designers who do not yet have direct access to the steels to be used for their structures.

Given that in simulation of marine structure components localization is often a better indicator of fracture onset than a fracture criterion determined with tensile tests (due to the large element size), simulation accuracy could be improved by stress state dependent localization criteria. For example, the Pack-Mohr approach (Pack & Mohr, 2017) is extended by consideration of localization at lower stress triaxialities.

5. RECENT AND UPCOMING ALS RESEARCH AREAS

This chapter reviews recent ALS related publications pertaining to new and emerging research areas. It identifies knowledge gaps, and where applicable, guidance and recommendations are provided.

5.1 Introduction

The future of maritime transport and utilization will bring new types of accidents, or re-shape the causes and consequences of familiar ones through the development of technology, climate change, changes in societal behaviour, and/or economic drivers. For example, Inmarsat (2021) reports that climate change raises concern about the safety of vessels in the future, citing "Climate change and the impact of extreme weather conditions are a growing cause for concern in the maritime sector. It is notable that all three years of data show a consistent rise in distress signals during November and December, which are months known for bad weather in the northern hemisphere." One particular consequence of this is that relatively small fishing vessels will be affected; with Inmarsat (2021) noting that "… fishing vessels consistently rank[ing] in the top two vessel types for distress calls over the three-year period …". Another example of changing accident scenarios as a function of technology development relates to increasing vessel size. Allianz (2021) reports (referring to the Ever Green grounding in March 2021): "As the Suez Canal incident demonstrated only too well, ever-increasing vessel sizes continue to pose a disproportionately large risk with costly groundings, fires and record levels of container losses at sea."

International regulations, goals, and guidelines surrounding allowable ship emissions are rapidly changing. Since January 1, 2013, the International Maritime Organization (IMO) has required a minimum energy efficiency level per capacity mile (e.g., tonne mile) for various types of commercial ships. Ever tightening (every 5 years) Energy Efficiency Design Index (EEDI) criteria are drivers of change for new build ships. IMO's new regulation IMO2020 came into effect Jan. 1, 2020, which limits the sulphur in fuel oil to 0.50% (mass by mass); which leads to reduced sulphur oxide (SOx) emissions. Important research into alternative fuels and methods of propulsion is underway for future new build ships. Presently, the IMO's Energy Efficiency Existing Ship Index (EEXI) is driving change to lower emissions for existing ships. Novel propulsion technologies under development in response to mandated emissions reductions will bring a need for new considerations about ship structural design and safety. McKinlay et al. (2021) present a case study comparing the volume and mass and design considerations of different energy sources providing 9270 MWh; namely LNG, diesel, hydrogen (gas), hydrogen (liquid), metal hydride, ammonia, methanol and Li-ion batteries. They found the three most promising candidates to be hydrogen, ammonia, and methanol; due to their potential to produce emission free electricity via a fuel cell. Other works often cite ammonia as a high-density and low-cost hydrogen carrier (Baldi et al., 2019). The accidental scenarios associated with the storage and use of these alternative fuels requires further study.

Rising interest for autonomous and/or remote-controlled surface ships and related shore control centres will bring a new set of challenges in unmanned ship operations exposing ships and maritime traffic, in general, to possible accidents. Wahlström et al. (2015) list possible problems due to human mistakes in remote control centres, such as information overload, boredom, mishaps during changeovers and handoffs, lack of feel of the vessel, constant reorientation to new tasks, delays in control and monitoring, and the need for human understanding in local knowledge and object differentiation (e.g., in differentiating between help-seekers and pirates). This list may be expanded with incompatibilities of monitoring systems, cyber attacks, lack of redundant systems on board the vessel, etc.

The European Council for Maritime Applied R&D (ECMAR) aims for zero-emission and zero-accident ships, see e.g., ECMAR position paper (ECMAR, 2017), while recognizing new challenges: human-machine interfaces, new offshore energy harvesting facilities, marine

biotechnology, arctic technologies, cyber security, etc. Adding to that, completely novel structures may exist in the future. Drummen and Olbert (2021) presented a conceptual design of a modular floating multi-purpose island, in response to the problems of increasing population, rising water levels, and the need for additional space for food growth and energy harvesting. The implementation of such new technologies must necessarily require the definition of the new associated hazards and risks.

Future concerns might well bring challenges like those recognized in the ongoing COVID-19 pandemic, such as: human errors due to crew fatigue, reducing operation costs at the expense of safety, cargo damage due to delays, and maintenance problems and breakdowns (Prosertek, 2020).

A review of the recent research efforts addressing some of the ALS concerns for the mentioned challenges is presented below.

5.2 Collision Avoidance

As mentioned above, ship collision is a significant threat to maritime safety. Further, autonomous ships are now a reality, with the successful first voyage of the MV Yara Birkeland (Schuler, 2021). Autonomous surface ships have a potential to reduce the costs and risks of maritime transport, however upcoming challenges are still enormous: from the technological transition required for a ship to operate autonomously, to legal requirements and societal changes to be addressed.

With the rise of machine learning algorithms and big data analytics, particularly in the line of rising interest in autonomous vessels development, there is growing research interest in intelligent systems in the service of ship collision avoidance. One research direction is oriented toward the minimization of ship collision risks. Abebe et al. (2021) developed a machine-learning estimation of ship collision risk based on collision risk index and gradient boosting regression (GBR) model. Zhang et al. (2020) proposed a method for detection of ship collision risk using convolutional neural network model (CNN) for interpretation and classification of ship-ship collision risks in encounter scenarios, based on recognition and interpretation AIS based image data. Wang et al. (2019) proposed a deep reinforcement learning obstacle avoidance decision-making (DRLOAD) algorithm for unmanned ship navigation in unknown environments. This paper addresses the fact that the marine environment is complex and volatile and that there is a need for an anthropomorphic decision-making algorithm learning from seafarers' experience. A simulation environment model was generated, as well as the sensor model and avoidance reward function.

Another research direction considers ship trajectory prediction as a tool for ship collision avoidance and ship maneuvering in restricted environments. Zhao et al. (2022) presented AIS data supported ship trajectory prediction using Empirical Model Decomposition (EMD) based on a machine learning framework. Shen et al. (2019) used a systematic approach in application of deep Q-learning applied to automatic collision avoidance, particularly in restricted waters, both by numerical simulations and experimental test. They demonstrated that deep reinforcement learning (DRL) has great potential in automatic collision avoidance actions. Ozturk et al. (2019) presented novel methodology to assess the navigational collision risk (NCR) in port based on machine learning and fuzzy inference. Simulation results were validated by ship-handling simulations performed by 20 expert pilots and tested in a port approach maneuvering scenario. Authors indicate the possible application of the methodology in auto-berthing systems and in cooperative collision avoidance situations. Zhao and Roh (2019) point out that "Developing a high-level autonomous collision avoidance system for ships that can operate in an unstructured and unpredictable environment is challenging." In their paper they proposed a method aimed to overcome the multi-ship collision avoidance problem based on a DRL algorithm. In their study, ships can autonomously decide to avoid collision while complying the COLREG requirements. Their proposed method indicates successful collision avoidance

performance. Zhang et al. (2019) discuss decision-making for the autonomous navigation of maritime autonomous surface ships in an uncertain environment. A decision-making system based on hierarchical deep reinforcement learning is proposed, consisting of two layers: the scene division layer and an autonomous navigation decision-making layer. In performed simulations obstacles such as ships, breakwater and shore bank were simulated in the environmental model.

Along with the most recent papers listed above, a comprehensive state-of-the-art review of the collision-avoidance navigation systems for Maritime Autonomous Surface Ships (MASS) is presented by Zhang et al. (2021). A summary of guidance documents is listed, as well as major advancements in maritime collision-avoidance navigation technologies and systems. Existing and prototype maritime autonomous surface ships are presented in a table form. Another literature survey, presented by Burmeister and Constapel (2021), considers collision avoidance and path planning. It investigates methods based on artificial intelligence, data-driven methods based on machine learning, and other data science approaches. It separately treats collision avoidance and motion and path planning. Both review articles from Zhang et al. (2021) and Burmeister and Constapel (2021) provide a comprehensive list of contemporary results in this growing research field.

5.3 Offshore Wind Turbines

Offshore wind turbines are at the forefront of the green transition. The number of offshore wind turbine installations, including both bottom fixed and floating types, is expected to grow at record speed in the coming decades. Energy coming from the wind and the sun are the two key sources of renewable energy recognized by the International Energy Agency (IEA) in the forecast of global energy production till 2050 in the IEA “Net Zero by 2050” report (IEA, 2021). IEA forecasts solar power to increase 20 times and wind power 11 times until 2050; becoming leading sources of electricity before 2030 and generating globally nearly 70% of electricity in 2050. International Renewable Energy Agency (IRENA) forecast a total of 4% of global power generation will come solely from offshore wind production plants, rising from approximately 20GW in 2018 to 520GW in 2050 (IRENA, 2018). At the same time, turbine size and capacity factors are constantly increasing. Offshore wind farms are often located near the coast close to traffic lanes and are exposed to the risk of collisions from visiting and passing ships due to human errors, unsuccessful avoidance maneuvers or free drifting of vessels following a propulsion damage. The challenges for ship-OWT collision analysis lie in the multidisciplinary nature of the problem including interactions of hydrodynamics, structural mechanics, and aerodynamics. Each of the three aspects requires considerable efforts for modelling accuracy. In addition, different designs of foundations exist for offshore wind turbines either bottom fixed or floating, and their performances under ALS loads may differ as well. Design standards for the ALS design of offshore wind turbines are not established. More research efforts are needed.

Jensen et al. (2018) pointed that while typical offshore wind farms are likely to use bottom-fixed foundations for years to come. Floating structures makes it possible to go even further offshore or use deeper locations, indicating the need for future research efforts in that direction. Yang et al. (2021) investigated mooring breakage effects of a 5MW barge-type floating offshore wind turbine. They concluded that the remaining mooring lines are able to take over the additional load so that mooring system is not at risk of progressive failure. Even so, notable changes in the platform sway and yaw motions are noticed. Yue et al. (2021) proposed a novel, fractal cross section of a fender structure protecting the tripod of the offshore wind turbine (OWT) and investigated its anti-collision performance. Model validation was done under the collision conditions involving a 5000t ship with a 2 m/s velocity. Collision resistance performance was tested for protection devices with different fractal order and both structural response and top OWT acceleration was examined. Jia et al. (2020) studied the response of a 4 MW offshore wind turbine under a collision load from the berthing of a maintenance ship as well as due to operational loads: wind, sea current and waves. Environmental parameters were used as

input in the test for normal operating conditions and further research is suggested for other load cases such as starting, stopping, idling, operation with fault, and so on. Han et al. (2019) studied anti-collision performance of a protective fender during collision of a ship and tripod foundation of an offshore wind turbine. Different material layouts for the fender were considered, namely rubber and aluminium foam inside of cylindrical steel plating. A 2500 t ship was considered in collision analysis with different initial speeds. In addition, a coefficient of restitution was defined to examine the progression of plastic deformation with the increase of ship velocity. Song et al. (2021) made a comparison of numerical and analytical methods of analysis of impact of a ship with a monopile-supported offshore wind turbine. A number of collision scenarios were analysed considering wind direction, wind speed, aerodynamic damping and other factors. Among these, impact velocity and wind direction affected the wind turbine response significantly. Further research is proposed for consideration of hydrodynamic loads, as well as floating wind turbines.

5.4 Floating Bridges

Following the pioneering work from Sha et al. (2017) and Moe et al. (2017), Sha et al. (2019) examined local and global responses of a floating bridge under ship-girder collisions. The finite element method was applied in a study of collision between a deformable ship structure and a floating steel box girder shaped bridge. The paper examines the local and global responses to determine the ratio of energy absorbed locally through elastic and plastic deformation, and the energy dissipated by the global bridge motion.

As bridges become more ambitious, there is a greater chance that they will face collision with ocean-going ships and boats. Motivated by Norway's ambitious plan to span fjords with floating bridges, Storheim et al. (2018) did an analysis of a potential submarine collision with the cables that might be used to support one span with a tension-leg platform.

5.5 LNG Leakage

Galierkova et al. (2021) studied maritime accidents with hazardous substances involving chemicals belonging to two groups: Hazardous and Noxious Substances (HNS) and oily substances. They point out that, while HNS spills are far less common than the oil spills, they have a potential to be more dangerous. In addition, oil spill consequences may be predicted with a certain level of confidence while HNS spills may vary significantly from one case to another. Cao et al. (2021) performed a safety analysis of a vent mast on an LNG powered ship during a low-temperature combustible gas leakage accident. Simulation of an LNG vapour cloud diffusion was carried out using the CFD method. Both concentration of gas and temperature field distribution were examined, and potentially dangerous areas were identified. They concluded that the proposed method could be used as a tool for determination of layout of equipment modules, optimization of leakage and dispersion detection systems and other uses. Jiao et al. (2021) performed extensive research on contemporary scientific contribution (2005-2019) to LNG safety related to quantitative risk assessment, LNG evaporated gas and other topics. A knowledge map analysis was created by examining Web of Science data, through the process of identification, screening, and eligibility. The aim of the study was not to point out specific papers but to reveal the existence of a total of 1122 articles published in 509 different journals considering the topic of LNG safety. The paper lists top 14 prolific journals with more than 10 LNG safety articles published, displays co-authorship networks, and lists the top 8 critical authors in LNG safety research. As such, the paper provides valuable information on the worldwide distribution of LNG safety knowledge. Iannaccone et al. (2021) performed numerical simulations of LNG tanks exposed to fire. A two-dimensional CFD model was developed, validated, and extended to large-scale tanks simulating fire engulfment scenarios. Time evolution of condensation and evaporation, as well as temperature contour plots are presented. The paper highlights the influence of thermodynamic and geometrical features over the spatial distribution of evaporating zones and temperature fields inside cryogenic tanks and indicates the need and direction for

further research. Park (2019) investigated the development of a design reference stress for determining ultimate crushing capacity of a membrane-type LNG cargo containment tank; specifically, the NO96 type. Crushing of a multi-material membrane-type structure due to the action of a sloshing load was examined numerically, using a nonlinear FE method. Load capacity of the bulkhead intersections was evaluated via a bending capacity assessment. The paper indicates the need for future studies of crushing failure at the LNG operating temperatures.

5.6 Fish Farming

FAO technical paper 549 (Kapetsky et al., 2013) indicated large, unrealized offshore mariculture potential from a spatial perspective. Another view of unrealized offshore mariculture potential relates to divorcing offshore installations from their present dependence on being moored. Free-floating and propelled installations represent offshore mariculture potential for the future. Global aquaculture production more than tripled in live-weight volume from 34 Mt in 1997 to 112 Mt in 2017, of which freshwater fish account for 75% of global edible aquaculture volume (Naylor et al., 2021), supporting the FAO conclusions. Holen et al. (2019) studied major accidents in Norwegian fish farming, such as explosion, fires, emissions/release, damage to structure, failure of life support and loss of well control. Among others, they concluded that risk management in fish farming must include major accident prevention strategies in addition to the management of long-term risk and sustainability during fish production. Safety4Sea (2018) lists primary reasons for ship collision with fishery farms, following 71 fisher farm entry claims in China alone, in 2017. However, the existing research effort is not proportional to the challenges related to fish farm safety.

Due to limited nearshore areas and its great impact to local ecosystems, the aquaculture industry is moving fish farms into more exposed sea regions where the environmental conditions are much more severe. However, harsher environmental loads and frequent aquaculture operations imply risk for accidental actions, such as ship collisions or extreme wave loads, where damage potential and possible consequences can be severe. The accidental actions may lead to undesired fish escape, which will cause major economic loss for the fish farming industry and is considered to have negative impact on the wild stocks. The designs of fish farming cages vary considerably from traditional flexible cages with plastic floating collars, to semi-flexible and 'rigid' cages. Examples can be found from two new designs of offshore aquaculture cages in Norwegian waters, the 'Ocean Farm 1' semi-submersible fish farm and the 'Havfarm1' ship-shaped fish farm. Design standards of offshore fish farms against accidental actions are lacking, and relevant research work is very limited as well. A recent work was carried out by Yu et al. (2019), where local and global responses of the Ocean Farm 1 semi-submersible fish farm subjected to collisions from a supply vessel was investigated. The fish farm structure was found to absorb most of the impact energy. Possible penetration of the net is indicated. The residual strength of the damaged fish farm to wave loads remains to be assessed. More research work on the analysis and design of different fish farm concepts under accidental actions is needed.

5.7 ALS and Resilience for Low- and Non-ice-class Ships Subject to Ice Impact

Accidental glacial ice impact (e.g., with an iceberg, growler, or bergy-bit) is a classic ALS scenario for low- and non-ice-class ships, as well as offshore structures (e.g., FPSOs operating in glacial ice infested waters). New ALS scenarios for these structures are emerging that are the result of predicted change in the operational environment in polar ice-covered waters. Many recent works have predicted and documented the ongoing decline in polar ice cover. This has incited increased focus on potential for polar resource extraction and transportation routes. As such, many more ships and potentially offshore structures are forecast to be operating in polar waters in the coming years. Due to the remoteness, lack of infrastructure, lack of search and rescue, and other challenges particular to the polar regions, new accident scenarios (amongst other scenarios) may give rise to the need for low- and non-ice-class ships to operate in marginal ice conditions. A relatively timely example of a new polar waters accident scenario that

may require the assistance of low- and/or non-ice-class ships is the evacuation of a cruise ship with thousands of people onboard. High-ice-class ships are relatively few in number and may not have the capacity to handle thousands of survivors; or may be too far away to assist in a timely manner. Environmental pollution scenarios (e.g., oil spill in marginal ice zones) are another potential accident scenario, among others (known and yet to be determined).

There are two related emerging areas of research: new accident scenarios associated with increased presence of ships and offshore structures in polar waters; and the resilience of low- and non-ice-class ships operating in ice. Regarding the latter, intentionally operating a ship in an environment that may induce ALS-like structural responses is, by definition, not an "accident scenario" (as this was done with intention). It is, rather, a question of ship structural "resilience". Analysis of structural resilience to ice loads for low- and non-ice-class ships is much more complex than the analysis required to design a hull to support ice loads, because the former ship types may violate some of the underlying design assumptions for ice-class ships, i.e.: their bow waterline normal frame angle is likely insufficient to induce flexure and/or roll/pitch in the impacted ice feature; their hull steel may not have sufficient ductility at operating temperatures in polar waters; their frame spacing may be large, they may not be able to effectively manoeuvre at low speed, etc.

In consideration of the resilience of low- and non-ice-class ships to ice loads, Dolny (2018) presents a methodology for assessing the structure of low-ice-classed ships to ice impact loads, with the goal of determining a "safe speed" that does not unduly impair the resilience of the ship. This work is based on Daley's (1999) update to Popov et al.'s (1967) impact and collision mechanics model which assumes that all motions are the result of an impulse along the normal to the hull at the point of collision. That method accounts for hydrodynamic added mass using constant assumed values, but does not consider sliding friction, hull curvature or buoyancy forces. Dolny's method (2018) defines an ice interaction scenario, then solves the mechanics of the ship-ice collision process which requires ice strength models for both ice crushing and flexural failure modes, and finally iterates through structural strength models to define limit conditions to predict a safe speed envelope. Dolny's method (2018) method improves on Daley's (1999) method by including modifications for steep normal frame angles and an updated ice flexural failure limit model that includes ice compression due to horizontal impact force, friction and dynamic support of the ice by the water foundation (based on work by Daley and Kendrick (2011) and Sazidy (2015)). Bobeldijk et al. (2021) used Dolny's method (2018) to determine the ice impact load on a non-ice-strengthened naval vessel and to apply that load as a moving load (2015; 2017) to evaluate three different hull structure designs. Much research is left to do regarding the assessment of resilience of low- and non-ice-class vessels. Some outstanding items are: analytical methods for a shared-energy approach for ice impacts (some progress by Price et al. (2021)) – including shared-energy analytical approaches for sliding ice impacts (e.g., by extending Liu et al. (2019)); development/calibration of numerical deformable ice models including appropriate treatment of spalling; further research into hull fracture response to moving/sliding ice loads (Quinton, 2015) with a view to accounting for the effect of the evolution of plastic states of stress on failure criteria (e.g., as in the benchmark study presented in the appendix below); definition of novel accident scenarios; definition of novel resilience scenarios; further development and calibration of "safe speed" predictions for low- and non-ice-class ships operating in ice.

5.8 Sea and Atmospheric Icing

While not a new or emerging area of research for ships and offshore structures, icing is receiving recent attention for these structures, as well as for offshore wind turbines (for which icing is a relatively new research area). Ice accretion is the accumulation of ice on surfaces from super-cooled water droplets. Ice accretion conditions depend on wind velocity, air temperature, and seawater temperature. In cold offshore environments, ice accretion has two sources, wave generated spray (seawater) and atmospheric wind generated spray (freshwater), with the wave

spray being the main contributor. Ice accretion adversely affects stability and safety of ships and offshore structures. In fact, United States Coast Guard (USCG, 2019) reports that icing conditions most likely played an important role in the sinking of the ship Destination in 2017. Dehghani-Sanij et al. (Dehghani-Sanij et al., 2017a, 2017b) describe other notable historical accidents due to extreme icing, and review past predictive formulas and models, which include droplet trajectories, liquid water content, spray movement, spray duration, mass balance, and heat flux models.

Samuelsen et al. (2017), Dehghani-Sanij et al. (2018), Bhatia and Khan (2019), and Mintu et al. (2019, 2020a, 2020b) present new models or updates for ice accretion prediction. Samuelsen et al. (2017) present a comprehensive dataset for ice accretion that include sea and wind conditions, ship speed, and icing rate, and propose a model based on the collected data. Dehghani-Sanij et al. (2018) develop a three-dimensional model for droplet trajectories of the spray cloud. Bhatia and Khan (2019) propose a probabilistic model based on spray flux and atmospheric temperature. Mintu et al. (2019) study the trajectory of sea spray with a multi-phase air-water simulation, using a smooth particle hydrodynamics computational fluid dynamics model. Mintu et al. (2020a), propose a model for spray flux generation model applicable to vessels of any size and Mintu et al. (2020b) study the frequency at which spray is generated.

Orimolade et al. (2017, 2018), and Mustafa et al. (2019) study ice accretion effects on ships and offshore structures. Orimolade et al. (2017) determine that ice accretion during polar low atmospheric conditions poses a greater safety risk for smaller vessels. Orimolade et al. (2018) studies the effects of icing on a semi-submersible rig and concludes that icing poses more of an operational risk than a safety risk to the rig. Mustafa et al. (2019) discuss risks related to ice accretion for offshore wind turbines from atmospheric and wave generated spray. On a final note, there is gap in recent knowledge related to the effects of ice accretion due to wave generated spray in offshore wind turbines and new studies on the area would be beneficial.

5.9 Implosion Loads

With the increasing presence of subsea systems comes an increased likelihood of hydrostatic pressure driven collapse of structures. Collapse in these cases can manifest itself as an implosion, or rapid collapse of the structure. Implosion generates a pressure load that is imparted to surrounding structures. The mechanics of implosion events have been studied by numerous researchers e.g. Turner & Ambrico (2012), Farhat et al. (2013), and Gish & Wierzbicki (2015). More recently, Kishore et al. (2020) have studied the effects of implosion pulses on nearby structures using digital image correlation (DIC).

5.10 Hydrogen

Although hydrogen adoption is still in its infancy, developments where hydrogen is used as a fuel to propel the ship are expected to increase in the near future. The main issues from safety perspective are the safe storage and use of hydrogen onboard ships. Because of the low volumetric density hydrogen occupies approximately 4 times more space compared to diesel fuels. Therefore, the available space in the ship must be utilized more effectively which can be a challenge from ALS perspective considering current safe distance requirements for storage tanks. Alternative design approaches must increasingly rely on accurate coupled simulation approaches (see Section 4.4.2) as besides the worst-case scenario, the probability of different other realistic scenarios becomes important in comparative analysis. Upon damage, low flash-point fuels such as hydrogen and natural gas, impose the risk of explosion in closed spaces (van Biert et al., 2016). For informed design decisions, multi-physics simulations must be performed including the leakage and explosion of hydrogen in various compartments, e.g. see Mao et al. (2021). Van Hoecke et al. (2021), in their review article, discuss the challenges in the use of hydrogen for maritime applications. With 238 references considered, this paper covers different aspects of hydrogen as an alternative fuel for shipping: including advantages and disadvantages of different hydrogen storage techniques as well as related challenges. Mao et al.

(2021) performed a simulation of hydrogen leakage and hydrogen diffusion as well as consequences of explosion in various compartments on a hydrogen fuel cell ship. Yuan et al. (2021) studied fine water mist application for suppression of hydrogen jet fires on hydrogen fuel cell ships. Vertical and horizontal jet fire scenarios were considered. Among other, they concluded that ambient wind speed is an important factor affecting the suppression effect of a fine water mist on jet fires.

5.11 Airplane strikes on structures

Paik and Park (2020) examined crashworthiness of a floating offshore nuclear power plant hull structure in the case of aircraft strike. The paper lists the advantages of local electrical power production, such as access to remote locations and the possibility of manufacturing in the shipyard (and not on a dedicated site) and lists existing and promising designs. Following this a nonlinear FEM method is applied for simulation of consequences in the case of aircraft collision with hull structure – considering the aircraft engine as a projectile most likely to penetrate double hull structure of the power plant. The paper considers use of ballasting material in the double-hull space as an energy absorbing design solution. Peng et al. (2021) performed a numerical simulation of base-isolated LNG storage tanks subjected to large commercial aircraft crash. While the paper address land-based storage tanks it described systematic numerical simulations for evaluating dynamic responses and damage failure of both structures: LNG tank and aircraft.

6. SUMMARY AND FINAL RECOMMENDATIONS

As per the mandate of this committee, recent research works, and international design rules and standards were reviewed with respect to concern for accidental limit states (ALS) of ships and offshore structures and their structural components under accidental conditions.

The committee considered the traditional accidents of collision, grounding, dropped objects, explosion, and fire on traditional structures, as well as identified work done (or lack thereof) towards assessing their effects on new(er) concepts (e.g., offshore wind turbines, autonomous ships, hydrogen fuel cell propulsion, etc.).

Where appropriate, recommendations and guidance were provided throughout the report. Summarized here are some of areas requiring further research related to accidents and accidental limit states, and hazard and risk identification, that were identified by the committee to be of contemporary and near-future importance: Autonomous ships; alternative fuels; new emissions regulations; ship-bridge collisions; consideration of intelligent human experience-based risk mitigation actions in hazard and risk analyses; the maritime use of batteries; LNG spillage (including effects on structural performance); offshore wind turbine ALS design standards as well as their use further offshore and in deeper waters; the resilience of low- and non-ice-class ships operating in ice; coupled consideration of hydro-plastic slamming; guidance and recommendations for FEA mass-scaling and inclusion of triaxiality based failure criterion for collision and grounding studies; and correlation between CFD fire analysis and practical engineering tools.

7. ACKNOWLEDGEMENTS

The authors would like to acknowledge the contributions of the following individuals to the development of this report:

- Icam Nantes: Chisom Bernard Umunnakwe, Ye Pyae Sone Oo, and Victor De Oliveira
- Memorial University of Newfoundland: Ahmed Youssri Elruby, and Sthéfano Lande Andrade
- TU Delft: Lucie Roussel
- Tallinn University of Technology: A. Sults

REFERENCES

AASHTO. (2009). *American Association of State Highway and Transportation Officials: Guide Specifications and Commentary for Vessel Collision Design of Highway Bridges*.

Abebe, M., Noh, Y., Seo, C., Kim, D., & Lee, I. (2021). Developing a Ship Collision Risk Index estimation model based on Dempster-Shafer theory. *Applied Ocean Research*, *113*, 102735. https://doi.org/10.1016/J.APOR.2021.102735

Abilio Ramos, M., Thieme, C. A., Utne, I. B., & Mosleh, A. (2020). Human-system concurrent task analysis for maritime autonomous surface ship operation and safety. *Reliability Engineering & System Safety*, *195*, 106697. https://doi.org/https://doi.org/10.1016/j.ress.2019.106697

Abilio Ramos, M., Utne, I. B., & Mosleh, A. (2019). Collision avoidance on maritime autonomous surface ships: Operators' tasks and human failure events. *Safety Science*, *116*, 33–44. https://doi.org/https://doi.org/10.1016/j.ssci.2019.02.038

Abrahamsen, B. C., Alsos, H. S., Aune, V., Fagerholt, E., Faltinsen, O. M., & Hellan, Ø. (2020). Hydroplastic response of a square plate due to impact on calm water. *Physics of Fluids*, *32*(8), 82103. https://doi.org/10.1063/5.0013858

ABS. (2013a). *Guidance Notes On Accidental Load Analysis and Design for Offshore Structures*.

ABS. (2013b). *RULES FOR BUILDING AND CLASSING FLOATING PRODUCTION INSTALLATIONS 2014* (p. 618). American Bureau of Shipping.

ABS. (2021). *Guidance Notes on Nonlinear Finite Element Analysis of Marine and Offshore Structures*.

Ahvenjärvi, S. (2016). The Human Element and Autonomous Ships. *TransNav, the International Journal on Marine Navigation and Safety of Sea Transportation*, *10*(3), 517–521. https://doi.org/10.12716/1001.10.03.18

Allianz. (2021). *Safety and Shipping Review 2021: An annual review of trends and developments in shipping losses and safety*. https://www.agcs.allianz.com/content/dam/onemarketing/agcs/agcs/reports/AGCS-Safety-Shipping-Review-2021.pdf

Alsos, H. S., Hopperstad, O. S., Törnqvist, R., & Amdahl, J. (2008). Analytical and numerical analysis of sheet metal instability using a stress based criterion. *International Journal of Solids and Structures*, *45*(7–8), 2042–2055. https://doi.org/10.1016/J.IJSOLSTR.2007.11.015

Amdahl, Jørgen. (2019). Impact from ice floes and icebergs on ships and offshore structures in Polar Regions. *IOP Conference Series: Materials Science and Engineering*, *700*(1), 12039. https://doi.org/10.1088/1757-899x/700/1/012039

Amdahl, Jørgen, & Holmas, T. (2016). ISUM for Offshore Frame Structures. In *ASME 2016 35th International Conference on Ocean, Offshore and Arctic Engineering*. https://doi.org/10.1115/OMAE2016-55053

Amdahl, Jørgen, & Yu, Z. (2021). *Design against ship collisions in accordance with the new DNV RP C204*.

Andrade, S. L., Quinton, B. W. T., Daley, C. G., & Gagnon, R. E. (2020). Numerical Study of Large Pendulum Ice Impact Loads. In *ASME 2020 39th International Conference on Ocean, Offshore and Arctic Engineering*. https://doi.org/10.1115/OMAE2020-19068

API RP 14J. (2001). *Recommended Practice for Design and Hazards Analysis for Offshore Production Facilities 2nd Edition* (p. 90). American Petroleum Institute (API).

API RP 2A. (2014). *Planning, Designing, and Constructing Fixed Offshore Platforms—Working Stress Design; Twenty-Second Edition*.

API RP 2FB. (2006). *Recommended Practice for the Design of Offshore Facilities Against Fire and Blast Loading, 1st Edition* (p. 74).

API RP 2MET. (2019). *Derivation of Metocean Design and Operating Conditions* (p. 280).

Atkins, A. G. (1988). Scaling in combined plastic flow and fracture. *International Journal of Mechanical Sciences*, *30*(3–4), 173–191. https://doi.org/10.1016/0020-7403(88)90053-7

Atkins, A. G. (1999). Scaling laws for elastoplastic fracture. *International Journal of Fracture*, *95*(1–4), 51–66. https://doi.org/http://dx.doi.org/10.1023/A:1018683830486

Atli-Veltin, B., Dekker, R., Brunner, S. K., & Walters, C. L. (2016). Wrinkling, Fracture, and Necking: The Various Failure Modes in Maritime Crash. In *ASME 2016 35th International Conference on Ocean, Offshore and Arctic Engineering*. https://doi.org/10.1115/OMAE2016-54148

Avachat, S., & Zhou, M. (2016). Compressive response of sandwich plates to water-based impulsive loading. *International Journal of Impact Engineering*, *93*, 196–210. https://doi.org/10.1016/j.ijimpeng.2016.03.007

Aven, T. (2010). On how to define, understand and describe risk. *Reliability Engineering & System Safety*, *95*(6), 623–631. https://doi.org/https://doi.org/10.1016/j.ress.2010.01.011

Aven, T. (2011). Selective critique of risk assessments with recommendations for improving methodology and practise. *Reliability Engineering & System Safety*, *96*(5), 509–514. https://doi.org/https://doi.org/10.1016/j.ress.2010.12.021

Aven, T. (2015). *Risk Analysis* (2nd Ed.). John Wiley & Sons, Ltd. https://doi.org/10.1002/9781119057819

Azzi, C., & Vassalos, D. (2011). Fire safety onboard passenger ships. *RINA, Royal Institution of Naval Architects - International Conference on Design and Operation of Passenger Ships - Papers*, 35–42.

Bakdi, A., Glad, I., Vanem, E., & Engelhardtsen, Ø. (2019). AIS-Based Multiple Vessel Collision and Grounding Risk Identification based on Adaptive Safety Domain. *Materials*, *8*, 5. https://doi.org/10.3390/jmse8010005

Baker, W. E., Westine, P. S., & Dodge, F. T. B. T. (1991). *Similarity Methods in Engineering Dynamics: Theory and Practice of Scale Modeling* (Vol. 12). Elsevier. https://www.sciencedirect.com/science/article/pii/B9780444881564500075

Baldi, F., Azzi, A., & Maréchal, F. (2019). From renewable energy to ship fuel: ammonia as an energy vector and mean for energy storage. *Computer Aided Chemical Engineering*, *46*, 1747–1752. https://doi.org/10.1016/B978-0-12-818634-3.50292-7

Barenblatt, G. I. (2003). *Scaling*. Cambridge University Press. https://doi.org/10.1017/CBO9780511814921

Basnet, S., Valdez Banda, O. A., Chaal, M., Hirdaris, S., & Kujala, P. (2020). *Comparison of system modelling techniques for autonomous ship systems*.

Bela, A., Le Sourne, H., Buldgen, L., & Rigo, P. (2017). Ship collision analysis on offshore wind turbine monopile foundations. *Marine Structures*, *51*, 220–241. https://doi.org/https://doi.org/10.1016/j.marstruc.2016.10.009

Berntsson, K., Kõrgesaar, M., Goncalves, B. R., & Romanoff, J. (2019). The influence of modelling weld effects when optimizing thin-walled structures for crashworthiness. *Proceedings of the International Offshore and Polar Engineering Conference*, *4*, 4280–4287.

Bhatia, K., & Khan, F. (2019). A predictive model to estimate ice accumulation on ship and offshore rig. *Ocean Engineering*, *173*, 68–76. https://doi.org/10.1016/J.OCEANENG.2018.12.060

Biehl, F., & Lehmann, E. (2006). Collisions of Ships and Offshore Wind Turbines: Calculation and Risk Evaluation. In *25th International Conference on Offshore Mechanics and Arctic Engineering* (pp. 663–670). https://doi.org/10.1115/OMAE2006-92270

Bijleveld, F. W., Hoogeland, M. G., Walters, C. L., & van Bergen, J. W. (2018). A Practical Approach to Ductile Material Failure During Raking Collisions. In *The 28th International Ocean and Polar Engineering Conference* (p. ISOPE-I-18-466).

Bin, S., Zhiqiang, H., Jin, W., & Zhaolong, Y. (2016). An analytical method to assess the damage and predict the residual strength of a ship in a shoal grounding accident scenario. *Journal of Ocean Engineering and Science*, *1*(2), 167–179. https://doi.org/https://doi.org/10.1016/j.joes.2016.03.007

Bleich, H. H., & Sandler, I. S. (1970). Interaction between structures and bilinear fluids. *International Journal of Solids and Structures*, *6*, 617–639.

Bobeldijk, M., Dragt, S., Hoogeland, M., & van Bergen, J. (2021). Assessment of the technical safe limit speed of a non-ice-strengthened naval vessel with representative and alternative side shell designs in ice-infested waters. *Ships and Offshore Structures*, *16*(sup1), 275–289. https://doi.org/10.1080/17445302.2021.1912475

Brochard, K., Le Sourne, H., & Barras, G. (2018). Extension of the string-on-foundation method to study the shock wave response of an immersed cylinder. *International Journal of Impact Engineering*, *117*, 138–152. https://doi.org/10.1016/J.IJIMPENG.2018.03.007

Brochard, K., Le Sourne, H., & Barras, G. (2020). Estimation of the response of a deeply immersed cylinder to the shock wave generated by an underwater explosion. *Marine Structures*, *72*, 102786. https://doi.org/10.1016/J.MARSTRUC.2020.102786

Buldgen, L., Le Sourne, H., & Pire, T. (2014). Extension of the super-elements method to the analysis of a jacket impacted by a ship. *Marine Structures*, *38*, 44–71. https://doi.org/10.1016/j.marstruc.2014.05.002

Burmeister, H.-C., Bruhn, W. C., & Rødseth, Ø. J. (2014). Can unmanned ships improve navigational safety? *Proceedings of the Transport Research Arena, TRA 2014*, 14–17.

Burmeister, H.-C., Bruhn, W. C., Rødseth, Ø. J., & Porathe, T. (2014). Autonomous Unmanned Merchant Vessel and its Contribution towards the e-Navigation Implementation: The MUNIN Perspective. *International Journal of E-Navigation and Maritime Economy*, *1*, 1–13. https://doi.org/https://doi.org/10.1016/j.enavi.2014.12.002

Burmeister, H.-C., & Constapel, M. (2021). Autonomous Collision Avoidance at Sea: A Survey. *Frontiers in Robotics and AI*, *8*, 297. https://doi.org/10.3389/frobt.2021.739013

Bužančić Primorac, B., Parunov, J., & Guedes Soares, C. (2020). Structural Reliability Analysis of Ship Hulls Accounting for Collision or Grounding Damage. *Journal of Marine Science and Application*, *19*(4), 717–733. https://doi.org/10.1007/s11804-020-00176-w

Cai, W., Zhu, L., & Qian, X. (2022). Dynamic responses of steel plates under repeated ice impacts. *International Journal of Impact Engineering*, *162*, 104129. https://doi.org/10.1016/J.IJIMPENG.2021.104129

Cai, W., Zhu, L., Yu, T. X., & Li, Y. (2020). Numerical simulations for plates under ice impact based on a concrete constitutive ice model. *International Journal of Impact Engineering*, *143*, 103594. https://doi.org/10.1016/J.IJIMPENG.2020.103594

Calle, M. A., Oshiro, R. E., & Alves, M. (2017). Ship collision and grounding: Scaled experiments and numerical analysis. *International Journal of Impact Engineering*, *103*. https://doi.org/10.1016/j.ijimpeng.2017.01.021

Calle, M. A., Salmi, M., Mazzariol, L. M., & Kujala, P. (2020). Miniature reproduction of raking tests on marine structure: Similarity technique and experiment. *Engineering Structures*, *212*, 110527. https://doi.org/https://doi.org/10.1016/j.engstruct.2020.110527

Cao, Y., Jia, Q., Wang, S., Jiang, Y., & Bai, Y. (2021). Safety design analysis of a vent mast on an LNG powered ship during a low-temperature combustible gas leakage accident. *Journal of Ocean Engineering and Science*. https://doi.org/10.1016/J.JOES.2021.06.001

CDRBC. (2017). *TB 10002-2017: Code for design on railway bridge and culvert*. National Railway Administration of the People's Republic of China.

Cerik, Burak C, & Choung, J. (2020). Progressive Collapse Analysis of Intact and Damaged Ships under Unsymmetrical Bending. In *Journal of Marine Science and Engineering* (Vol. 8, Issue 12). https://doi.org/10.3390/jmse8120988

Cerik, Burak Can. (2017). Large inelastic deformation of aluminium alloy plates in high-speed vessels subjected to slamming. *Journal of Marine Science and Technology*, *22*(2), 301–312. https://doi.org/10.1007/s00773-016-0411-0

Cerik, Burak Can, & Choung, J. (2020). On the prediction of ductile fracture in ship structures with shell elements at low temperatures. *Thin-Walled Structures*, *151*, 106721. https://doi.org/10.1016/J.TWS.2020.106721

Cerik, Burak Can, Lee, K., Park, S. J., & Choung, J. (2019). Simulation of ship collision and grounding damage using Hosford-Coulomb fracture model for shell elements. *Ocean Engineering*, *173*, 415–432. https://doi.org/10.1016/J.OCEANENG.2019.01.004

Cerik, Burak Can, Park, B., Park, S. J., & Choung, J. (2019). Modeling, testing and calibration of ductile crack formation in grade DH36 ship plates. *Marine Structures*, *66*, 27–43. https://doi.org/10.1016/J.MARSTRUC.2019.03.003

Chaal, M., Valdez Banda, O. A., Glomsrud, J. A., Basnet, S., Hirdaris, S., & Kujala, P. (2020). A framework to model the STPA hierarchical control structure of an autonomous ship. *Safety Science*, *132*, 104939. https://doi.org/https://doi.org/10.1016/j.ssci.2020.104939

Chen, B. Q., & Guedes Soares, C. (2020). Numerical investigation on the influence of stiffeners on the crushing resistance of web girders in ship grounding. *Developments in the Collision and Grounding of Ships and Offshore Structures - Proceedings of the 8th International Conference on Collision and Grounding of Ships and Offshore Structures, ICCGS 2019*, 49–56. https://doi.org/10.1016/j.marstruc.2018.10.003

Chen, P. (2020). *Probabilistic Risk Analysis for Ship Collision-Theory and Application for Conventional and Autonomous Ships* [Delft University of Technology]. https://doi.org/https://doi.org/10.4233/uuid:b8275053-49a0-4d77-aaea-27a92758f6e8

Cheon, J. S., Jang, B.-S., Yim, K. H., Lee, H. D., Koo, B.-Y., & Ju, H.-B. (2016). A study on slamming pressure on a flat stiffened plate considering fluid–structure interaction. *Journal of Marine Science and Technology*, *21*(2), 309–324. https://doi.org/10.1007/s00773-015-0353-y

Cho, S. R., Dessi, D., Engle, A., Gu, X., Ha, T. B., Hodgson, T., Imakita, A., Kapsenberg, G., Kukkanen, T., Malenica, S., Moan, T., Senjanovic, I., & Singh, S. P. (2009). COMMITTEE V.7 IMPULSIVE PRESSURE LOADING AND RESPONSE ASSESSMENT. In *17th International Ship and Offshore Structures Congress Volume 2* (p. 66).

Cho, U., Dutson, A. J., Wood, K. L., & Crawford, R. H. (2005). An advanced method to correlate scale models with distorted configurations. *Journal of Mechanical Design, Transactions of the ASME*, *127*(1), 78–85. https://doi.org/10.1115/1.1825044

Cole, R. H. (1948). *Underwater explosions.* Princeton Univ. Press.

Conti, F., Le Sourne, H., Vassalos, D., Kujala, P., Lindroth, D., Kim, S. J., & Hirdaris, S. (2021). A comparative method for scaling SOLAS collision damage distributions based on ship crashworthiness – application to probabilistic damage stability analysis of a passenger ship. *Ships and Offshore Structures*, 1–17. https://doi.org/10.1080/17445302.2021.1932023

Costas, M., Morin, D., Hopperstad, O. S., Børvik, T., & Langseth, M. (2019). A through-thickness damage regularisation scheme for shell elements subjected to severe bending and membrane deformations. *Journal of the Mechanics and Physics of Solids*, *123*, 190–206. https://doi.org/10.1016/J.JMPS.2018.08.002

Coutinho, C. P., Baptista, A. J., & Dias Rodrigues, J. (2016). Reduced scale models based on similitude theory: A review up to 2015. *Engineering Structures*, *119*, 81–94. https://doi.org/10.1016/J.ENGSTRUCT.2016.04.016

Czujko, J., & Paik, J. K. (2012). Hydrocarbon explosion – assessing and managing hydrocarbon explosion and fire risks in offshore installations. *Marine Technology*, *49*, 23–25.

Czujko, J., & Paik, J. K. (2015). A new method for accidental limit states design of thin-walled structures subjected to hydrocarbon explosion loads. *Ships and Offshore Structures*, *10*(5), 460–469. https://doi.org/10.1080/17445302.2015.1031206

Daley, C. G. (1999). Energy Based Ice Collision Forces. *Poac 99*, *1*, 1–20.

Daley, C. G., Daley, K. H., Dolny, J., & Quinton, B. W. T. (2017). Overload response of flatbar frames to ice loads. *Ships and Offshore Structures*, *12*. https://doi.org/10.1080/17445302.2016.1254520

Daley, C. G., & Kendrick, A. (2011). *BMT Report 6931DFR.Rev00: Safe speeds in ice*.

de Vos, J., Hekkenberg, R. G., & Valdez Banda, O. A. (2021). The Impact of Autonomous Ships on Safety at Sea – A Statistical Analysis. *Reliability Engineering & System Safety*, *210*,

107558. https://doi.org/https://doi.org/10.1016/j.ress.2021.107558
Decius, J. C. (1948). Dimensional analysis: An approach from transformation theory and a criterion for scaling model experiments. *Journal of the Franklin Institute*, *245*(5), 379–387. https://doi.org/10.1016/0016-0032(48)90002-7
Deeb, H., Mehdi, R. A., & Hahn, A. (2017). A review of damage assessment models in the maritime domain. *Ships and Offshore Structures*, *12*(sup1), S31–S54. https://doi.org/10.1080/17445302.2016.1278317
Dehghani-Sanij, A. R., Dehghani, S. R., Naterer, G. F., & Muzychka, Y. S. (2017a). Sea spray icing phenomena on marine vessels and offshore structures: Review and formulation. *Ocean Engineering*, *132*, 25–39. https://doi.org/10.1016/J.OCEANENG.2017.01.016
Dehghani-Sanij, A. R., Dehghani, S. R., Naterer, G. F., & Muzychka, Y. S. (2017b). Marine icing phenomena on vessels and offshore structures: Prediction and analysis. *Ocean Engineering*, *143*, 1–23. https://doi.org/10.1016/J.OCEANENG.2017.07.049
Dehghani, S. R., Naterer, G. F., & Muzychka, Y. S. (2018). 3-D trajectory analysis of wave-impact sea spray over a marine vessel. *Cold Regions Science and Technology*, *146*, 72–80. https://doi.org/10.1016/J.COLDREGIONS.2017.11.016
Derradji-Aouat, A. (2000). A unified failure envelope for isotropic fresh water ice and iceberg ice. *ETCE/OMAE 2000 Joint Conference, February 14-17*.
DeRuntz, Jr., J. A. (1989). The underwater shock analysis code and its applications. *60th Shock and Vibration Symposium Vol. I*, 89–107.
Ding, B.-D., Lü, H.-L., Li, X., Liu, J.-W., & Liu, Q. (2015). Experimental study on single-layer cylindrical reticulated shell under impact force. *Zhendong Gongcheng Xuebao/Journal of Vibration Engineering*, *28*(5), 692–702. https://doi.org/10.16385/j.cnki.issn.1004-4523.2015.05.003
DNVGL-OS-A101. (2019). *Safety principles and arrangements, Edition July 2019*.
DNVGL-OS-C101. (2019). *Design of offshore steel structures, general - LRFD method, 2019 Edition*.
DNVGL-RP-C204. (2019). *Structural design against accidental loads, Edition 2019-09*.
DNVGL-RP-C208. (2019). *Determination of structural capacity by non-linear finite element analysis methods, September 2019 Edition*.
DNVGL-RU-OU-0503. (2018). *Offshore fish farming units and installations, Edition July 2018*.
DNVGL-RU-SHIP. (2020). *Ch.2 Propulsion, power generation and auxiliary systems* (p. 377).
DNVGL-SI-0166. (2018). *Verification for compliance with Norwegian shelf regulations, July 2018 Edition*.
DNVGL-ST-0119. (2018). *Floating wind turbine structures. Edition July 2018*.
DNVGL-ST-0437. (2016). *Loads and site conditions for wind turbines, Edition November 2016*.
Dolny, J. (2018). *Methodology for Defining Technical Safe Speeds for Light Ice-Strengthened Government Vessels Operating In Ice*. http://www.shipstructure.org/pdf/473.pdf
Drummen, I., & Olbert, G. (2021). Conceptual Design of a Modular Floating Multi-Purpose Island. *Frontiers in Marine Science*, *8*, 86. https://doi.org/10.3389/fmars.2021.615222
Du, L., Goerlandt, F., & Kujala, P. (2020). Review and analysis of methods for assessing maritime waterway risk based on non-accident critical events detected from AIS data. *Reliability Engineering & System Safety*, *200*, 106933. https://doi.org/https://doi.org/10.1016/j.ress.2020.106933
Du, L., Valdez Banda, O. A., Goerlandt, F., Huang, Y., & Kujala, P. (2020). A COLREG-compliant ship collision alert system for stand-on vessels. *Ocean Engineering*, *218*, 107866. https://doi.org/https://doi.org/10.1016/j.oceaneng.2020.107866
Du, L., Valdez Banda, O. A., Goerlandt, F., Kujala, P., & Zhang, W. (2021). Improving Near Miss Detection in Maritime Traffic in the Northern Baltic Sea from AIS Data. *Journal of Marine Science and Engineering*, *9*(2). https://doi.org/10.3390/jmse9020180
Du, L., Valdez Banda, O. A., Huang, Y., Goerlandt, F., Kujala, P., & Zhang, W. (2021). An empirical ship domain based on evasive maneuver and perceived collision risk. *Reliability*

Engineering & System Safety, *213*, 107752. https://doi.org/https://doi.org/10.1016/j.ress.2021.107752

Echeverry Jaramillo, S., Márquez Duque, L., Le Sourne, H., & Rigo, P. (2019). Numerical crashworthiness analysis of a spar floating offshore wind turbine impacted by a ship. In Carlos Guedes Soares (Ed.), *Developments in the Collision and Grounding of Ships and Offshore Structures: Proceedings of the 8th International Conference on Collision and Grounding of Ships and Offshore Structures*. Routledge Taylor & Francis Group. https://doi.org/10.1201/9781003002420

ECMAR. (2017). *A VISION FOR EUROPEAN MARITIME RDI 2030: ECMAR Position Paper*. https://www.ecmar.eu/media/1817/ecmar-position-paper.pdf

Ehlers, S., & Østby, E. (2012). Increased crashworthiness due to arctic conditions – The influence of sub-zero temperature. *Marine Structures*, *28*(1), 86–100. https://doi.org/10.1016/J.MARSTRUC.2012.05.004

Ekeberg, O.-C., Shipilova, O., Birknes-Berg, J., Lande, R. H., & Johansen, A. (2018). *Glacial Ice Impact, Report No. 2017-0425, Rev. 2* (p. 69). DNV GL.

Eliopoulou, E., Papanikolaou, A., & Voulgarellis, M. (2016). Statistical analysis of ship accidents and review of safety level. *Safety Science*, *85*, 282–292. https://doi.org/https://doi.org/10.1016/j.ssci.2016.02.001

EMSA. (2021). *Annual overview of marine casualties and incidents 2021* (p. 150). European Maritime Safety Agency.

Eurocode. (2002). *EN 1991-1-2 Part 1-2: General actions - Actions on structures exposed to fire*.

Eurocode. (2005). *EN 1993-1-2 Part 1-2: General - Structural fire design*.

Fan, C., Wróbel, K., Montewka, J., Gil, M., Wan, C., & Zhang, D. (2020). A framework to identify factors influencing navigational risk for Maritime Autonomous Surface Ships. *Ocean Engineering*, *202*, 107188. https://doi.org/https://doi.org/10.1016/j.oceaneng.2020.107188

Farhat, C., Wang, K. G., Main, A., Kyriakides, S., Lee, L. H., Ravi-Chandar, K., & Belytschko, T. (2013). Dynamic implosion of underwater cylindrical shells: Experiments and Computations. *International Journal of Solids and Structures*, *50*(19), 2943–2961. https://doi.org/10.1016/J.IJSOLSTR.2013.05.006

Fu, S., Gao, X., & Chen, X. (2018). The similarity law and its verification of cylindrical lattice shell model under internal explosion. *International Journal of Impact Engineering*, *122*, 38–49. https://doi.org/10.1016/j.ijimpeng.2018.08.010

Gagnon, R. E., Andrade, S. L., Quinton, B. W. T., Daley, C. G., & Colbourne, B. (2020). Pressure distribution data from large double-pendulum ice impact tests. *Cold Regions Science and Technology*, *175*, 103033. https://doi.org/10.1016/J.COLDREGIONS.2020.103033

Galieriková, A., Dávid, A., Materna, M., & Mako, P. (2021). Study of maritime accidents with hazardous substances involved: comparison of HNS and oil behaviours in marine environment. *Transportation Research Procedia*, *55*, 1050–1064. https://doi.org/10.1016/J.TRPRO.2021.07.182

Gao, Y., Dong, Y., Xiao, L., Wang, F., & Feng, S. (2018). Preliminary Similarity Analysis on the Deformation Dynamic Response of Thin Plates Subjected to Blast and Impact Loadings. *Propellants, Explosives, Pyrotechnics*, *43*(6), 583–594. https://doi.org/10.1002/prep.201700279

Gauch, E., LeBlanc, J., & Shukla, A. (2018). Near field underwater explosion response of polyurea coated composite cylinders. *Composite Structures*, *202*, 836–852. https://doi.org/https://doi.org/10.1016/j.compstruct.2018.04.048

Geers, T. L. (1978). Doubly asymptotic approximations for transient motions of submerged structures. *The Journal of the Acoustical Society of America*, *64*(5), 1500–1508. https://doi.org/10.1121/1.382093

Gish, L. A., & Wierzbicki, T. (2015). Estimation of the underwater implosion pulse from cylindrical metal shells. *International Journal of Impact Engineering*, *77*, 166–175.

https://doi.org/10.1016/J.IJIMPENG.2014.11.018
Goerlandt, F., & Kujala, P. (2011). Traffic simulation based ship collision probability modeling. *Reliability Engineering & System Safety*, *96*(1), 91–107. https://doi.org/https://doi.org/10.1016/j.ress.2010.09.003
Goerlandt, F., & Kujala, P. (2014). On the reliability and validity of ship–ship collision risk analysis in light of different perspectives on risk. *Safety Science*, *62*, 348–365. https://doi.org/https://doi.org/10.1016/j.ssci.2013.09.010
Goerlandt, F., Laine, V., Bal-Beşikçi, E., Baldauf, M., Al-Quhali, M. A., & Koldenhof, Y. (2019). End-user and stakeholder views on selected risk assessment tools for marine oil spill preparedness and response, including future research and development needs. *TransNav : International Journal on Marine Navigation and Safety of Sea Transportation*, *13*(1), 213–220.
Goerlandt, F., & Montewka, J. (2015). Maritime transportation risk analysis: Review and analysis in light of some foundational issues. *Reliability Engineering & System Safety*, *138*, 115–134. https://doi.org/https://doi.org/10.1016/j.ress.2015.01.025
Goerlandt, F., Montewka, J., Kuzmin, V., & Kujala, P. (2015). A risk-informed ship collision alert system: Framework and application. *Safety Science*, *77*, 182–204. https://doi.org/https://doi.org/10.1016/j.ssci.2015.03.015
GSDHBC. (2015). *JTG D60-2015: General Specifications for Design of Highway Bridges and Culverts*. Ministry of Transport of the People's Republic of China.
Haag, S. R., Hoogeland, M. G., & Vredeveldt, A. W. (2017). Grounding Damage Estimate Through Acceleration Measurements. In *ASME 2017 36th International Conference on Ocean, Offshore and Arctic Engineering*. https://doi.org/10.1115/OMAE2017-61732
Han, Z., Li, C., Deng, Y., & Liu, J. (2019). The analysis of anti-collision performance of the fender with offshore wind turbine tripod impacted by ship and the coefficient of restitution. *Ocean Engineering*, *194*, 106614. https://doi.org/10.1016/J.OCEANENG.2019.106614
Haugen, S., & Vinnem, J. E. (2015). Perspectives on risk and the unforeseen. *Reliability Engineering and System Safety*, 1–5. https://doi.org/DOI:101016/jress201412009
Haver, S. (2019). Airgap and safety: Metocean induced uncertainties affecting airgap assessments. *Marine Structures*, *63*, 406–428. https://doi.org/https://doi.org/10.1016/j.marstruc.2017.09.006
Herrnring, H., & Ehlers, S. (2021). A Finite Element Model for Compressive Ice Loads Based on a Mohr-Coulomb Material and the Node Splitting Technique. *Journal of Offshore Mechanics and Arctic Engineering*, *144*(2). https://doi.org/10.1115/1.4052746
Hodges, J. L., Lattimer, B. Y., & Luxbacher, K. D. (2019). Compartment fire predictions using transpose convolutional neural networks. *Fire Safety Journal*, *108*, 102854. https://doi.org/https://doi.org/10.1016/j.firesaf.2019.102854
Holen, S. M., Yang, X., Utne, I. B., & Haugen, S. (2019). Major accidents in Norwegian fish farming. *Safety Science*, *120*, 32–43. https://doi.org/10.1016/J.SSCI.2019.05.036
Hoo Fatt, M. S., & Sirivolu, D. (2017). Marine composite sandwich plates under air and water blasts. *Marine Structures*, *56*, 163–185. https://doi.org/10.1016/J.MARSTRUC.2017.08.004
Hoo Fatt, M. S., & Wierzbicki, T. (1991). Damage of plastic cylinders under localized pressure loading. *International Journal of Mechanical Sciences*, *33*(12), 999–1016. https://doi.org/10.1016/0020-7403(91)90055-8
Hu, Z., Wang, G., Yao, Q., & Yu, Z. (2016). Rapid prediction of structural responses of double-bottom structures in shoal grounding scenario. *Journal of Marine Science and Application*, *15*(1), 73–85. https://doi.org/10.1007/s11804-016-1344-z
Iannaccone, T., Scarponi, G. E., Landucci, G., & Cozzani, V. (2021). Numerical simulation of LNG tanks exposed to fire. *Process Safety and Environmental Protection*, *149*, 735–749. https://doi.org/10.1016/J.PSEP.2021.03.027
IEA. (2021). *Net Zero by 2050*. https://www.iea.org/reports/net-zero-by-2050

IMO. (1973). *International Convention for the Prevention of Pollution from Ships (MARPOL)*.
IMO. (1974). *International Convention for the Safety of Life at Sea (SOLAS)*.
IMO. (2007). *Convention on the International Regulations for Preventing Collisions at Sea, 1972 (COLREGs)*.
IMO. (2014). *Res. MSC.370(93) Amendments to the international code for the construction and equipment of ships carrying liquefied gasses in bulk (IGC Code)* (p. 195).
IMO. (2015). *Res. MSC.391(95) Adoption of the International Code of Safety for Ships using Gases or other Low-flashpoint Fuels (IGF Code)*.
IMO. (2016). *Res. MSC.420(97) Interim recommendations for carriage of liquified hydrogen in bulk*.
IMO. (2018). *MSC-MEPC.2/Circ.12/Rev.2 Revised guidelines for formal safety assessment (FSA) for use in the IMO rule-making process* (p. 71).
Ince, S. T., Kumar, A., & Paik, J. K. (2017). A new constitutive equation on ice materials. *Ships and Offshore Structures*, *12*(5), 610–623. https://doi.org/10.1080/17445302.2016.1190122
Ince, S. T., Kumar, A., Park, D. K., & Paik, J. K. (2017). An advanced technology for structural crashworthiness analysis of a ship colliding with an ice-ridge: Numerical modelling and experiments. *International Journal of Impact Engineering*, *110*, 112–122. https://doi.org/10.1016/J.IJIMPENG.2017.02.014
Inmarsat. (2021). *The future of maritime safety*. https://www.inmarsat.com/en/insights/maritime/2021/the-future-of-maritime-safety.html
IRENA. (2018). *Offshore innovation widens renewable energy options*. https://www.irena.org/publications/2018/Sep/Offshore-innovation-widens-renewable-energy-options
ISO 19900:2019. (2019). *Petroleum and natural gas industries — General requirements for offshore structures, Ed. 3* (p. 64).
ISO 19901-1:2015. (2015). *Petroleum and natural gas industries — Specific requirements for offshore structures — Part 1: Metocean design and operating considerations*.
ISO 19901-3:2014. (2014). *Petroleum and natural gas industries — Specific requirements for offshore structures — Part 3: Topsides structure, Ed. 2* (p. 117).
ISO 19902:2007. (2007). *Petroleum and natural gas industries — Fixed steel offshore structures, Ed. 1* (p. 622).
ISO 19902:2020. (2020). *Petroleum and natural gas industries — Fixed steel offshore structures, Ed. 2* (p. 565).
ISO 19903:2019. (2019). *Petroleum and natural gas industries — Concrete offshore structures, Ed. 2* (p. 115).
ISO 19904-1:2019. (2019). *Petroleum and natural gas industries — Floating offshore structures — Part 1: Ship-shaped, semi-submersible, spar and shallow-draught cylindrical structures, Ed. 2* (p. 200).
ISO 19905-1:2016. (2016). *Petroleum and natural gas industries — Site-specific assessment of mobile offshore units — Part 1: Jack-ups, Ed. 2* (p. 320).
ISO 19905-3:2021. (2021). *Petroleum and natural gas industries — Site-specific assessment of mobile offshore units — Part 3: Floating units, Ed. 2* (p. 22).
ISO 19906:2019. (2019). *Petroleum and natural gas industries — Arctic offshore structures*.
ISO 31000:2018. (2018). *Risk Management*.
Jalonen, R., Tuominen, R., & Wahlström, M. (2017). *Safety of Unmanned Ships - Safe Shipping with Autonomous and Remote Controlled Ships* (Aalto University Publication Series SCIENCE + TECHNOLOGY; 5/2017). Aalto University. http://urn.fi/URN:ISBN:978-952-60-7480-1
Jensen, K. S., Petersen, S. J., & Pedersen, R. R. (2018). European offshore wind engineering – past, present and future. *Proceedings of the Institution of Civil Engineers - Civil Engineering*, *171*(4), 159–165. https://doi.org/10.1680/jcien.17.00040
Jia, H., Qin, S., Wang, R., Xue, Y., Fu, D., & Wang, A. (2020). Ship collision impact on the

structural load of an offshore wind turbine. *Global Energy Interconnection*, *3*(1), 43–50. https://doi.org/10.1016/J.GLOEI.2020.03.009

Jiang, D., Wu, B., Cheng, Z., Xue, J., & van Gelder, P. H. A. J. M. (2021). Towards a probabilistic model for estimation of grounding accidents in fluctuating backwater zone of the Three Gorges Reservoir. *Reliability Engineering & System Safety*, *205*, 107239. https://doi.org/https://doi.org/10.1016/j.ress.2020.107239

Jiang, P., Tian, C. J., Xie, R. Z., & Meng, D. S. (2006). Experimental investigation into scaling laws for conical shells struck by projectiles. *International Journal of Impact Engineering*, *32*(8), 1284–1298. https://doi.org/10.1016/j.ijimpeng.2004.09.015

Jiao, Y., Wang, Z., Liu, J., Li, X., Chen, R., & Chen, W. (2021). Backtracking and prospect on LNG supply chain safety. *Journal of Loss Prevention in the Process Industries*, *71*, 104433. https://doi.org/10.1016/J.JLP.2021.104433

Jones, N. (1973). Slamming Damage. *Journal of Ship Research*, *17*(02), 80–86. https://doi.org/10.5957/jsr.1973.17.2.80

Jones, N. (2012). *Structural Impact (2nd Edition)*. Cambridge University Press. http://site.ebrary.com/lib/alltitles/docDetail.action?docID=10533163&ppg=447

Kapetsky, J. M., Aguilar-Manjarrez, J., & Jenness, J. (2013). *FAO Fisheries and Aquaculture Technical Paper No. 549: A global assessment of offshore mariculture potential from a spatial perspective*.

Kennard, E. H. (1943). Cavitation in an Elastic Liquid. *Phys. Rev.*, *63*(5–6), 172–181. https://doi.org/10.1103/PhysRev.63.172

Kim, H., Daley, C. G., & Kim, H. (2018). Evaluation of large structural grillages subjected to ice loads in experimental and numerical analysis. *Marine Structures*, *61*, 467–502. https://doi.org/10.1016/J.MARSTRUC.2018.06.015

Kim, K. J., Lee, J. H., Park, D. K., Jung, B. G., Han, X., & Paik, J. K. (2016). An experimental and numerical study on nonlinear impact responses of steel-plated structures in an Arctic environment. *International Journal of Impact Engineering*, *93*, 99–115. https://doi.org/10.1016/J.IJIMPENG.2016.02.013

Kim, S. J., Kõrgersaar, M., Ahmadi, N., Taimuri, G., Kujala, P., & Hirdaris, S. (2021). The influence of fluid structure interaction modelling on the dynamic response of ships subject to collision and grounding. *Marine Structures*, *75*, 102875. https://doi.org/https://doi.org/10.1016/j.marstruc.2020.102875

Kishore, S., Naik Parrikar, P., & Shukla, A. (2021). Response of an underwater cylindrical composite shell to a proximal implosion. *Journal of the Mechanics and Physics of Solids*, *152*, 104414. https://doi.org/https://doi.org/10.1016/j.jmps.2021.104414

Kishore, S., Senol, K., Naik Parrikar, P., & Shukla, A. (2020). Underwater implosion pressure pulse interactions with submerged plates. *Journal of the Mechanics and Physics of Solids*, *143*, 104051. https://doi.org/10.1016/J.JMPS.2020.104051

Kong, X., Li, X., Zheng, C., Liu, F., & Wu, W.-G. (2017). Similarity considerations for scale-down model versus prototype on impact response of plates under blast loads. *International Journal of Impact Engineering*, *101*, 32–41. https://doi.org/10.1016/j.ijimpeng.2016.11.006

Kõrgesaar, M. (2019). The effect of low stress triaxialities and deformation paths on ductile fracture simulations of large shell structures. *Marine Structures*, *63*, 45–64. https://doi.org/https://doi.org/10.1016/j.marstruc.2018.08.004

Kõrgesaar, M., Jalasto, T., & Alsos, H. S. (2021). WeldInp – Method to include welded zones in large numerical ABAQUS FE models. In J Amdahl & C. Guedes Soares (Eds.), *Developments in the Analysis and Design of Marine Structures: Proceedings of the 8th International Conference on Marine Structures (MARSTRUCT 2021, 7-9 June 2021, Trondheim, Norway)* (p. 6). CRC Press.

Kõrgesaar, M., Romanoff, J., St-Pierre, L., & Varsta, P. (2019). Effect of weld modelling on crashworthiness optimization. In *Trends in the Analysis and Design of Marine Structures* (p. 7). CRC Press.

Kõrgesaar, M., & Storheim, M. (2020). Treatment of Bending Deformations in Maritime Crash Analyses. In *ASME 2020 39th International Conference on Ocean, Offshore and Arctic Engineering*. https://doi.org/10.1115/OMAE2020-19272

Le Sourne, H., Donner, R., Besnier, F., & Ferry, M. P. (2001). External dynamics of ship-submarine collision. *2nd International Conference on Collision and Grounding of Ships*, 137–144.

Le Sourne, H., Kim, S. J., Taimuri, G., Conti, F., Bae, H., Ahmed, M., Pineau, J.-P., Looten, T., Kaydihan, L., Kujala, P., & Hirdaris, S. (2021). *A comparison of crashworthiness methods for the assessment of ship damage extents*.

Le Sourne, H., Pineau, J.-P., Umunnakwe, C. B., Wesoly, T., & Dorival, O. (2021). On the influence of buoyancy forces, failure strain and friction coefficient on the damage extent of a grounded ship. In *Developments in the Analysis and Design of Marine Structures: Proceedings of the 8th International Conference on Marine Structures (MARSTRUCT 2021, 7-9 June 2021, Trondheim, Norway)* (pp. 229–235). https://doi.org/10.1201/9781003230373-27

Le Sourne, H., Pire, T., Hsieh, J. R., & Rigo, P. (2016). New analytical developments to study local and global deformations of an offshore wind turbine jacket impacted by a ship. *Proceedings of the 7th International Conference on Collision and Grounding of Ships and Offshore Structures (ICCGS'16)*, 15–18.

Lee, S.-G., Lee, J.-S., Lee, H.-S., Park, J.-H., & Jung, T.-Y. (2017). Full-scale Ship Collision, Grounding and Sinking Simulation Using Highly Advanced M&S System of FSI Analysis Technique. *Procedia Engineering*, *173*, 1507–1514. https://doi.org/https://doi.org/10.1016/j.proeng.2016.12.232

Lee, S., & Hong, J.-W. (2020). Parametric studies on smoothed particle hydrodynamic simulations for accurate estimation of open surface flow force. *International Journal of Naval Architecture and Ocean Engineering*, *12*, 85–101. https://doi.org/https://doi.org/10.1016/j.ijnaoe.2019.07.003

Leelachai, A. (2020). *Progressive collapse of damaged ship structures* [Newcastle University]. http://theses.ncl.ac.uk/jspui/handle/10443/5149

Leveson, N. G. (2011). Applying systems thinking to analyze and learn from events. *Safety Science*, *49*(1), 55–64. https://doi.org/https://doi.org/10.1016/j.ssci.2009.12.021

Li, S., Hu, Z. Q., & Benson, S. D. (2019). A cyclic progressive collapse method to predict the bending response of a ship hull girder . In C.Guedes Soares & J. Parunov (Eds.), *7th International Conference on Marine Structures, MARSTRUCT 2019* (pp. 149-157 BT-Trends in the Analysis and Design o). https://doi.org/10.1201/9780429298875-16

Lim, G. J., Cho, J., Bora, S., Biobaku, T., & Parsaei, H. (2018). Models and computational algorithms for maritime risk analysis: a review. *Annals of Operations Research*, *271*(2), 765–786. https://doi.org/10.1007/s10479-018-2768-4

Liu, B., Dong, A., Villavicencio, R., Liu, K., & Guedes Soares, C. (2020). Experimental and numerical study on the penetration of stiffened aluminium alloy plates punched by a hemi-cylindrical indenter. *Ships and Offshore Structures*. https://doi.org/10.1080/17445302.2020.1835052

Liu, Bin, & Guedes Soares, C. (2016a). Analytical method to determine the crushing behaviour of girders with stiffened web. *International Journal of Impact Engineering*, *93*, 49–61. https://doi.org/https://doi.org/10.1016/j.ijimpeng.2016.02.008

Liu, Bin, & Guedes Soares, C. (2016b). Experimental and numerical analysis of the crushing behaviour of stiffened web girders. *International Journal of Impact Engineering*, *88*, 22–38.

Liu, Bin, Villavicencio, R., Pedersen, P. T., & Guedes Soares, C. (2021). Analysis of structural crashworthiness of double-hull ships in collision and grounding. *Marine Structures*, *76*, 102898. https://doi.org/https://doi.org/10.1016/j.marstruc.2020.102898

Liu, Z., & Amdahl, J. (2010). A new formulation of the impact mechanics of ship collisions and

its application to a ship–iceberg collision. *Marine Structures*, *23*, 360–384. https://doi.org/10.1016/j.marstruc.2010.05.003

Liu, Z., & Amdahl, J. (2019). On multi-planar impact mechanics in ship collisions. *Marine Structures*, *63*, 364–383. https://doi.org/https://doi.org/10.1016/j.marstruc.2018.10.006

Liu, Z., Amdahl, J., & Løset, S. (2011). Plasticity based material modelling of ice and its application to ship–iceberg impacts. *Cold Regions Science and Technology*, *65*(3), 326–334. https://doi.org/10.1016/J.COLDREGIONS.2010.10.005

Lloyd's Register. (2014a). *Guidance Notes for Risk Based Analysis: Collisions* (p. 29).

Lloyd's Register. (2014b). *Guidance Notes for Risk Based Analysis: Fire Loads and Protection*.

Lloyd's Register. (2015). *Guidance Notes for the Risk Based Analysis: Explosion Loads*.

Lloyd's Register. (2016). *Guidance Notes for Collision Assessment for the Location of Low-flashpoint Fuel Tanks* (p. 9).

Lu, W., Amdahl, J., Lubbad, R., Yu, Z., & Løset, S. (2021). Glacial ice impacts: Part I: Wave-driven motion and small glacial ice feature impacts. *Marine Structures*, *75*, 102850. https://doi.org/https://doi.org/10.1016/j.marstruc.2020.102850

Lu, W., Yu, Z., Lubbad, R., Amdahl, J., Løset, S., & Kim, E. (2020). *Glacial Ice Actions: Executive Summary of NORD ST20 2019/313 and NORD ST19, Report No. ArcISo_2019_Ptil03* (p. 57). ArcISo AS.

Lu, W., Yu, Z., van den Berg, M., Lubbad, R., Amdahl, J., Løset, S., & Kim, E. (2019). *Assessment of Structural Damage due to Glacial Ice Impact (ST19), Report No. ArcISo_2018_Ptil01* (p. 98). https://doi.org/10.13140/RG.2.2.14957.33761

Lu, W., Yu, Z., van den Berg, M., Monteban, D., Lubbad, R., Hornnes, V., Amdahl, J., Løset, S., & Kim, E. (2019). *Loads, Design and Operations of Floaters in the North, Report No. ArcISo_2019_Ptil02* (p. 234). ArcISo AS.

Lu, Y., Liu, K., Wang, Z., & Tang, W. (2020). Dynamic behavior of scaled tubular K-joints subjected to impact loads. *Marine Structures*, *69*. https://doi.org/10.1016/j.marstruc.2019.102685

Luo, Z., Zhu, Y. P., Zhao, X. Y., & Wang, D. Y. (2014). Determination method of dynamic distorted scaling laws and applicable structure size intervals of a rotating thin-wall short cylindrical shell. *Proceedings of the Institution of Mechanical Engineers, Part C: Journal of Mechanical Engineering Science*, *229*(5), 806–817. https://doi.org/10.1177/0954406214541645

Luo, Z., Zhu, Y. P., Zhao, X. Y., & Wang, D. Y. (2015). High-order vibrations dynamic scaling laws of distorted scaled models of thin-walled short cylindrical shells. *Mechanics Based Design of Structures and Machines*, *43*(4), 514–534. https://doi.org/10.1080/15397734.2015.1044610

Ma, B., Zhu, L., Tian, L., & Zhu, Z. (2021). Design formula for the ship plate under severe slamming. In *The 31st International Ocean and Polar Engineering Conference* (p. ISOPE-I-21-4133).

Ma, L., & Swan, C. (2020). An experimental study of wave-in-deck loading and its dependence on the properties of the incident waves. *Journal of Fluids and Structures*, *92*, 102784. https://doi.org/https://doi.org/10.1016/j.jfluidstructs.2019.102784

Ma, S., Chen, Y., Wang, Z., Wang, J., Lyu, L., & Wei, W. (2021). Similarity Law between Centrifuge Scale Test and Prototype Underwater Explosion. *Shock and Vibration*, *2021*. https://doi.org/10.1155/2021/8582026

Mair, H. U. (1999). Benchmarks for Submerged Structure Response to Underwater Explosions. *Shock and Vibration*, *6*, 743708. https://doi.org/10.1155/1999/743708

Man, Y., Lundh, M., Porathe, T., & MacKinnon, S. N. (2015). From Desk to Field - Human Factor Issues in Remote Monitoring and Controlling of Autonomous Unmanned Vessels. *Procedia Manufacturing*, *3*, 2674–2681. https://doi.org/https://doi.org/10.1016/j.promfg.2015.07.635

Mao, X., Ying, R., Yuan, Y., Li, F., & Shen, B. (2021). Simulation and analysis of hydrogen

leakage and explosion behaviors in various compartments on a hydrogen fuel cell ship. *International Journal of Hydrogen Energy*, *46*(9), 6857–6872. https://doi.org/10.1016/J.IJHYDENE.2020.11.158

Maritime Knowledge Centre, TNO, & TUDelft. (2017). *Final Report - Framework CO2 reduction in shipping*.

Mazaheri, A. (2009). *Probabilistic Modeling of Ship Grounding* . http://appmech.tkk.fi/fi/julkaisut/TKK-AM-10.pdf

Mazzariol, L. M., & Alves, M. (2019a). Experimental verification of similarity laws for impacted structures made of different materials. *International Journal of Impact Engineering*, *133*. https://doi.org/10.1016/j.ijimpeng.2019.103364

Mazzariol, L. M., & Alves, M. (2019b). Similarity laws of structures under impact load: Geometric and material distortion. *International Journal of Mechanical Sciences*, *157–158*, 633–647. https://doi.org/10.1016/j.ijmecsci.2019.05.011

McKinlay, C. J., Turnock, S. R., & Hudson, D. A. (2021). Route to zero emission shipping: Hydrogen, ammonia or methanol? *International Journal of Hydrogen Energy*, *46*(55), 28282–28297. https://doi.org/10.1016/J.IJHYDENE.2021.06.066

Meng, Q., Qu, X., Yong, K. T., & Wong, Y. H. (2011). QRA model-based risk impact analysis of traffic flow in urban road tunnels. *Risk Analysis : An Official Publication of the Society for Risk Analysis*, *31*(12), 1872–1882. https://doi.org/10.1111/j.1539-6924.2011.01624.x

Meng, Q., Weng, J., & Qu, X. (2010). A probabilistic quantitative risk assessment model for the long-term work zone crashes. *Accident Analysis & Prevention*, *42*(6), 1866–1877. https://doi.org/https://doi.org/10.1016/j.aap.2010.05.007

Min, D., Heo, Y., Shin, D., Kim, S., & Cho, S. (2013). On the plastic and fracture damage of polar class vessel structures subjected to impact loadings. In *Collision Grounding Ships and Offshore Structures* (pp. 213–220). CRC Press.

Mintu, S. A., Molyneux, D., & Colbourne, B. (2019). *Multi-Phase Simulation of Droplet Trajectories of Wave-Impact Sea Spray Over a Vessel*. *Volume 2:* https://doi.org/10.1115/OMAE2019-95799

Mintu, S. A., Molyneux, D., & Colbourne, B. (2020a). *Ship-Wave Impact Generated Sea Spray: Part 1 — Formulating Liquid Water Content and Spray Cloud Duration*. *Volume 6A:* https://doi.org/10.1115/OMAE2020-18223

Mintu, S. A., Molyneux, D., & Colbourne, B. (2020b). *Ship-Wave Impact Generated Sea Spray: Part 2 — Formulating Spray Frequency*. *Volume 6A:* https://doi.org/10.1115/OMAE2020-18224

Moan, T., Amdahl, J., & Ersdal, G. (2019). Assessment of ship impact risk to offshore structures - New NORSOK N-003 guidelines. *Marine Structures*, *63*, 480–494. https://doi.org/https://doi.org/10.1016/j.marstruc.2017.05.003

Moe, O. H., Sha, Y., Veie, J., & Amdahl, J. (2017). Analysis of tether anchored floating suspension bridge subjected to large ship collisions. *Procedia Engineering*, *199*, 2488–2493. https://doi.org/10.1016/J.PROENG.2017.09.413

Mokhtari, M., Nam, W., & Amdahl, J. (2021). Thermal analysis of marine structural steel EH36 subject to non-spreading cryogenic spills. Part II: finite element analysis. *Ships and Offshore Structures*, 1–10. https://doi.org/10.1080/17445302.2021.1979920

Montewka, J., Goerlandt, F., & Kujala, P. (2014). On a systematic perspective on risk for formal safety assessment (FSA). *Reliability Engineering & System Safety*, *127*, 77–85. https://doi.org/https://doi.org/10.1016/j.ress.2014.03.009

Montewka, J., Wróbel, K., Heikkilä, E., Valdez Banda, O. A., Goerlandt, F., & Haugen, S. (2018). *Challenges, solution proposals and research directions in safety and risk assessment of autonomous shipping*.

Moulas, D., Shafiee, M., & Mehmanparast, A. (2017). Damage analysis of ship collisions with offshore wind turbine foundations. *Ocean Engineering*, *143*, 149–162. https://doi.org/https://doi.org/10.1016/j.oceaneng.2017.04.050

Mouritz, A. P. (2019). Advances in understanding the response of fibre-based polymer composites to shock waves and explosive blasts. *Composites Part A: Applied Science and Manufacturing*, *125*. https://doi.org/10.1016/j.compositesa.2019.105502

Mousavi, M., Ghazi, I., & Omaraee, B. (2017). Risk Assessment in the Maritime Industry. *Engineering, Technology & Applied Science Research*, *7*(1 SE-), 1377–1381. https://doi.org/10.48084/etasr.836

Mujeeb-Ahmed, M. P. P., Ince, S. T. S. T., & Paik, J. K. (2020). Computational models for the structural crashworthiness analysis of a fixed-type offshore platform in collisions with an offshore supply vessel. *Thin-Walled Structures*, *154*, 106868. https://doi.org/https://doi.org/10.1016/j.tws.2020.106868

Mustafa, A., Barabadi, A., & Markeset, T. (2019). Risk assessment of wind farm development in ice proven area. *Proceedings of the 25th International Conference on Port and Ocean Engineering under Arctic Conditions June 9-13*, 13. Proceedings of the 25th International Conference on%0APort and Ocean Engineering under Arctic Conditions

Naylor, R. L., Hardy, R. W., Buschmann, A. H., Bush, S. R., Cao, L., Klinger, D. H., Little, D. C., Lubchenco, J., Shumway, S. E., & Troell, M. (2021). A 20-year retrospective review of global aquaculture. *Nature*, *591*(7851), 551–563. https://doi.org/10.1038/s41586-021-03308-6

Newton, R. E. T. T.-E. of cavitation on underwater shock loading-P. 1. (1978). *No Title*. http://hdl.handle.net/10945/29264

Nguyen, S., Chen, P. S.-L., Du, Y., & Thai, V. V. (2021). An Operational Risk Analysis Model for Container Shipping Systems considering Uncertainty Quantification. *Reliability Engineering & System Safety*, *209*, 107362. https://doi.org/https://doi.org/10.1016/j.ress.2020.107362

Noam, T., Dolinski, M., & Rittel, D. (2014). Scaling dynamic failure: A numerical study. *International Journal of Impact Engineering*, *69*, 69–79. https://doi.org/10.1016/j.ijimpeng.2014.02.011

Noh, M. H., Cerik, B. C., Han, D., & Choung, J. (2018). Lateral impact tests on FH32 grade steel stiffened plates at room and sub-zero temperatures. *International Journal of Impact Engineering*, *115*, 36–47. https://doi.org/10.1016/J.IJIMPENG.2018.01.007

NORSOK N-001:2010. (2010). *Integrity of offshore structures, 7th Ed.*

NORSOK N-003:2017. (2017). *Actions and action effects, 3rd Ed.*

NORSOK N-004:2004. (2004). *Design of steel structures, 2nd Ed.*

NORSOK N-004:2013. (2013). *Design of steel structures* (p. 288).

NORSOK Z-013. (2010). *Risk and emergency preparedness assessment Rev. 3*.

Norwegian Maritime Directorate. (1991). *Regulations of 20 December 1991 No. 878 on stability, watertight subdivision and watertight/weathertight means of closure on mobile offshore units* (p. 18).

Ommani, B., Berthelsen, P. A., & Firoozkoohi, R. (2018). *OC2018 A-116 - Loads, design and operation of floaters in the Arctic - Ptil – NORD ST20* (p. 165). SINTEF Ocean AS.

Orimolade, A. P., Gudmestad, O. T., & Wold, L. E. (2017). Vessel stability in polar low situations. *Ships and Offshore Structures*, *12*(sup1), S82–S87. https://doi.org/10.1080/17445302.2016.1259954

Orimolade, A. P., Larsen, S., & Gudmestad, O. T. (2018). Vessel stability in polar low situations: case study for semi-submersible drilling rigs. *Ships and Offshore Structures*, *13*(3), 303–309. https://doi.org/10.1080/17445302.2017.1372959

OSHA. (2016). *Recommended Practices for Safety and Health Programs* (p. 40). Occupational Safety and Health Administration. https://www.osha.gov/sites/default/files/OSHA3885.pdf

Oshiro, R. E., & Alves, M. (2004). Scaling impacted structures. *Archive of Applied Mechanics*, *74*(1), 130–145. https://doi.org/10.1007/s00419-004-0343-8

Oshiro, R. E., & Alves, M. (2012). Predicting the behaviour of structures under impact loads using geometrically distorted scaled models. *Journal of the Mechanics and Physics of*

Solids, *60*(7), 1330–1349. https://doi.org/10.1016/j.jmps.2012.03.005

Otto, S., Pedersen, P. T., Samuelides, M. S., & Sames, P. C. (2002). Elements of risk analysis for collision and grounding of a RoRo passenger ferry. *Marine Structures*, *15*(4), 461–474. https://doi.org/https://doi.org/10.1016/S0951-8339(02)00014-X

Ozbas, B. (2013). Safety Risk Analysis of Maritime Transportation: Review of the Literature. *Transportation Research Record*, *2326*(1), 32–38. https://doi.org/10.3141/2326-05

Ozturk, U., Birbil, S. I., & Cicek, K. (2019). Evaluating navigational risk of port approach manoeuvrings with expert assessments and machine learning. *Ocean Engineering*, *192*, 106558. https://doi.org/10.1016/J.OCEANENG.2019.106558

Pack, K., & Mohr, D. (2017). Combined necking & fracture model to predict ductile failure with shell finite elements. *Engineering Fracture Mechanics*, *182*, 32–51. https://doi.org/10.1016/J.ENGFRACMECH.2017.06.025

Paik, J. K. (2017). Collision risk assessment of a VLCC class tanker. *Transactions of the Society of Naval Architects and Marine Engineers*.

Paik, J. K. (2020a). Computational models for gas cloud temperature analysis in fires. In *Topics in Safety, Risk, Reliability and Quality* (Vol. 37). https://doi.org/10.1007/978-981-13-8245-1_8

Paik, J. K. (2020b). Computational models for structural crashworthiness analysis in fires. In *Topics in Safety, Risk, Reliability and Quality* (Vol. 37). https://doi.org/10.1007/978-981-13-8245-1_12

Paik, J. K. (2020c). *Quantitative Collision Risk Assessment and Management - Advanced Structural Safety Studies: With Extreme Conditions and Accidents* (J. K. Paik (ed.); pp. 417–474). Springer Singapore. https://doi.org/10.1007/978-981-13-8245-1_14

Paik, J. K. (2020d). *Quantitative Grounding Risk Assessment and Management BT - Advanced Structural Safety Studies: With Extreme Conditions and Accidents* (J. K. Paik (ed.); pp. 475–506). Springer Singapore. https://doi.org/10.1007/978-981-13-8245-1_15

Paik, J. K., Czujko, J., Kim, B. J., Seo, J. K., Ryu, H. S., Ha, Y. C., Janiszewski, P., & Musial, B. (2011). Quantitative assessment of hydrocarbon explosion and fire risks in offshore installations. *Marine Structures*, *24*(2), 73–96. https://doi.org/https://doi.org/10.1016/j.marstruc.2011.02.002

Paik, J. K., Kim, K. J., Lee, J. H., Jung, B. G., & Kim, S. J. (2017). Test database of the mechanical properties of mild, high-tensile and stainless steel and aluminium alloy associated with cold temperatures and strain rates. *Ships and Offshore Structures*, *12*(sup1), S230–S256. https://doi.org/10.1080/17445302.2016.1262729

Paik, J. K., Lee, D. H., Noh, S. H., Park, D. K., & Ringsberg, J. W. (2020a). Full-scale collapse testing of a steel stiffened plate structure under cyclic axial-compressive loading. *Structures*, *26*, 996–1009. https://doi.org/10.1016/J.ISTRUC.2020.05.026

Paik, J. K., Lee, D. H., Noh, S. H., Park, D. K., & Ringsberg, J. W. (2020b). Full-scale collapse testing of a steel stiffened plate structure under axial-compressive loading triggered by brittle fracture at cryogenic condition. *Ships and Offshore Structures*, *15*(sup1), S29–S45. https://doi.org/10.1080/17445302.2020.1787930

Paik, J. K., Lee, D. H., Park, D. K., & Ringsberg, J. W. (2021). Full-scale collapse testing of a steel stiffened plate structure under axial-compressive loading at a temperature of −80°C. *Ships and Offshore Structures*, 1–16. https://doi.org/10.1080/17445302.2020.1791685

Paik, J. K., & Park, J. H. (2020). Impact crashworthiness of a floating offshore nuclear power plant hull structure in a terrorist attack with an aircraft strike. *Ships and Offshore Structures*, *15*(sup1), S176–S189. https://doi.org/10.1080/17445302.2020.1757197

Paik, J. K., Ryu, M. G., He, K., Lee, D. H., Lee, S. Y., Park, D. K., & Thomas, G. (2021a). Full-scale fire testing to collapse of steel stiffened plate structures under lateral patch loading (part 1)–without passive fire protection. *Ships and Offshore Structures*, *16*(3), 227–242. https://doi.org/10.1080/17445302.2020.1764705

Paik, J. K., Ryu, M. G., He, K., Lee, D. H., Lee, S. Y., Park, D. K., & Thomas, G. (2021b). Full-

scale fire testing to collapse of steel stiffened plate structures under lateral patch loading (part 2)–with passive fire protection. *Ships and Offshore Structures*, *16*(3), 243–254. https://doi.org/10.1080/17445302.2020.1764706

Paik, J. K., & Shin, Y. S. (2006). Structural damage and strength criteria for ship stiffened panels under impact pressure actions arising from sloshing, slamming and green water loading. *Ships and Offshore Structures*, *1*(3), 249–256. https://doi.org/10.1533/saos.2006.0109

Pangestu, L. A., Ng, C. Y., Kajuputra, A. E., Muzammil, M. K., & Sabtu, S. (2020). *Wave-in-Deck Force on Fixed Jacket Platforms by Silhoutte Method and Detailed Component Method BT - Advancement in Emerging Technologies and Engineering Applications* (C. L. Saw, T. K. Woo, S. S. a/l Karam Singh, & D. Asmara Bin Salim (eds.); pp. 415–429). Springer Singapore.

Park, Y. IL. (2019). Ultimate crushing strength criteria for GTT NO96 LNG carrier cargo containment system under sloshing load. *Ocean Engineering*, *188*, 106224. https://doi.org/10.1016/J.OCEANENG.2019.106224

Pedersen, P. T. (2010). Review and application of ship collision and grounding analysis procedures. In *Marine Structures* (Vol. 23, Issue 3, pp. 241–262). https://doi.org/https://doi.org/10.1016/j.marstruc.2010.05.001

Pedersen, P. T., & Zhang, S. (1998). Absorbed energy in ship collisions and grounding : Revising Minorsky's empirical method. *Journal of Ship Research*, *44*, 140–154.

Peng, Q., Wu, H., Zhang, R. F., & Fang, Q. (2021). Numerical simulations of base-isolated LNG storage tanks subjected to large commercial aircraft crash. *Thin-Walled Structures*, *163*, 107660. https://doi.org/10.1016/J.TWS.2021.107660

Perez-Martin, M. J., Holmen, J. K., Thomesen, S., Hopperstad, O. S., & Børvik, T. (2019). Dynamic Behaviour of a High-Strength Structural Steel at Low Temperatures. *Journal of Dynamic Behavior of Materials*, *5*(3), 241–250. https://doi.org/10.1007/s40870-019-00206-x

Pineau, J.-P., & Le Sourne, H. (2021). *Rapid assessment of ship bottom sliding on paraboloid shaped rock* (pp. 254–261). https://doi.org/10.1201/9781003230373-30

Pineau, J.-P., Le Sourne, H., & Soulhi, Z. (2021). Rapid assessment of ship raking grounding on elliptic paraboloid shaped rock. *Ships and Offshore Structures*, *16*(sup1), 106–121. https://doi.org/10.1080/17445302.2021.1927357

Pire, T., Echeverry Jaramillo, S., Rigo, P., Buldgen, L., & Le Sourne, H. (2017). *Validation of a simplified method for the crashworthiness of offshore wind turbine jackets using finite elements simulations*. https://doi.org/10.1201/9781315157368-57

Pire, T., Le Sourne, H., Echeverry, S., & Rigo, P. (2018). Analytical formulations to assess the energy dissipated at the base of an offshore wind turbine jacket impacted by a ship. *Marine Structures*, *59*, 192–218. https://doi.org/https://doi.org/10.1016/j.marstruc.2018.02.002

Popov, Y. N., Faddeev, O. V., Kheisin, D. E., & Yakovlev, A. A. (1969). *Strength of ships sailing in ice* (p. 233). Defense Technical Information Center.

Popov, Y. N., Faddeyev, 0. V., Kheysin, D. Y., & Yakovlev, A. A. (1967). *Strength of ships sailing in ice*. Sudostroyeniye Publishing House.

Porathe, T., Hoem, Å., Rødseth, Ø. J., Fjørtoft, K., & Johnsen, S. O. (2018). At least as safe as manned shipping? Autonomous shipping, safety and "human error." In *Safety and Reliability – Safe Societies in a Changing World* (p. 9). CRC Press. https://www.taylorfrancis.com/chapters/oa-edit/10.1201/9781351174664-52/least-safe-manned-shipping-autonomous-shipping-safety-human-error-porathe-hoem-rødseth-fjørtoft-johnsen

Porfiri, M., & Gupta, N. (2009). A review of research on impulsive loading of marine composites. In *Major Accomplishments in Composite Materials and Sandwich Structures: An Anthology of ONR Sponsored Research*. https://doi.org/10.1007/978-90-481-3141-9_8

Price, A., Quinton, B. W. T., & Veitch, B. (2021). Shared-Energy Prediction Model for Ship-Ice Interactions. In *SNAME Maritime Convention* (p. D021S004R005).

https://doi.org/10.5957/SMC-2021-033

Prosertek. (2020). *5 challenges the maritime transport industry must face due to COVID-19*. Webpage. https://prosertek.com/en/blog/challenges-maritime-transport-covid-19/

Pu, Q., Liu, J., Gou, H., Bao, Y., & Xie, H. (2019). Finite element analysis of long-span rail-cum-road cable-stayed bridge subjected to ship collision. *Advances in Structural Engineering*, *22*(11), 2530–2542. https://doi.org/10.1177/1369433219846953

Purba, P. H., Dinariyana, A. A. B., Handani, D. W., & Rachman, A. F. (2020). Application of Formal Safety Assessment for Ship Collision Risk Analysis in Surabaya West Access Channel. *IOP Conference Series: Earth and Environmental Science*, *557*(1), 12034. https://doi.org/10.1088/1755-1315/557/1/012034

Qu, X., Meng, Q., & Suyi, L. (2011). Ship collision risk assessment for the Singapore Strait. *Accident Analysis & Prevention*, *43*(6), 2030–2036. https://doi.org/https://doi.org/10.1016/j.aap.2011.05.022

Qu, X., Yang, Y., Liu, Z., Jin, S., & Weng, J. (2014). Potential crash risks of expressway on-ramps and off-ramps: A case study in Beijing, China. *Safety Science*, *70*, 58–62. https://doi.org/https://doi.org/10.1016/j.ssci.2014.04.016

Quinton, B. W. T. (2015). *Experimental and Numerical Investigation of Moving Loads on Hull Structures: Vol. PhD*. Memorial University of Newfoundland.

Quinton, B. W. T., Daley, C. G., Gagnon, R. E., & Colbourne, D. B. (2017). Guidelines for the nonlinear finite element analysis of hull response to moving loads on ships and offshore structures. *Ships and Offshore Structures*, *12*. https://doi.org/10.1080/17445302.2016.1261391

Ramberg, H. F. (2011). *High energy ship collisions with bottom supported offshore wind turbines*. Norges Teknisk-Naturvitenskapelige Universitet.

Ren, L., Ma, H., Shen, Z., Wang, Y., & Zhao, K. (2019). Blast resistance of water-backed metallic sandwich panels subjected to underwater explosion. *International Journal of Impact Engineering*, *129*, 1–11. https://doi.org/https://doi.org/10.1016/j.ijimpeng.2019.02.009

Rippe, C. M., & Lattimer, B. Y. (2021). Post-fire modeling of aluminum structures using a kinetic driven approach. *Fire Safety Journal*, *120*, 103132. https://doi.org/https://doi.org/10.1016/j.firesaf.2020.103132

Rødseth, Ø. J., & Burmeister, H.-C. (2015). Risk Assessment for an Unmanned Merchant Ship. *TransNav, the International Journal on Marine Navigation and Safety of Sea Transportation*, *9*(3), 357–364. https://doi.org/10.12716/1001.09.03.08

Røed, W., Mosleh, A., Vinnem, J. E., & Aven, T. (2009). On the use of the hybrid causal logic method in offshore risk analysis. *Reliability Engineering & System Safety*, *94*(2), 445–455. https://doi.org/https://doi.org/10.1016/j.ress.2008.04.003

Rudan, S., Ćatipović, I., Berg, R., Völkner, S., & Prebeg, P. (2019). Numerical study on the consequences of different ship collision modelling techniques. *Ships and Offshore Structures*, *14*(sup1), 387–400. https://doi.org/10.1080/17445302.2019.1615703

Ryu, M. G., He, K., Lee, D. H., Park, S.-I., Thomas, G., & Paik, J. K. (2021). Finite element modeling for the progressive collapse analysis of steel stiffened-plate structures in fires. *Thin-Walled Structures*, *159*. https://doi.org/10.1016/j.tws.2020.107262

Sadeghi, H., Davey, K., Darvizeh, R., & Darvizeh, A. (2019). Scaled models for failure under impact loading. *International Journal of Impact Engineering*, *129*(Complete), 36–56. https://doi.org/10.1016/j.ijimpeng.2019.02.010

Safety4sea. (2018). *Ship collision risk increases as China sees more fishery farms*. Website. https://safety4sea.com/ship-collision-risk-increases-as-china-sees-more-fishery-farms/?__cf_chl_jschl_tk__=pmd_62PvrZz_PRYbwMsDyuMlPMrKcZIoBmPyX2ZI4RvsU3Y-1633803705-0-gqNtZGzNAlCjcnBszQi9

Samuelides, M. S., Ventikos, N., & Gemelos, I. C. (2009). Survey on grounding incidents: Statistical analysis and risk assessment. *Ships and Offshore Structures*, *4*(1), 55–68.

https://doi.org/10.1080/17445300802371147
Samuelsen, E. M., Edvardsen, K., & Graversen, R. G. (2017). Modelled and observed sea-spray icing in Arctic-Norwegian waters. *Cold Regions Science and Technology*, *134*, 54–81. https://doi.org/10.1016/J.COLDREGIONS.2016.11.002
Sazidy, M. S. (2015). *Development of Velocity Dependent Ice Flexural Failure Model and Application to Safe Speed* [Memorial University of Newfoundland]. http://research.library.mun.ca/id/eprint/8452
Schiffer, A., & Tagarielli, V. L. (2014). The dynamic response of composite plates to underwater blast: Theoretical and numerical modelling. *International Journal of Impact Engineering*, *70*, 1–13. https://doi.org/https://doi.org/10.1016/j.ijimpeng.2014.03.002
Schiffer, A., & Tagarielli, V. L. (2015). The response of circular composite plates to underwater blast: Experiments and modelling. *Journal of Fluids and Structures*, *52*, 130–144. https://doi.org/10.1016/J.JFLUIDSTRUCTS.2014.10.009
Schuler, M. (2021). *Yara Debuts Yara Birkeland, the World's First Autonomous and Emission-Free Containership*. GCaptain.
Seo, B., Truong, D. D., Cho, S.-R., Kim, D., Park, S.-K., & Shin, H. (2018). A study on accumulated damage of steel wedges with dead-rise 10 due to slamming loads. *International Journal of Naval Architecture and Ocean Engineering*.
Sha, Y., & Amdahl, J. (2019). A simplified analytical method for predictions of ship deckhouse collision loads on steel bridge girders. *Ships and Offshore Structures*, *14*(sup1), 121–134. https://doi.org/10.1080/17445302.2018.1560881
Sha, Y., Amdahl, J., & Dørum, C. (2017). Dynamic responses of a floating bridge subjected to ship collision load on bridge girders. *Procedia Engineering*, *199*, 2506–2513. https://doi.org/10.1016/J.PROENG.2017.09.425
Sha, Y., Amdahl, J., & Dørum, C. (2019). Local and Global Responses of a Floating Bridge Under Ship–Girder Collisions. *Journal of Offshore Mechanics and Arctic Engineering*, *141*(3). https://doi.org/10.1115/1.4041992
Sha, Y., Amdahl, J., & Liu, K. (2019). Design of steel bridge girders against ship forecastle collisions. *Engineering Structures*, *196*, 109277. https://doi.org/https://doi.org/10.1016/j.engstruct.2019.109277
Shams, A., Lopresto, V., & Porfiri, M. (2017). Modeling fluid-structure interactions during impact loading of water-backed panels. *Composite Structures*, *171*, 576–590. https://doi.org/10.1016/J.COMPSTRUCT.2017.02.098
Shen, H., Hashimoto, H., Matsuda, A., Taniguchi, Y., Terada, D., & Guo, C. (2019). Automatic collision avoidance of multiple ships based on deep Q-learning. *Applied Ocean Research*, *86*, 268–288. https://doi.org/10.1016/J.APOR.2019.02.020
Shin, H., Seo, B., & Cho, S.-R. (2018). Experimental investigation of slamming impact acted on flat bottom bodies and cumulative damage. *International Journal of Naval Architecture and Ocean Engineering*, *10*(3), 294–306. https://doi.org/https://doi.org/10.1016/j.ijnaoe.2017.06.004
Siddharth, B., Hallowell, M. R., Van Boven, L., Welker, K. M., Golparvar-Fard, M., & Gruber, J. (2020). Using Augmented Virtuality to Examine How Emotions Influence Construction-Hazard Identification, Risk Assessment, and Safety Decisions. *Journal of Construction Engineering and Management*, *146*(2), 4019102. https://doi.org/10.1061/(ASCE)CO.1943-7862.0001755
Skoglund, V. J. (1967). *Similitude: Theory and Applications*. International Textbook Company.
Snyman, I. M. (2010). Impulsive loading events and similarity scaling. *Engineering Structures*, *32*(3), 886–896. https://doi.org/10.1016/j.engstruct.2009.12.014
Sone Oo, Y. P., Le Sourne, H., & Dorival, O. (2020). On the applicability of Taylor's theory to the underwater blast response of composite plates. *International Journal of Impact Engineering*, *145*, 103677. https://doi.org/10.1016/J.IJIMPENG.2020.103677
Sone Oo, Y. P., Le Sourne, H., & Dorival, O. (2021a). Development of Analytical Formulae to

Determine the Response of Submerged Composite Plates Subjected to Underwater Explosion. In *Lecture Notes in Civil Engineering: Vol. 64 LNCE*. https://doi.org/10.1007/978-981-15-4672-3_17

Sone Oo, Y. P., Le Sourne, H., & Dorival, O. (2021b). A coupled closed-form/Doubly Asymptotic Approximation approach for the response of orthotropic plates subjected to an underwater explosion. *Ships and Offshore Structures*, *16*(sup1), 171–185. https://doi.org/10.1080/17445302.2021.1918962

Song, M., Jiang, Z., & Yuan, W. (2021). Numerical and analytical analysis of a monopile-supported offshore wind turbine under ship impacts. *Renewable Energy*, *167*, 457–472. https://doi.org/https://doi.org/10.1016/j.renene.2020.11.102

Song, M., Kim, E., Amdahl, J., Ma, J., & Huang, Y. (2016). A comparative analysis of the fluid-structure interaction method and the constant added mass method for ice-structure collisions. *Marine Structures*, *49*, 58–75. https://doi.org/https://doi.org/10.1016/j.marstruc.2016.05.005

Song, Q., Dong, Y., Cui, M., & Yu, B. (2017). A similarity method for predicting the residual velocity and deceleration of projectiles during impact with dissimilar materials. *Advances in Mechanical Engineering*, *9*(7). https://doi.org/10.1177/1687814017705598

Song, Y., & Wang, J. (2019). Development of the impact force time-history for determining the responses of bridges subjected to ship collisions. *Ocean Engineering*, *187*, 106182. https://doi.org/https://doi.org/10.1016/j.oceaneng.2019.106182

Sormunen, O.-V., Kõrgesaar, M., Tabri, K., Heinvee, M., Urbel, A., & Kujala, P. (2016). Comparing rock shape models in grounding damage modelling. *Marine Structures*, *50*, 205–223.

Standards Norway. (2009). *NS 9415:2009 Marine fish farms: Requirements for site survey, risk analyses, design, dimensioning, production, installation and operation*.

Storheim, M., Alsos, H. S., & Amdahl, J. (2018). Evaluation of Nonlinear Material Behavior for Offshore Structures Subjected to Accidental Actions. *Journal of Offshore Mechanics and Arctic Engineering*, *140*(4). https://doi.org/10.1115/1.4038585

Storheim, M., & Dørum, C. (2018). *An Evaluation of Submarine Collisions to a TLP*. *Volume 3:* https://doi.org/10.1115/OMAE2018-78364

Storheim, M., & Lian, G. (2018). An Assessment of Load and Response for Horizontal Slamming Loads From Model Scale Experiments. In *ASME 2018 37th International Conference on Ocean, Offshore and Arctic Engineering*. https://doi.org/10.1115/OMAE2018-78355

Storheim, M., Notaro, G., Johansen, A., & Amdahl, J. (2016). *Comparison of ABAQUS and LS-DYNA in simulations of ship collisions*.

Szłapczyński, R., & Niksa-Rynkiewicz, T. (2018). A Framework of A Ship Domain-Based Near-Miss Detection Method Using Mamdani Neuro-Fuzzy Classification. *Polish Maritime Research*, *25*(s1), 14–21. https://doi.org/doi:10.2478/pomr-2018-0017

Szłapczyński, R., & Szlapczynska, J. (2016). An analysis of domain-based ship collision risk parameters. *Ocean Engineering*, *126*, 47–56. https://doi.org/https://doi.org/10.1016/j.oceaneng.2016.08.030

Tabri, K., Naar, H., & Kõrgesaar, M. (2020). Ultimate strength of ship hull girder with grounding damage. *Ships and Offshore Structures*, *15*(sup1), S161–S175. https://doi.org/10.1080/17445302.2020.1827631

Taylor, G. I. (1963). The pressure and impulse of submarine explosion waves on plates. *The Scientific Papers of GI Taylor*, *3*, 287–303.

Terndrup Pedersen, P., & Zhang, S. (1998). On Impact mechanics in ship collisions. *Marine Structures*, *11*(10), 429–449. https://doi.org/https://doi.org/10.1016/S0951-8339(99)00002-7

Thieme, C. A., Utne, I. B., & Haugen, S. (2018). Assessing ship risk model applicability to Marine Autonomous Surface Ships. *Ocean Engineering*, *165*, 140–154. https://doi.org/https://doi.org/10.1016/j.oceaneng.2018.07.040

Tran, P., Wu, C., Saleh, M., Bortolan Neto, L., Nguyen-Xuan, H., & Ferreira, A. J. M. (2021). Composite structures subjected to underwater explosive loadings: A comprehensive review. *Composite Structures*, *263*. https://doi.org/10.1016/j.compstruct.2021.113684

Travanca, J., & Hao, H. (2014). Dynamics of steel offshore platforms under ship impact. *Applied Ocean Research*, *47*, 352–372.

Travanca, J., & Hao, H. (2015). Energy dissipation in high-energy ship-offshore jacket platform collisions. *Marine Structures*, *40*, 1–37.

Truong, D. D., Jang, B.-S., Janson, C.-E., Ringsberg, J. W., Yamada, Y., Takamoto, K., Kawamura, Y., & Ju, H.-B. (2021). Benchmark study on slamming response of flat-stiffened plates considering fluid-structure interaction. *Marine Structures*, *79*, 103040. https://doi.org/https://doi.org/10.1016/j.marstruc.2021.103040

Truong, D. D., Jang, B.-S., Ju, H.-B., & Han, S. W. (2020). Prediction of slamming pressure considering fluid-structure interaction. Part I: numerical simulations. *Ships and Offshore Structures*, 1–22. https://doi.org/10.1080/17445302.2020.1816732

Truong, D. D., Shin, H. K., & Cho, S.-R. (2018). Permanent set evolution of aluminium-alloy plates due to repeated impulsive pressure loadings induced by slamming. *Journal of Marine Science and Technology*, *23*(3), 580–595. https://doi.org/10.1007/s00773-017-0494-2

Tu, S., Ren, X., Kristensen, T. A., He, J., & Zhang, Z. (2018). Study of low-temperature effect on the fracture locus of a 420-MPa structural steel with the edge tracing method. *Fatigue & Fracture of Engineering Materials & Structures*, *41*(8), 1649–1661. https://doi.org/https://doi.org/10.1111/ffe.12803

Turner, S. E., & Ambrico, J. M. (2012). Underwater Implosion of Cylindrical Metal Tubes. *Journal of Applied Mechanics*, *80*(1). https://doi.org/10.1115/1.4006944

USCG. (2019). *Report of the Marine Board of Investigation into the Commercial Fishing Vessel Destination Sinking and Loss of the Vessel with all Six Crewmembers Missing and Presumed Deceased Approximately 4.4 NM Northwest of St. George Island, Alaska on February 11, 20*. https://media.defense.gov/2019/Mar/03/2002095494/-1/-1/0/REPORT OF INVESTIGATION FISHING VESSEL DESTINATION.PDF

Utne, I. B., Rokseth, B., Sørensen, A. J., & Vinnem, J. E. (2020). Towards supervisory risk control of autonomous ships. *Reliability Engineering & System Safety*, *196*, 106757. https://doi.org/https://doi.org/10.1016/j.ress.2019.106757

Valdez Banda, O. A., & Goerlandt, F. (2018). A STAMP-based approach for designing maritime safety management systems. *Safety Science*, *109*, 109–129. https://doi.org/https://doi.org/10.1016/j.ssci.2018.05.003

Valdez Banda, O. A., Jalonen, R., Goerlandt, F., Montewka, J., & Kujala, P. (2014). *Hazard Identification in Winter Navigation*.

Valdez Banda, O. A., Kannos, S., Goerlandt, F., van Gelder, P. H. A. J. M., Bergström, M., & Kujala, P. (2019). A systemic hazard analysis and management process for the concept design phase of an autonomous vessel. *Reliability Engineering & System Safety*, *191*, 106584. https://doi.org/https://doi.org/10.1016/j.ress.2019.106584

Valdez Banda, O. A., Kujala, P., & Hirdaris, S. (2021). Virtual special Issue: Autonomous vessels safety. *Safety Science*, *136*, 105144. https://doi.org/https://doi.org/10.1016/j.ssci.2020.105144

van Biert, L., Godjevac, M., Visser, K., & Aravind, P. V. (2016). A review of fuel cell systems for maritime applications. *Journal of Power Sources*, *327*, 345–364. https://doi.org/10.1016/J.JPOWSOUR.2016.07.007

Van Hoecke, L., Laffineur, L., Campe, R., Perreault, P., Verbruggen, S. W., & Lenaerts, S. (2021). Challenges in the use of hydrogen for maritime applications. *Energy Environ. Sci.*, *14*(2), 815–843. https://doi.org/10.1039/D0EE01545H

Vassalos, D., Azzi, C., & Pennycott, A. (2010, January). Crisis Management Onboard Passenger Ships. *International Conference on Human Performance at Sea HPAS, 2010*.

Ventikos, N. (2013). Exploring Fire Incidents/Accidents Onboard Cruise and Passenger Ships.

SPOUDAI - Journal of Economics and Business, *63*(3–4), 146–157. https://spoudai.unipi.gr/index.php/spoudai/article/view/73

Ventikos, N., Lambrinakis, K., Nitsopoulos, S., & Lyridis, D. (2006). *Fires/Explosions Onboard Greek Vessels: The Hazards, the Records and the Statistical Trends*.

Veritec. (1988). *Handbook of Accidental Loads*.

Viste-Ollestad, I., Andersen, T. L., Oma, N., & Zachariassen, S. (2016). *Investigation of an incident with fatal consequences on COSLInnovator, 30 December 2015* (p. 47). Petroleum Safety Authority Norway.

Vredeveldt, A. W., Werter, N., Van Dijk, T., Van Den Boom, S., & Coppejans, O. (2021). Improving crashworthiness calculations for safe containment of hazardous fuels. *MARSTRUCT2021*.

Wahlström, M., Hakulinen, J., Karvonen, H., & Lindborg, I. (2015). Human Factors Challenges in Unmanned Ship Operations – Insights from Other Domains. *Procedia Manufacturing*, *3*, 1038–1045. https://doi.org/https://doi.org/10.1016/j.promfg.2015.07.167

Walters, C. L. (2014). Framework for adjusting for both stress triaxiality and mesh size effect for failure of metals in shell structures. *International Journal of Crashworthiness*, *19*(1), 1–12. https://doi.org/10.1080/13588265.2013.825366

Wan, Y., Zhu, L., Fang, H., Liu, W., & Mao, Y. (2019). Experimental testing and numerical simulations of ship impact on axially loaded reinforced concrete piers. *International Journal of Impact Engineering*, *125*, 246–262. https://doi.org/https://doi.org/10.1016/j.ijimpeng.2018.11.016

Wanchoo, P., Matos, H., Rousseau, C.-E., & Shukla, A. (2021). Investigations on air and underwater blast mitigation in polymeric composite structures – A review. *Composite Structures*, *263*. https://doi.org/10.1016/j.compstruct.2020.113530

Wang, C., Zhang, X., Cong, L., Li, J., & Zhang, J. (2019). Research on intelligent collision avoidance decision-making of unmanned ship in unknown environments. *Evolving Systems*, *10*(4), 649–658. https://doi.org/10.1007/s12530-018-9253-9

Wang, D., Fan, F., Zhi, X., & Shen, S. (2011). Experimental study on single-layer reticulated dome under impact. *Jianzhu Jiegou Xuebao/Journal of Building Structures*, *32*(8), 34–41.

Wang, Gaohui, Wang, Y., Lu, W., Zhou, W., Chen, M., & Yan, P. (2016). On the determination of the mesh size for numerical simulations of shock wave propagation in near field underwater explosion. *Applied Ocean Research*, *59*, 1–9. https://doi.org/10.1016/J.APOR.2016.05.011

Wang, Ge, Tang, S., & Shin, Y. S. (2002). Direct Calculation Approach And Design Criteria For Wave Slamming of an FPSO Bow. *International Journal of Offshore and Polar Engineering*, *12*(04).

Wang, L., Wang, J., Shi, M., Fu, S., & Zhu, M. (2021). Critical risk factors in ship fire accidents. *Maritime Policy & Management*, *48*(6), 895–913. https://doi.org/10.1080/03088839.2020.1821110

Wang, S., Xu, F., Zhang, X., Yang, L., & Liu, X. (2021). Material similarity of scaled models. *International Journal of Impact Engineering*, *156*. https://doi.org/10.1016/j.ijimpeng.2021.103951

Wang, Y.-F., Li, Y. L., Zhang, B., Yan, P. N., & Zhang, L. (2015). Quantitative Risk Analysis of Offshore Fire and Explosion Based on the Analysis of Human and Organizational Factors. *Mathematical Problems in Engineering*, *2015*, 537362. https://doi.org/10.1155/2015/537362

Wang, Y.-F., Wang, L.-T., Jiang, J.-C., Wang, J., & Yang, Z.-L. (2020). Modelling ship collision risk based on the statistical analysis of historical data: A case study in Hong Kong waters. *Ocean Engineering*, *197*, 106869. https://doi.org/https://doi.org/10.1016/j.oceaneng.2019.106869

Wei, D., & Hu, C. (2019). Scaling of An Impacted Reticulated Dome Using Partial Similitude Method. In *Latin American journal of solids and structures.* (Vol. 16, Issue 2). M Alves.

https://doi.org/10.1590/1679-78255342
Wiegard, B., & Ehlers, S. (2020). Pragmatic regularization of element-dependent effects in finite element simulations of ductile tensile failure initiation using fine meshes. *Marine Structures*, *74*, 102823. https://doi.org/10.1016/J.MARSTRUC.2020.102823
Wierzbicki, T., & Suh, M. S. (1988). Indentation of tubes under combined loading. *International Journal of Mechanical Sciences*, *30*(3), 229–248. https://doi.org/https://doi.org/10.1016/0020-7403(88)90057-4
Woelke, P. B. (2020). Simplification of the Gurson model for large-scale plane stress problems. *International Journal of Plasticity*, *125*, 331–347. https://doi.org/10.1016/J.IJPLAS.2019.10.004
Woelke, P. B., Londono, J., Knoerr, L., Dykeman, J., & Malcolm, S. (2018). Fundamental Differences between Fracture Behavior of Thin Sheets under Plane Strain Bending and Tension. *IOP Conference Series: Materials Science and Engineering*, *418*, 012078. https://doi.org/10.1088/1757-899X/418/1/012078
Wróbel, K., Krata, P., Montewka, J., & Hinz, T. (2016). Towards the Development of a Risk Model for Unmanned Vessels Design and Operations. *TransNav, the International Journal on Marine Navigation and Safety of Sea Transportation*, *10*(2), 267–274. https://doi.org/10.12716/1001.10.02.09
Wróbel, K., Montewka, J., & Kujala, P. (2017). Towards the assessment of potential impact of unmanned vessels on maritime transportation safety. *Reliability Engineering & System Safety*, *165*, 155–169. https://doi.org/https://doi.org/10.1016/j.ress.2017.03.029
Wróbel, K., Montewka, J., & Kujala, P. (2018). Towards the development of a system-theoretic model for safety assessment of autonomous merchant vessels. *Reliability Engineering & System Safety*, *178*, 209–224. https://doi.org/https://doi.org/10.1016/j.ress.2018.05.019
Wu, J., Chong, ji, Long, Y., Zhou, Y., Yu, Y., & Liu, J. (2018). Experimental study on the deformation and damage of cylindrical shell-water-cylindrical shell structures subjected to underwater explosion. *Thin-Walled Structures*, *127*, 654–665. https://doi.org/https://doi.org/10.1016/j.tws.2018.03.002
Wu, W. (武文斌), Zhang, A.-M. (张阿漫), Liu, Y.-L. (刘云龙), & Liu, M. (刘谋斌). (2020). Interaction between shock wave and a movable sphere with cavitation effects in shallow water. *Physics of Fluids*, *32*(1), 16103. https://doi.org/10.1063/1.5133991
Yan-jie, S. (2011). Study on influencing factors of risk of offshore platforms under fire and gas explosion disaster. *Ocean Engineering*.
Yang, Y., Bashir, M., Li, C., & Wang, J. (2021). Investigation on mooring breakage effects of a 5 MW barge-type floating offshore wind turbine using F2A. *Ocean Engineering*, *233*, 108887. https://doi.org/10.1016/J.OCEANENG.2021.108887
Yang, Z., Yang, Z., & Yin, J. (2018). Realising advanced risk-based port state control inspection using data-driven Bayesian networks. *Transportation Research Part A: Policy and Practice*, *110*, 38–56. https://doi.org/https://doi.org/10.1016/j.tra.2018.01.033
Youssef, S. A. M., & Paik, J. K. (2018). Hazard identification and scenario selection of ship grounding accidents. *Ocean Engineering*, *153*, 242–255. https://doi.org/https://doi.org/10.1016/j.oceaneng.2018.01.110
Yu, Z. (2017). *Hydrodynamic and structural aspects of ship collisions* [Norwegian University of Science and Technology]. http://hdl.handle.net/11250/2461937
Yu, Z., & Amdahl, J. (2018). A review of structural responses and design of offshore tubular structures subjected to ship impacts. *Ocean Engineering*, *154*, 177–203. https://doi.org/https://doi.org/10.1016/j.oceaneng.2018.02.009
Yu, Z., & Amdahl, J. (2021). A numerical solver for coupled dynamic simulation of glacial ice impacts considering hydrodynamic-ice-structure interaction. *Ocean Engineering*, *226*, 108827. https://doi.org/https://doi.org/10.1016/j.oceaneng.2021.108827
Yu, Z., Amdahl, J., Greco, M., & Xu, H. (2019a). Hydro-plastic response of beams and stiffened panels subjected to extreme water slamming at small impact angles, Part I: An analytical

solution. *Marine Structures*, *65*, 53–74. https://doi.org/https://doi.org/10.1016/j.marstruc.2019.01.002

Yu, Z., Amdahl, J., Greco, M., & Xu, H. (2019b). Hydro-plastic response of beams and stiffened panels subjected to extreme water slamming at small impact angles, part II: Numerical verification and analysis. *Marine Structures*, *65*, 114–133. https://doi.org/https://doi.org/10.1016/j.marstruc.2019.01.003

Yu, Z., Amdahl, J., Kristiansen, D., & Bore, P. T. (2019). Numerical analysis of local and global responses of an offshore fish farm subjected to ship impacts. *Ocean Engineering*, *194*, 106653. https://doi.org/10.1016/J.OCEANENG.2019.106653

Yu, Z., Amdahl, J., Rypestøl, M., & Cheng, Z. (2022). Numerical modelling and dynamic response analysis of a 10 MW semi-submersible floating offshore wind turbine subjected to ship collision loads. *Renewable Energy*, *184*, 677–699. https://doi.org/https://doi.org/10.1016/j.renene.2021.12.002

Yu, Z., Amdahl, J., & Sha, Y. (2018). Large inelastic deformation resistance of stiffened panels subjected to lateral loading. *Marine Structures*, *59*, 342–367. https://doi.org/https://doi.org/10.1016/j.marstruc.2018.01.005

Yu, Z., Cao, A., & Amdahl, J. (2021). Experimental and numerical validation of an analytical hydro-plastic model for the prediction of structural damage in extreme water slamming. In J. Amdahl & C. Guedes Soares (Eds.), *Developments in the Analysis and Design of Marine Structures: Proceedings of the 8th International Conference on Marine Structures (MARSTRUCT 2021, 7-9 June 2021, Trondheim, Norway)* (p. 8). CRC Press.

Yu, Z., Liu, Z., & Amdahl, J. (2019). Discussion of assumptions behind the external dynamic models in ship collisions and groundings. *Ships and Offshore Structures*, *14*(sup1), 45–62. https://doi.org/10.1080/17445302.2018.1556234

Yu, Z., Lu, W., van den Berg, M., Amdahl, J., & Løset, S. (2021). Glacial ice impacts: Part II: Damage assessment and ice-structure interactions in accidental limit states (ALS). *Marine Structures*, *75*, 102889. https://doi.org/https://doi.org/10.1016/j.marstruc.2020.102889

Yuan, Y., Wu, S., & Shen, B. (2021). A numerical simulation of the suppression of hydrogen jet fires on hydrogen fuel cell ships using a fine water mist. *International Journal of Hydrogen Energy*, *46*(24), 13353–13364. https://doi.org/10.1016/J.IJHYDENE.2021.01.130

Yue, X., Han, Z., Li, C., & Zhao, X. (2021). The study on structure design of fender of offshore wind turbine based on fractal feature during collision with ship. *Ocean Engineering*, *236*, 109100. https://doi.org/10.1016/J.OCEANENG.2021.109100

Zhang, S., Villavicencio, R., Zhu, L., & Pedersen, P. T. (2017). Impact mechanics of ship collisions and validations with experimental results. *Marine Structures*, *52*, 69–81.

Zhang, S., Villavicencio, R., Zhu, L., & Pedersen, P. T. (2019). Ship collision damage assessment and validation with experiments and numerical simulations. *Marine Structures*, *63*, 239–256. https://doi.org/https://doi.org/10.1016/j.marstruc.2018.09.005

Zhang, W., Wang, Y., & Du, J.-Y. (2010). Research on similarity of dynamic response of ship grillage subjected to transient load. *Binggong Xuebao/Acta Armamentarii*, *31*(SUPPL. 1), 172–178.

Zhang, Weibin, Feng, X., Goerlandt, F., & Liu, Q. (2020). Towards a Convolutional Neural Network model for classifying regional ship collision risk levels for waterway risk analysis. *Reliability Engineering & System Safety*, *204*, 107127. https://doi.org/10.1016/J.RESS.2020.107127

Zhang, X., Wang, C., Jiang, L., An, L., & Yang, R. (2021). Collision-avoidance navigation systems for Maritime Autonomous Surface Ships: A state of the art survey. *Ocean Engineering*, *235*, 109380. https://doi.org/10.1016/J.OCEANENG.2021.109380

Zhang, X., Wang, C., Liu, Y., & Chen, X. (2019). Decision-Making for the Autonomous Navigation of Maritime Autonomous Surface Ships Based on Scene Division and Deep Reinforcement Learning. *Sensors*, *19*(18). https://doi.org/10.3390/s19184055

Zhang, Y., & Hu, Z. Q. (2021). A nonlinear numerical simulation approach for the dynamic

response analysis of floating wind turbine under ship impact scenario. *8th International Conference on Marine Structures (MARSTRUCT 2021)*.

Zhang, Z. F., Wang, C., Wang, L. K., Zhang, A. M., & Silberschmidt, V. V. (2018). Underwater explosion of cylindrical charge near plates: Analysis of pressure characteristics and cavitation effects. *International Journal of Impact Engineering*, *121*, 91–105. https://doi.org/10.1016/J.IJIMPENG.2018.06.009

Zhao, J., Lu, J., Chen, X., Yan, Z., Yan, Y., & Sun, Y. (2022). High-fidelity data supported ship trajectory prediction via an ensemble machine learning framework. *Physica A: Statistical Mechanics and Its Applications*, *586*, 126470. https://doi.org/10.1016/J.PHYSA.2021.126470

Zhao, L., & Roh, M. Il. (2019). COLREGs-compliant multiship collision avoidance based on deep reinforcement learning. *Ocean Engineering*, *191*, 106436. https://doi.org/10.1016/J.OCEANENG.2019.106436

Zhu, L., Cai, W., Chen, M., Tian, Y., & Bi, L. (2020). Experimental and numerical analyses of elastic-plastic responses of ship plates under ice floe impacts. *Ocean Engineering*, *218*, 108174. https://doi.org/https://doi.org/10.1016/j.oceaneng.2020.108174

Zhu, L., Gao, J., & Li, Y. (2018). Numerical Analysis on the Response of Deck Plates Laterally Impacted by a Rectangular Indenter. In *ASME 2018 37th International Conference on Ocean, Offshore and Arctic Engineering*. https://doi.org/10.1115/OMAE2018-78023

Zu, M. A. A. (2019). *A Numerical Investigation of the Slamming Event Through FSI Analysis* [Chalmers tekniska högskola]. https://hdl.handle.net/20.500.12380/300346

APPENDIX A - BENCHMARK STUDY ON FULL-SCALE STIFFENED PANEL IMPACT AND FRACTURE WITH COMPLEX INDUCED STATE OF STRESS

A1 BENCHMARK SYNOPSIS

This benchmark study was affected by the COVID-19 pandemic restrictions in that the five required novel full-scale stiffened panel impact experiments and the associated mechanical properties experiments were substantially delayed. As such, the amount of time that benchmark participants had to participate was severely reduced, and only four participants contributed numerical predictions to the benchmark study. Therefore, the committee has decided not to print the results of the novel laboratory experiments at this time, so that the "blind" nature of the benchmark may be preserved and so the benchmark study may be extended to new participants. The complete benchmark study including experiment results and new participant contributions will be published later. Reported herein are the benchmark study details and the results of four participant contributions.

The benchmark scenario to be considered is the dynamic nonlinear full-scale structural response and fracture of a stiffened hull panel subject to an energy-limited medium-speed impact with two types of rigid indenters: smooth, and non-smooth. The smooth indenter nominally induces a biaxial state of stress in the impacted structure, throughout the entire impact. The non-smooth indenter nominally induces an evolving state of stress in the impacted structure as the impact progresses from start to finish.

The purpose of this benchmark is to determine whether existing FEA tools can accurately model fracture for structures undergoing changing/evolving states of stress during an impact. To support this benchmark study, five novel full-scale large double-pendulum impact experiments were conducted in Summer 2021 at Memorial University of Newfoundland (MUN). A stiffened panel was subject to three successive impacts using a smooth indenter. No fracture of any part of the stiffened panel was observed during any of the three impacts. Next, another stiffened panel with the same scantlings was subject to two successive impacts using a non-smooth indenter. The non-smooth indenter punched completely through the panel during the second impact. The experiment results of only the first impact with the smooth indenter, as well as various material properties data, were provided to the benchmark participants so that they might calibrate their numerical models. The benchmark participants were asked to numerically predict the behaviour of each of the five experiments (i.e., the 3 successive smooth indenter impacts, and the 2 successive non-smooth indenter impacts).

As the induced state of stress in actual ship collisions is a priori unknown, it is desired to know if a single finite element modeling approach can accurately predict hull fracture for impacts involving evolving states of stress. Therefore, if benchmark participants can accurately predict the impact force, residual displacement, and hull fracture (or lack thereof) for all five experiments, then this success indicates that the current state of the art for finite element analysis is sufficient to model ship hull fracture for evolving states of impact induced structural stress.

A2 INTRODUCTION

Ship collision, allision, and grounding scenarios, as well as other accidental impacts (e.g., impact with a pier) have been the subject of many studies. Methods of assessing hull damage have evolved from Minorsky's method, through to simplified finite element analysis (FEA), through to fully nonlinear FEA. Recent developments in both computing power as well as available simulation technologies have enabled sophisticated nonlinear FEA of ship collisions to be performed in a reasonable amount of time. Several recent studies have compared the results of fully numerical FEA simulations of stiffened plate hull structures with similar laboratory experiments. In most of these experiments, the stiffened hull structure was loaded to fracture by a smooth spherical indenter using a hydraulic actuator. This approach tends to induce a state of stress of primarily quasi-static biaxial tension. Recent simulations of these experiments

produce results that are in good agreement with the experiments in terms of fracture initiation, fracture propagation, and structural failure mechanisms. There are limitations with this approach: 1. Fracture strain is known to be dependent on the state of stress at fracture. Specifically, fracture strain may be different for uniaxial tension, biaxial tension, plane strain tension, shear, and for combined states of stress; 2. Fracture strain criteria tend to be calibrated based on constant states of stress (e.g., bi-axial tension, or pure shear); 3. In practice, the body impacting a ship will likely not be a smooth spheroid, but instead have some non-optimal shape; thereby inducing localized stress states that may not be purely biaxial tension. Additionally, even with a smooth spherical indenter, any sliding or tearing motion of the indenter will induce a state of stress that is variable with time.

The objective of this benchmark study is to determine whether existing numerical modeling technologies are appropriate for predicting hull damage and fracture due to time-varying states of stress; or whether the development of new technologies are required. To accomplish this objective, five controlled laboratory impact experiments on two stiffened panel structures were conducted using MUN's large "limited-energy" double-pendulum impact apparatus: three successive impacts (no fracture) of a stiffened panel with a smooth spherical indenter; and two successive impacts to fracture of a stiffened panel with a non-smooth indenter.

Benchmark participants were given the results of the first smooth indenter impact to provide them a means of numerical model calibration. Benchmark participants were then asked to predict the impact force, residual displacement, and hull fracture (or lack thereof) for all five experiments.

A3 LABORATORY EXPERIMENTS

The limited-energy stiffened panel impact experiments were carried out at MUN, in the Summer of 2021, using the newly upgraded large double-pendulum apparatus (see Figure 8). The recent double-pendulum upgrades consist of a new extremely stiff pendulum carriage (right side of pendulum in Figure 8 (left)) capable of providing clamped boundary conditions for replaceable stiffened hull panels (see Figure 8 (right)). Further upgrades include the creation of interchangeable smooth and non-smooth rigid indenters.

The smooth indenter (Figure 9 (left)) is mounted to an extension arm that is connected to the indenter carriage (left side of pendulum in Figure 8 (left)). Its purpose is to induce a state of primarily biaxial tension in the impacted structure. Dimensions for the smooth indenter are given below in section 0. The non-smooth indenter (Figure 9 (right)) is interchangeable with the smooth indenter. Its purpose is to induce a state of stress in the impacted structure that evolves (with dramatic change) as the impact progresses with time. The non-smooth indenter consists of a spherical cap transitioning into a tetrahedron-like shape with hard chines. The spherical cap portion makes initial contact with the hull plating and nominally induces a state of biaxial tension in the impacted structure (similar to the smooth indenter), however, as the impact progresses, the hard chines and subsequent change in indenter shape (to the tetrahedron-like portion) evolved the induced state of stress to be a state of combined tension and shear. Dimensions for the non-smooth indenter are given below in section 0.

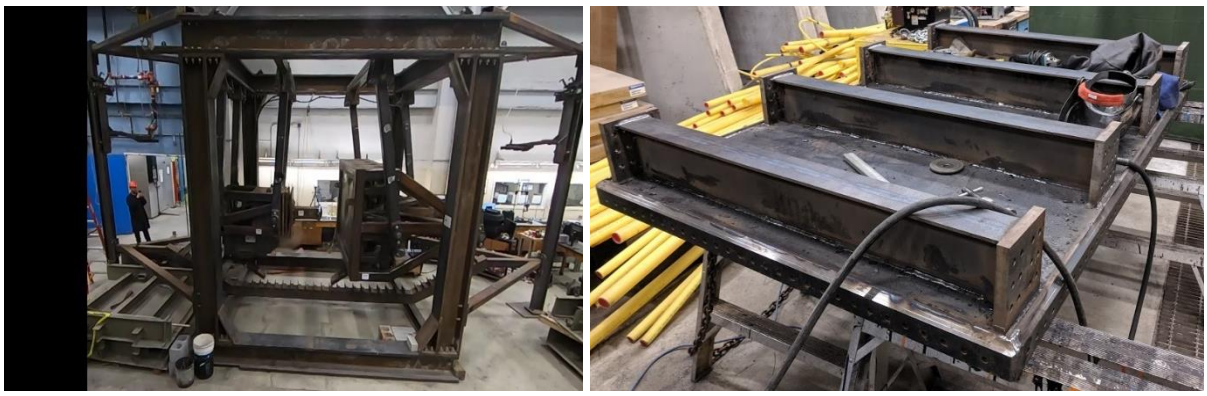

Figure 8: Large double-pendulum apparatus (left) and replaceable stiffened hull panel (right).

Figure 9: Smooth (left) and non-smooth (right) indenters shown mounted.

A3.1 Stiffened Panel Boundary Conditions and Dimensions

The impacted hull grillages used in the experiments are similar to Figure 8 (right). There are 4-stiffeners spaced equally. Thick steel end plates (visible in Figure 8 (right)) welded to the stiffeners are bolted to the panel carriage; thus, providing clamped boundary conditions to the stiffeners. Thick plate borders are welded to the stiffened panel plate boundaries, and are bolted to the panel carriage; thus, providing clamped boundary conditions to the plating. The bolts were tensioned prior to the experiments, and strain in the stiffened panels supporting carriage were monitored during the experiments. Results indicate that the panel carriage provided effective clamped boundary conditions to the stiffened panel.

If one assumes that the effect of the thick steel plates welded to the end of the stiffeners is negligible on the overall structural behaviour, then the stiffener webs and flanges may be considered to be the same length as the corresponding plate dimension. For this idealization, the dimensions of the stiffened panel are Plate: 2.032 x 1.36 x 0.0079 [m] (80 x 53.543 x 5/16 [in.]); Stiffener Web: 1.36 x 0.170 x 0.0079 [m] (53.543 x 6.688 x 5/16 [in.]); Stiffener Flange: 1.36 x 0.1016 x 0.0079 [m] (53.543 x 4.0 x 5/16 [in.]); and Stiffener Spacing: 609.45 mm (24 in.).

A3.2 Stiffened Panel Friction and Mechanical Properties

Mechanical properties were provided to participants in the following formats: data from indenter-plate friction experiments; steel grade requirements; mill certificate tensile tests; standard dogbone laboratory tensile tests; and two modified Mohr-Coulomb models generated from fracture experiments and FE modeling conducted at TUDelft were provided by TUDelft. All experiments were conducted using the same steel that the stiffened panels were constructed from. Benchmark participants were free to use whatever material data they preferred. Experiment data will be published with the complete benchmark study, at a later date.

A3.2.1 Friction data

Unlubricated steel-on-steel friction tests between the smooth indenter and a steel plate from the same plate steel used to create the stiffened hull panels were performed at MUN in July 2021. The average static and dynamic coefficients of friction were found to be 0.2598 and 0.1943, respectively.

A3.2.2 Steel grade requirements

The stiffened panel steel grade is CSA G40.21 300W (44W), requiring: a minimum yield strength of 300 MPa (44 ksi); an ultimate tensile strength of 450 to 585 MPa (65 to 85 ksi); and a minimum elongation of 23% in 50.8mm (2") gauge length and 20% min in 203.2mm (8") gauge length.

A3.2.3 Mill certificate mechanical properties

The steel for both stiffened panels was taken from the same production run. The Mill Certificate reports data for two tensile tests. For Test 1: yield strength is 324 MPa (47 ksi); ultimate tensile strength is 489.5 MPa (71 ksi); and minimum elongation is 26% min in 203.2mm (8") gauge length. For Test 2: yield strength is 351.6 MPa (51 ksi); tensile strength is 517.1 MPa (75 ksi); and minimum elongation is 24% min in 203.2mm (8") gauge length.

A3.2.4 Standard Dogbone Laboratory Tensile Tests

ASTM Standard (E8) flat "dogbone" shaped laboratory tensile tests were conducted at MUN. Tests were performed with full-thickness samples taken at 0° (i.e., parallel), 45°, and at 90° (i.e., perpendicular) to the rolling direction. The average material property values are given in Table 1.

Table 1: Average material property values for tensile test categories.

Category	E [GPa]	σ_y [MPa]	$\sigma_{avg,plateau}$ [MPa]	$\varepsilon_{plateau,max}$ [-]	ε_{ult} [MPa]	ε_{ult} [-]	ε_f [-]
0DEG Avg.	219.9	332.5	336.0	0.02093	495.9	0.19339	0.37660
45DEG Avg.	206.9	334.9	336.5	0.02126	495.9	0.19415	0.37027
90DEG Avg.	215.0	333.2	337.8	0.02103	497.4	0.19121	0.34915
Overall Avg.	214.0	333.6	336.8	0.02107	496.4	0.19291	0.36534

A3.2.5 TUDelft Modified Mohr-Coulomb models

TUDelft conducted fracture experiments and performed associated finite element modeling to generate two modified Mohr-Coulomb models for the steel used in these stiffened panels. The input parameters for these models are given in Table 2.

Table 2: Modified Mohr-Coulomb parameters.

Parameter	General Plasticity Model	von Mises Plasticity Model
A [MPa]	944	944
N [-]	0.29	0.29
c_1 [-]	0.06	0.06
c_2 [MPa]	537	543
c_3 [-]	0.99	-

A3.3 Smooth Indenter Dimensions

The smooth indenter consists of a spherical cap with radius 25.4 cm (10 in.) and height 5.08 cm (2 in.) on a cylinder with diameter 30.48 cm (12 in.) and height 2.54 cm (1.0 in.). The indenter is made of Hardox® 500 hardened steel (500 HBW) and may be considered to not have undergone plastic deformation during the impact. No material test data is available, but standard elastic steel parameters may be used. "Solid" CAD geometry of the smooth indenter was provided to the participants.

A3.4 Non-smooth Indenter Dimensions

The non-smooth indenter is a modified version of the smooth indenter. The top portion retains the spherical geometry with radius 25.4 cm (10 in.). The remainder has been shaped to provide discontinuous changes of curvature. The geometry is difficult to describe further, however the geometry was provided to participants as a "solid" CAD model. The indenter is made of Hardox® 500 hardened steel (500 HBW) and may be considered to not have undergone plastic deformation during the impact. No material test data is available, but standard elastic steel parameters may be used.

A3.5 Carriage Mass and Impact Speed Parameters

The total mass of the pendulum's indenter carriage was 4661 kg. The total mass of the pendulum's panel carriage (including the panel itself, which also includes the stiffener and plate boundary structure steel) was 4685 kg. All experiments began at a starting pendulum angle of 50° from the vertical axis. The horizontal impact speed at the point of initial impact as a function of starting pendulum angle is given by the formula:

$$\dot{x} = \sqrt{2gL \cdot (1 - \cos\theta)} \quad (1)$$

where: g is gravitational acceleration; L is the length of the pendulum arm; and θ is the staring angle (measured from the vertical axis).

At 50°: each pendulum carriage has a theoretical impact speed of 3.743 m/s; all actual experiment impact speeds (verified by highspeed digital image correlation) were within +5% of 3.743 m/s; the indenter pendulum carriage has a maximum kinetic energy of 32.66 kJ; the panel pendulum carriage has a maximum kinetic energy of 32.82 kJ; the total impact energy is the sum of the kinetic energies of both carriages, i.e., 65.48 kJ.

A3.6 Path of Pendulum Carriages prior to Impact

Referring to Figure 10, the origin (0,0) of the reference x-z axes is shown at the bottom of the black circle. This origin is the location of initial impact between the indenter and the stiffened panel.

The carriage supporting the grillage is depicted by the horizontal blue line on the left-hand side of the figure. The 2m long swingarms supporting the carriage are also shown in blue. The initial position of the stiffened panel is shown as point xg, zg. If one imagines the entire carriage, grillage, and swingarms as a simple pendulum with all masses lumped at point xg, zg, then the dashed blue line represents the effective pendulum arm for this simple pendulum.

The carriage supporting the indenter is depicted by the horizontal red line on the right-hand side of the figure. The 2m long swingarms supporting the carriage are also shown in red. The initial position of the indenter is shown as point xi, zi. If one imagines the entire carriage, indenter, and swingarms as a simple pendulum with all masses lumped at point xi, zi, then the dashed red line represents the pendulum arm for this simple pendulum.

Both carriages are shown at an initial starting position of 50° measured from a vertical axis. The blue and red dots on the lower part of the black circle (with radius 2m) depict the path that each carriage, respectively, must follow to the impact point.

As shown in Figure 10, the impact occurs as the result of two pendulums colliding (hence the term “double pendulum apparatus”). Each carriage acts as the mass of a simple pendulum. The displacement of each carriage (i.e., the motion of each pendulum mass) is prescribed by the equation of a circle defined by the length of the pendulum arms (2m). The vertical center of gravity for each carriage is coindicant with the lower end of the pendulum arms.

The point of impact occurs when both pendulum carriages are hanging vertically (i.e., as they would at rest). This implies that the initial impact occurs when both pendulum carriages are moving with maximum horizontal velocity and zero vertical velocity. This further implies that the effective pivot points for both pendulum arms are coincident (as shown in Figure 10). It is important to note that when the carriages move past this initial point of impact, they start to regain a vertical velocity component.

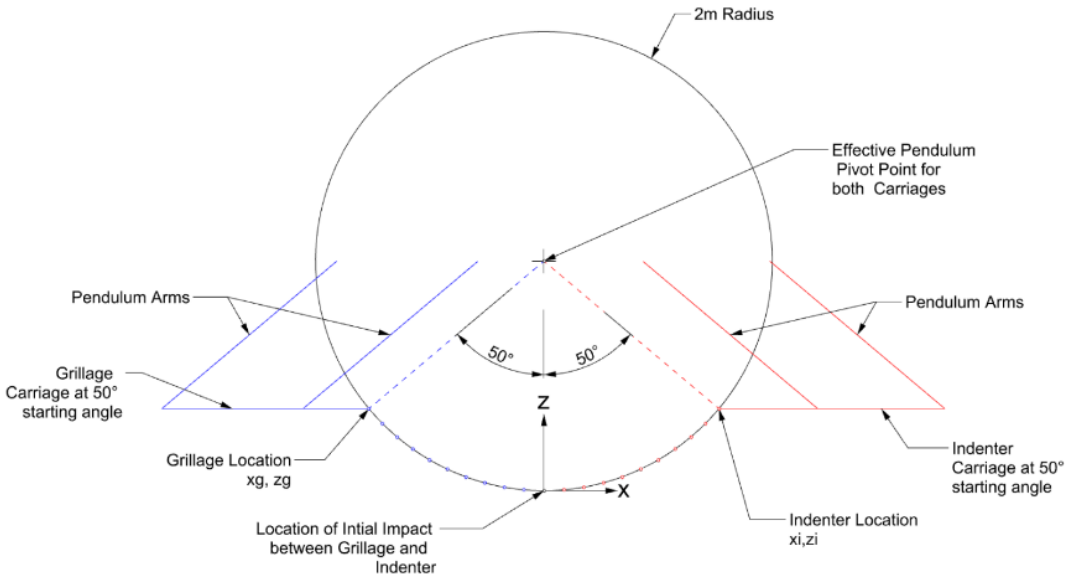

Figure 10: Pendulum Impact Details.

A3.7 Provided Experimental Results

Regarding experiments with the smooth indenter, three successive impacts were carried out on the same stiffened panel. No fracture was observed in the stiffened panel after each impact (and thus after all impacts).

Regarding the impact experiments with the non-smooth indenter, two successive impacts were carried out on the same stiffened panel. No fracture was observed after the 1st impact, but the imprint of the indenter was clearly outlined in the plating of the stiffened panel (see Figure 11 (left)). Fracture occurred during the second impact (see Figure 11 (right)).

Figure 11: Plating after 1st non-smooth impact (left) and after 2nd non-smooth impact (right)

A3.7.1 FEA calibration data for smooth indenter impact 1

The following experiment data for the 1st impact for the smooth indenter were provided to participants as means to calibrate their numerical model: impact force-time history; impact impulse time history; and residual dent depth as a function of distance from the center of the panel (i.e., the impact point). This data was given to participants in ".csv" format.

A3.8 Benchmark Results

As discussed above, the committee decided to extend this benchmark study to more participants and publish an expanded study, which is ongoing. In order to maintain the integrity of this "blind" benchmark study, the results of the experiments for the second and third smooth indenter impacts; as well as for both non-smooth indenter impacts are not reported here. Instead, the employed finite element methodologies, results of the calibration simulations, and numerical predictions for the remaining experiments by the four participants who contributed, to date, are to be presented.

A3.8.1 Numerical model details

The following refers to Table 3 below. All participants employed a double-precision explicit time-integration finite element solver. Three used 4-node reduced-integration shell elements, and one used fully integrated shell elements. All used 4-noded shells, however there is a considerable range in average element size: from 7.5 mm to 20 mm (excluding the 50 mm shells used by Participant 4 outside of the impact zone). However, for the non-smooth impacts, the average element size for three of the participants was similar at 7.5, 8, and 10 mm. Three participants utilized five through-thickness integration points, while one used two.

Table 3: Solver and element details

Participant	Solver	Element Type	Average Element Size	NIPS
1	LS-Dyna Explicit R11.0.0 DP	BT Shell 4-node	20 mm	5
2	LS-Dyna Explicit R9.3.1 DP	BT Shell 4-node w/ Stiffness HG	15 mm (smooth) 7.5 mm (non-smooth)	5
3	LS-Dyna Explicit R11.1 DP	Type 16 Shell 4-node w/ thinning	8 mm	2
4	Abaqus Explicit 2021hf6 DP	S4R Shell 4-node (except transitions)	10 mm (impact region) 50 mm (remainder)	5

DP=double precision; BT=Belytschko-Tsay; HG=hourglass control;
NIPS=# through-thickness int. pts.

Each participant modeled the ideal grillage (dimensions given above).

Regarding contact definitions, all participants employed a standard penalty contact formulation with sliding friction (using the provided values for static and dynamic friction), with the following exceptions: Participant 4 used a “softened” (scale-method) pressure-overclosure relationship for normal contact force calculations; and Participant 2 employed a split-pinball segment-based contact for the non-smooth experiment simulations.

Regarding pendulum carriage rigid body motion constraints, there was a range of methodologies employed. As mentioned above, a characteristic of the large double-pendulum apparatus is that both pendulum carriages swing in a circular path. While the motion of both carriages is exactly horizontal at the point of initial impact, once the pendulum carriages pass this point, they begin to regain vertical elevation (however slightly). The question arises as to whether participants should account (in some manner) for the vertical motion of the indenter and stiffened panel as both pass the initial point of impact. As the pendulum arms are 2m long, and the penetration of the indenter into the stiffened panel is comparably small, one might argue that a linear approximation is sufficient. Another question regarding pendulum carriage rigid body motion was whether to provide kinetic energy to both the indenter and the stiffened panel, or just one of the two and fix the other. The final consideration for rigid body motion of each pendulum carriage is that each carriage is supported by pendulum arms near its front and near its rear, and therefore the carriages do not rotate about their center of gravity as they swing.

Participant 1 chose to constrain all rigid body motions of the stiffened panel and impart an initial velocity of 3.931 m/s to only the indenter. Further, Participant 1 assumed linear motion for the first impact for each of the smooth and non-smooth cases. For each subsequent impact, Participant 1 resolved the horizontal and vertical velocity components at the new point of impact based on the residual deformation from the previous impact; however, a circular path for the indenter was not enforced. It should be noted that the mass of Participant 1’s indenter was not reported but would have had to equal the mass of both pendulum carriages in order to achieve the appropriate impact energy.

Participants 2 and 4 imparted an initial velocity of 3.743 m/s to both the indenter and the stiffened panel, and they both allowed for circular motion for both the indenter and the stiffened panel. They both enforced no rotation about the centers of gravity of the indenter and the stiffened panel.

Participant 3 allowed for only linear motion and imparted an initial velocity of 3.743 m/s to both the indenter and the stiffened panel.

Regarding boundary conditions for the stiffened panel: all Participants enforced a clamped boundary condition at the perimeter of the plate and at the ends of the stiffeners.

Regarding material modelling, each participant took a unique approach. Participant 1 employed a piecewise linear elasto-plastic material model (Mat_24 in LS-Dyna). They used the provided Ramberg-Osgood power law strain-hardening curve with an enforced Lüders plateau that was based on a 45DEG material tensile test (presented above) conducted at MUN. They employed Cowper-Symonds strain-rate hardening with parameters C=3200 and p=5. They employed an equivalent plastic failure strain of 0.207, based on Paik (2017), which initiated element erosion.

Participant 2 used a Hollomon-type power law hardening rule with an enforced Lüders plateau based on the material tensile tests conducted at MUN. They performed numerical tensile tests and found good agreement. They used a Bressan-Williams-Hill (BWH) instability failure criterion proposed by Alsos (2008) that incited element erosion. A through-thickness integration point is failed by setting the stresses to zero once the failure criterion is satisfied. Final element erosion occurs once the middle integration point fails.

Participant 3 used a piecewise linear elasto-plastic material model (Mat_24 in LS-Dyna). Their strain hardening data was Swift fit of a traditional true stress-strain conversion of the MUN 45° engineering stress-strain data, up to the maximum value, and then extended. An equivalent plastic failure strain of 0.36543 was the failure criterion, which induced element erosion. The participant did not disclose the method of determining the failure criterion.

Participant 4 used a J2 plasticity material model based on a Swift fit of the engineering stress-strain curve, including the Lüders plateau. They used 2FS-ex failure criteria based on Kõrgesaar (2019) and calibrated based on Walters' framework (Walters, 2014) using the material experiments conducted by TUDelft (discussed above). The failure criteria incited element erosion.

A4 RESULTS

As mentioned above, with the exception of "smooth indenter impact 1" (i.e., the data for which was sent to the participants), the participants' numerical predictions are compared with each other, but not with the actual experiment results. This was done at this point in time to maintain the integrity of the "blind" benchmark, so it may be extended to other participants for future publication.

Table 4 presents a summary of the participants numerical predictions for maximum impact force and residual dent depth for each of the five experiments (i.e., three consecutive impacts of one stiffened panel with the smooth indenter, and two consecutive impacts of another stiffened panel with the non-smooth indenter). The predictions for "Smooth 1" are also accompanied by the experimental results and associated prediction error. Regarding numerical model calibration, Participants 2, 3 and 4 predicted the peak impact force with excellent accuracy (<5% error). Residual dent depth (i.e., dent depth after removal of the impact force) was over-predicted in all cases by at least 10%, however participants were grouped into 96-97mm and 104-105mm bins. Regarding predictions for the remaining experiments, Participants 2, 3, and 4 predicted similar maximum impact force for all except the non-smooth indenter 2 impact. There was considerable scatter in prediction of residual dent depth for all participants. Participant 1 consistently predicted higher impact loads than the other participants. This may be partly due to the higher impact speed used, as well as the different impact mechanics associated with

their choice to fix the stiffened panel's rigid body motions. It is interesting to note that Participants 1 and 3 consistently predict lower residual dent depth than Participants 2 and 4. No failure was correctly predicted for the three consecutive smooth indenter impact simulations. All participants correctly predicted failure during the second non-smooth indenter impact for the second stiffened panel.

Table 4: Summary of results

Max Impact Force [kN]						
Participant	Smooth 1	Error	Smooth 2	Smooth 3	Non-smooth 1	Non-smooth 2
Experiment	1338	-	-	-	-	-
1	1607	20%	2156	2589	1614	1898
2	1378	3%	1873	2257	1337	1763
3	1380	3%	1870	2237	1305	1411
4	1395	4%	1812	2283	1328	1399
Residual Dent Depth [mm]						
Participant	Smooth 1	Error	Smooth 2	Smooth 3	Non-smooth 1	Non-smooth 2
Experiment	87	-	-	-	-	Fail
1	96.0	10%	128.7	153.8	99.7	Fail
2	104.0	20%	140.0	169.0	106.0	Fail
3	96.7	11%	116.1	128.0	95.8	Fail
4	104.9	21%	148.8	174.9	106.2	Fail

Figure 12 shows the results of the numerical predictions for impact force vs. time for the first stiffened panel impact with the smooth indenter. The experimental impact force is also given, as these data were provided to the participants to calibrate their numerical models. It is clear from the figure that the impact force and duration were captured well by Participants 2, 3 and 4. Participant 1 overestimated the impact force by approximately 20%, and the impact duration by approximately a factor of two. The latter is due to Participant 1's choice to hold the stiffened panel fixed in space instead of giving it an initial velocity.

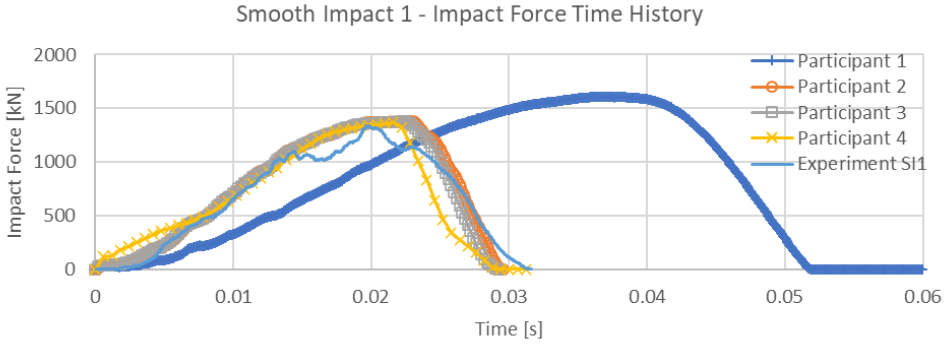

Figure 12: Experimental results and numerical predictions for "smooth impact 1"

Figure 13 shows impact force results for the second consecutive smooth indenter impact on the same stiffened panel. Participants 2 and 3 had very similar predictions. Participant 4's

prediction is initially much stiffer than the other participants, but their maximum impact force is comparable.

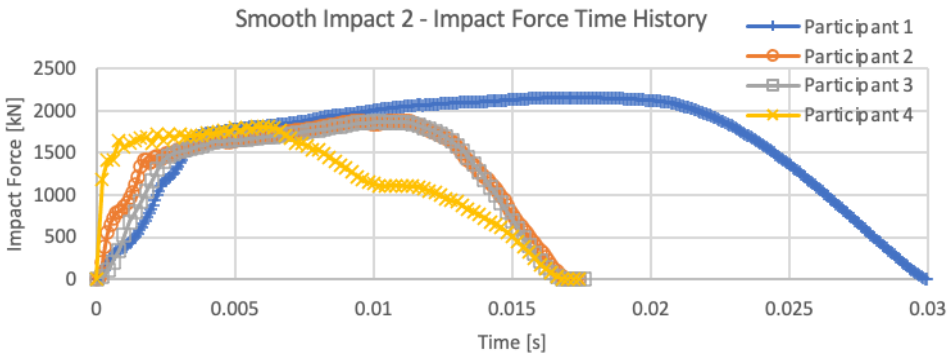

Figure 13: Experimental results and numerical predictions for "smooth impact 2"

Figure 14 shows impact force results for the third and final consecutive smooth indenter impact. The initial force spike in Participant 4's prediction is suspected to be due to a contact detection issue, and so this part of the curve is ignored regarding the peak force reported in Table 4. Again, Participants 2 and 3 provided very similar predictions.

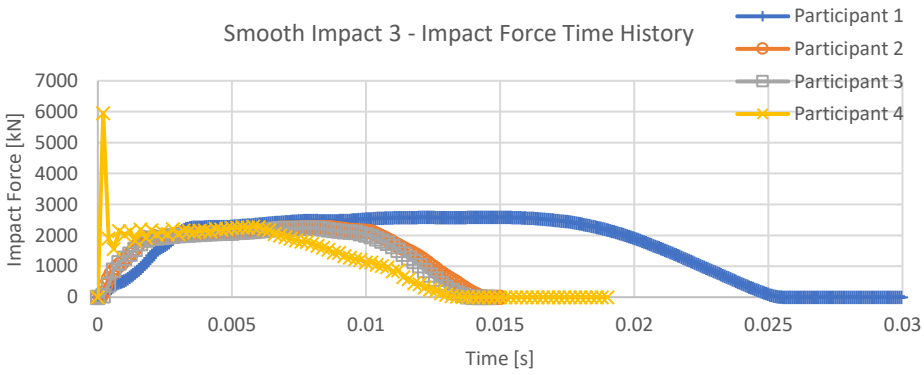

Figure 14: Experimental results and numerical predictions for "smooth impact 3"

Figure 15 shows impact force results for the first impact on a new stiffened panel using the non-smooth indenter. The predictions of Participants 2, 3, and 4 agree well.

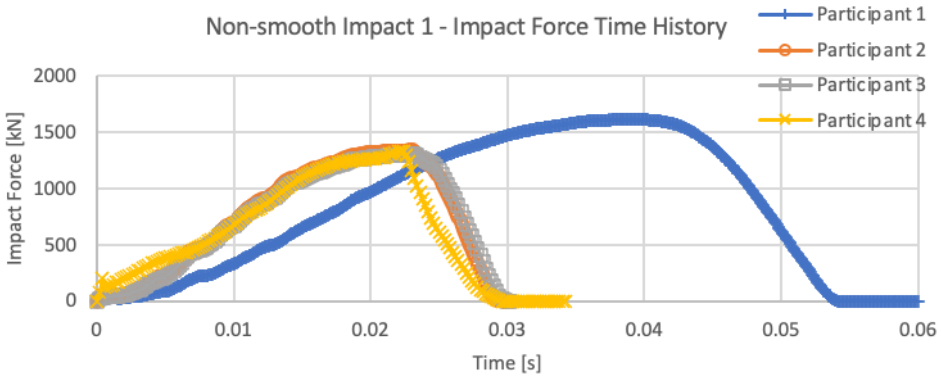

Figure 15: Experimental results and numerical predictions for "non-smooth impact 1"

Figure 16 shows impact force results for the second and final consecutive impact using the non-smooth indenter. All participants correctly predict complete punch-through fracture of the

indenter through the panel's plating. Participants 1 and 2 predict similar peak impact force; as do Participants 3 and 4, however there is a significant gap between both groups' predictions. There is no agreement regarding their prediction of the duration of the impact prior to punch through.

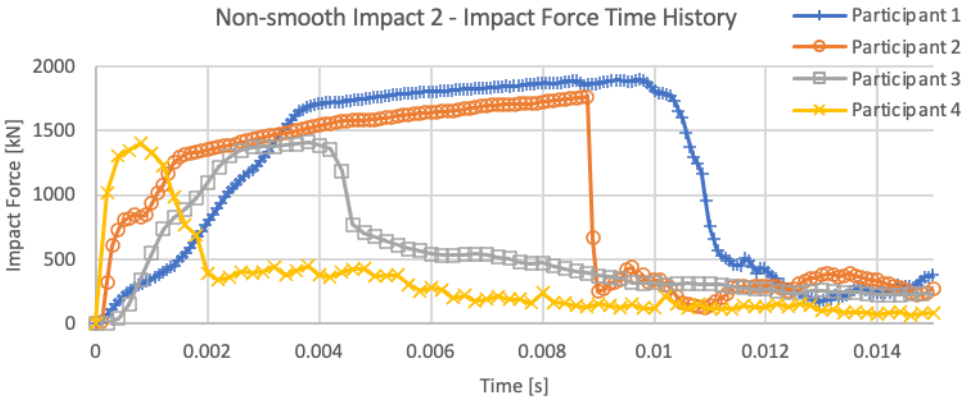

Figure 16: Experimental results and numerical predictions for "non-smooth impact 2"

A5 CONCLUSIONS AND FUTURE WORK

Unfortunately, due to delays in conducting the experiments caused by the COVID-19 pandemic, relatively few participants were able to complete this benchmark study in the time available. As such, the conclusions that can be drawn from the study, as reported here, are few. Some initial conclusions are that the constraints (or lack thereof) placed on the indenter and stiffened panel are important. Participant 1 constrained all rigid body motion for the stiffened panel, and as such, overpredicted the impact duration for all experiments by nearly a factor of 2. This has implications when strain rate effects are also considered, as the predicted strain-rate is approximately half of the actual. Also, from Figure 16 it is evident that the different failure criterion employed by the participants result in different impact force-time behaviours when predicting punch-through.

No conclusions will be made at this point about whether current FEA technology can effectively simulate a state of stress that is evolving from primarily biaxial tension to combined biaxial tension and shear. These conclusions will be drawn when the results of the extended benchmark study (i.e., to more participants) are reported and compared with the experiment results at a later date.